**Aalborg Universitet**

**AALBORG UNIVERSITY**
DENMARK

**Experimental Validation and Proof-of-concept of 5G Dense Small Cells Networks in Indoor Environments**

Wassie, Dereje Assefa

Publication date:
2019

Document Version
Publisher's PDF, also known as Version of record

Link to publication from Aalborg University

# EXPERIMENTAL VALIDATION AND PROOF-OF-CONCEPT OF 5G DENSE SMALL CELLS NETWORKS IN INDOOR ENVIRONMENTS

**BY**
**DEREJE ASSEFA WASSIE**

DISSERTATION SUBMITTED 2019

# Experimental Validation and Proof-of-concept of 5G Dense Small Cells Networks in Indoor Environments

Ph.D. Dissertation
## Dereje Assefa Wassie

# Curriculum Vitae

Dereje Assefa Wassie

Dereje Assefa Wassie received B.S. in Electrical Engineering from Jimma University, Ethiopia and M.S. in Telecommunication Engineering from Aalborg University, Denmark in 2008 and 2011 respectively. He is currently pursuing Ph.D. degree in Wireless Communications in the Department of Electronic Systems at Aalborg University. His main research interests include measurement system design and experimental analysis of the 5G communication concepts related to mobile broadband communications and industrial IoT.

Curriculum Vitae

# Abstract

Mobile communications have experienced significant developments in the last few years, and have provided services to our society and played a tremendous role in the way we communicate. Our society is continuously demanding more reliable, and better services. To fullfil such demands, industries and academia have been designing the fifth generation (5G) mobile communication system. In the 5G system, indoor dense small cells deployments are considered as one of the key enablers to increase the capacity and reliability of a network. Network densification brings many strong links that can be harnessed for improving the reliability by connecting a user terminal to multiple access points. The strong links can also be independently exploited to provide connections to different user terminals for improving the network capacity. However, these will be challenged by the increased level of inter-cell interferences that result from the presence of dense cells operating in almost fully occupied bands (i.e., sub-6 GHz bands).

Inter-cell Interference coordinations, advanced receivers, and spatial domain interference mitigation techniques (i.e., methods that rely on limiting the number of desired streams in multi-antenna transceiver systems) have been explored as possible solutions to deal with the interference. Advanced receivers and spatial domain schemes, on the other hand, have shown playing an essential role in combating the interference in dense small cells networks. These techniques are believed to be promising technologies in fulfilling the enhanced mobile broadband target of the 5G system. Similarly, multi-connectivity methods are considered as a promising scheme for achieving other 5G system targets such as very high reliability. Indeed, such technological advancements require comprehensive analysis and examination before being acknowledged for inclusion in the new technological innovations or standards. In literature, the validation of such technologies is typically carried out in a system-level simulation where simplified channel models and an abstract of the reference scenarios are usually employed. Such an approach may not fully grasp the realistic operating conditions. Therefore, it is essential to verify the potential benefits of the technologies in real operating conditions. This PhD thesis addresses the experimental validation of such

technologies in real indoor small cells scenarios. The entire work of this PhD project is carried out under several groups of studies. The first part of the study addresses the design and development of an experimental testbed and validation methodology. An agile multi-node experimental testbed has been designed in the context of distributed network setup for supporting a wide range of wireless experimental validation activities.

The second part of the project focuses on the experimental validation of several interference mitigation techniques (i.e., inter-cell interference coordination, advanced receivers) in indoor scenarios. The potential benefit of the techniques toward combating the interference in indoor dense small cells networks has been investigated using the multi-node testbed system. The experimental results verified that advanced receivers and spatial domain techniques are viable solutions toward combating the interference in indoor dense small cells networks. The results have also demonstrated that the potential of advanced receivers can further be improved by using interference aware rank adaptation algorithms.

The third part of the project focuses on wireless network reliability studies in indoor industrial scenarios. The first part of this study aims in investigating the radio propagation conditions, which has limited coverage in existing literature. The results obtained from the study showed that high shadowing levels and waveguiding effect severely impact the propagation conditions. Such conditions limit the reliability of a wireless network; therefore, wireless diversity techniques such as spatial diversity could be employed for enhancing reliability. In this regard, the second part of this study addresses an initial experimental analysis of multi-connectivity solutions in real indoor industrial scenarios. The obtained results -from experimental analysis- demonstrated that usage of multi-connectivity solutions could play a vital role in improving the reliability in indoor industrial scenarios. The results also showed that the physical layer multi-connectivity solution provides better reliability performance than higher layer multi-connectivity solution.

# Dansk Resume

I de senere år er der sket en signifikant udvikling indenfor mobilkommunikation, som har tilgængeliggjort services og har spillet en vigtig rolle for den måde vi kommunikerer. Men der kræves fortsat bedre og mere pålidelige service. For at leve op til disse krav har industrien og forskningen designet den femte generation (5G) af mobilkommunikation. I 5G systemet bliver konceptet små indendørsceller betragtet som en af de vigtigste elementer i at forøge kapaciteten og pålideligheden af netværket. Forøgelsen af tætheden af celler i netværket muliggør at der kan laves mange forbindelser som kan udnyttes til at forøge pålideligheden ved at forbinde brugerterminaler til flere access punkter. Forbindelserne kan også udnyttes uafhængigt af hinanden til at forbinde flere enheder og derved forøge kapaciteten på netværket. Dette vil dog blive besværliggjort af den forhøjede interferens imellem celler, som opstår når cellerne opererer i et næsten fuldt udnyttet frekvensbånd (f.eks. under 6 GHz frekvensbånd).

Intercelle interferenskoordinering, avancerede receivere, og spatial domæne interferens reducerings teknikker (f.eks. metoder som bygger på at begrænse antallet af ønskede streams i et multiantenne transceiver system) er alle blevet undersøgt som mulige løsninger til at håndtere interferens. Avancerede receivere og spatial domæne systemer har vist at de spiller en vigtig rolle i at bekæmpe interferens i småcelle netværk. Der er en tro på at disse teknikker vil sørge for at teknologien lever op til kravene til 5G systemet. På samme måde betragtes multiforbindelsesmetoder som en lovende tilgang for at opfylde andre krav til 5G systemet, så som ultra høj pålidelighed. Sådanne teknologifremskridt kræver omfattende analyse og forskning før de inddrages som en del af standarden af systemet. I litteraturen bliver valideringen af sådanne teknologier typisk udført i en systemniveau simulering, hvor simplificerede kanalmodeller og en abstraktion af referencescenarier bliver anvendt. Sådan en tilgang er ikke sikret til fulde at dække de realistiske operationelle omstændigheder. Derfor er det essentielt at verificere de potentielle fordele ved teknologierne under rigtige operationelle omstændigheder. Denne PhD afhandling adresserer den eksperimentelle validering af sådanne teknologier i rigtige indendørs småcelle scenarier. Arbejdet i dette PhD pro-

jekt er udført indenfor forskellige forskningsområder. Det første område adresserer design og udvikling af en eksperimentel testbed samt en valideringsmetode. En agil multinode eksperimentel testbed er blevet designet i konteksten af et distribueret netværkssetup som supporterer en bred vifte af trådløse eksperimentelle valideringsaktiviteter.

Det andet område af projektet fokuserer på den eksperimentelle validering af flere forskellige interferens reduceringsteknikker (f.eks. intercelle interferenskoordinering og avancerede receivere) i indendørsscenarier. Potentielle fordele ved teknikker til at bekæmpe interferens i tætte indendørs småcellenetværk er blevet undersøgt ved hjælp af det førnævnte multinode testbed. De eksperimentelle resultater verificerede at avancerede receivere og spatial domæne teknikker er funktionsdygtige løsninger til at bekæmpe interferens i tætte indendørscellenetværk. Resultaterne demonstrerer også at potentialet af avancerede receivere kan forbedres mere endnu ved at bruge interferensbevist rank tilpasningsalgoritmer.

Det tredje område af projektet fokuserer på studier af pålideligheden af trådløse indendørsnetværk i industrielle scenarier. Den første del af dette studie sigter at undersøge signaludbredelsen, hvilket kun er begrænset dækket i den eksisterende litteratur. Resultaterne i dette studie viser at høje niveauer af shadowing og effekten af waveguiding har en kritisk påvirkning på signaludbredelsen. Sådanne forhold begrænser pålideligheden af trådløse netværk. Derfor kan diversitetsteknikker anvendes for at forøge pålideligheden, så som spatial diversitet. I den sammenhæng adresserer den anden del af dette studie en indledende eksperimentel analyse af multiforbindelsesløsninger i rigtige indendørs industrielle scenarier. De opnåede resultater – fra eksperimentel analyse – demonstrerer at brugen af multiforbindelsesløsninger kan spille en vital rolle i at forbedre pålideligheden i indendørs scenarier. Resultaterne viser også at multiforbindelsesløsninger implementeret på det fysiske lag giver bedre pålidelighed end løsninger implementeret på højere lag.

# Contents

Contents

Contents

# List of Abbreviations

**1G** First Generation

**2G** Second Generation

**3G** Third Generation

**3GPP** 3rd Generation Partnership Project

**4G** Fourth Generation

**5G** Fifth Generation

**ADC** Analog-to-Digital Converter

**AP** Access Point

**CAZAC** Constant Amplitude Zero Autocorrelation Sequence

**CCDF** Complementary Cumulative Distribution Function

**CSG** Closed Subscriber Group

**CTF** Channel Transfer Function

**DC** Direct Current

**DFT** Discrete Fourier Transform

**DIR** Dominant Interferer Ratio

**DOF** Degrees of Freedom

**ECDF** Empirical Complementary Cumulative Distribution Function

**eICC** enhanced Inter-cell Interference Coordination

**eMBB** enhanced Mobile Broadband

**FDD** Frequency Division Duplex

**FDM**  Frequency-Division Multiplexing

**FFT**  Fast Fourier Transform

**FPGA**  Field Programmable Gate Array

**FRP**  Frequency Reuse Planning

**GPS**  Global Postioning System

**ICC**  Inter-cell Interference Coordination

**ICM**  Interference Covariance Matrix

**IDFT**  Inverse Discrete Fourier Transform

**IFFT**  Inverse Fast Fourier Transform

**IMPEX**  Implementation Expenditure

**IP**  Internet Protocol

**IRC**  Interference Rejection Combining

**JT**  Joint Transmission

**KPI**  Key Performance Indicator

**LOS**  Line-of-sight

**LTE**  Long Term Evolution

**LTE-A**  LTE-Advanced

**MCS**  Modulation and Coding Scheme

**MIMO**  Multiple-Input Multiple-Output

**MLE**  Maximum Likelihood Estimation

**mMTC**  massive Machine Type Communication

**mmWave**  Millimeter Wave

**MRC**  Maximal-Ratio Combining

**MRP**  Maximum Rank Planning

**NI**  National Instruments

**NTP**  Network Time Protocol

**NTS**  Network Time System

List of Abbreviations

**OFDM** Orthogonal Frequency-Division Multiplexing

**OSG** Open Subscriber Group

**PDCP** Packet Data Convergence Protocol

**PL** Path Loss

**PTP** Precision Time Protocol

**RAT** Radio Access Technology

**RF** Radio Frequency

**RLC** Radio Link Control

**RS** Reference Signal

**SDR** Software-defined Radio

**SF-LSE** Superfast Line spectral Estimation

**SFN** Single Frequency Network

**SIC** Successive Interference Cancellation

**SINR** Signal-to-Interference Plus Noise Ratio

**SRA** Selfish Rank Adaptation

**TCP** Transmission Control Protocol

**TDD** Time Division Duplex

**TDM** Time Division Multiplexing

**UE** User Equipment

**UPS** Uninterruptible Power Supply

**URLLC** Ultra-Reliable Low-Latency Communications

**USRP** universal Software Radio Peripheral

**VRA** Victim-aware Rank Adaptation

**ZC** Zadoff-Chu

List of Abbreviations

# Thesis Details

**Thesis Title:** Experimental Validation and Proof-of-concept of 5G Dense Small Cells Networks in Indoor Environments.

**Ph.D. Student:** Dereje Assefa Wassie

**Supervisors:** Prof. Preben Morgensen, Aalborg University.
Assoc. Prof. Gilberto Berardinelli, Aalborg University.
Asst. Prof. Fernando Menezes Leitão Tavares, Aalborg University.

The research described in this PhD thesis has been carried out at the Wireless Communication Networks (WCN) section in the Department of Electronic Systems, Aalborg University, Denmark. This work was performed in parallel with the mandatory courses required to attain the PhD degree.

The main body of this thesis contains the following research articles.

Paper A: Dereje A. Wassie, I. Rodriguez, G. Berardinelli, F. M. L. Tavares, T. B. Sørensen, T. L. Hansen and P. Mogensen, "An Agile Multi-Node Multi-Antenna Wireless Channel Sounding System," *IEEE Acess*, 2019.

Paper B: Dereje A. Wassie, G. Berardinelli, F. M. L. Tavares, O. Tonelli, T. B. Sørensen and P. Mogensen, "Experimental evaluation of interference rejection combining for 5G small cells," *IEEE Wireless Communications and Networking Conference (WCNC)*, 2015.

Paper C: Dereje A. Wassie, G. Berardinelli, D. Catania, F. M. L. Tavares, T. B. Sorensen and P. Mogensen, "Experimental Evaluation of Interference Suppression Receivers and Rank Adaptation in 5G Small Cells," *IEEE Vehicular Technology Conference (VTC2015-Fall)*, 2015.

Paper D: Dereje A. Wassie, G. Berardinelli, F. M. L. Tavares, T. B. Sorensen and P. Mogensen, "Experimental Verification of Interference Mitigation Techniques for 5G Small Cells," *IEEE Vehicular Technology Conference (VTC Spring)*, 2015.

Paper E: Dereje A. Wassie, G. Berardinelli, F. M. L. Tavares, T. B. Sorensen and P. Mogensen,"An Experimental Study of Advanced Receivers in a Practical Dense Small Cells Network," *Multiple Access Communications (MACOM) conference*, 2016.

Paper F: Dereje A. Wassie, I. Rodriguez, G. Berardinelli, F. M. L. Tavares, T. B. Sørensen, F. M. L. Tavares and P. Mogensen," Radio Propagation Analysis of Industrial Scenarios within the Context of Ultra-Reliable Communication," *IEEE Vehicular Technology Conference (VTC Spring)*, 2018.

Paper G: E. J. Khatib, Dereje A. Wassie, G. Berardinelli, I. Rodriguez and P. Mogensen, "Multi-Connectivity for Ultra-Reliable Communication in industrial scenarios," *IEEE Vehicular Technology Conference (VTC Spring)*, 2019.

This thesis has been submitted for assessment in partial fulfillment of the PhD degree. The thesis is based on submitted or published research articles which are listed above. Parts of the articles are used directly or indirectly in the extended summary of the thesis. As part of the assessment, co-author statements have been made available to the assessment committee and are also available at the Faculty.

# Acknowledgements

The completion of this PhD project is the result of an extraordinary journey accompanied by hard work, humility, trust, and many kind people generous support. It gives me great pleasure in extending my gratitude to my supervisors, Preben Morgensen, Gilberto Berardinelli, and Fernando Menezes Leitão Tavares for sharing their expertise and guidance.

Troels Bundgaard Sørensen, my teacher & colleague, thank you very much for all the discussion and valuable support on various aspects of the research. Ignacio Rodriguez Larrad and Emil J. Khatib, thank you very much for your valuable technical input during our collaboration that greatly improved this work. I also would like to express my heartfelt gratitude to each of my colleagues at WCN Section and colleagues from Nokia Bell Labs for their collaborations, and providing a pleasant work environment. In addition, I want to express my appreciation to my friends: German Corrales Madueno, Laura Luque Sanchez, Lucas Chavarria Gimenez and Lars Mikkelsen for your encouragement and advice during this journey.

Finally, I want to express my heartfelt gratitude to my beloved family (Worknesh Tarkegne, Assefa Wassie, Dr. Mesert Assefa, Dr. Solomon Assefa, and Meriam Yacob) for your unconditional love and encouragement. This journey would not be possible without your never-lasting love and support.

<div align="right">

Dereje Assefa Wassie
Aalborg University, April 2019

</div>

Acknowledgements

# Part I

# Introduction

# Introduction

Wireless communications have played a huge role in the way our society communicates and provided an immense social impact and notable economic growth over the last few decades [1]. Different generations of wireless communication technologies (cf. Fig. I.1), ranging from analog voice services offered by First Generation (1G) to the broadband data services of the latest fourth generation (4G), have been introduced in the last three decades (approximately every ten years). These generations of wireless technologies are optimized for increasing the data rates towards providing better services to the society. However, our society continues demanding more and better mobile broadband services. These demands have been rising exponentially year by year [1]. Besides, the number of internet-connected devices via a wireless network is increasing tremendously. Also, there is a need for a highly reliable wireless communication for wireless control & automation in industrial environments and vehicular communications. Such a need for highly reliable connections may not be achievable by just using the current wireless communication systems only. To satisfy these diverse need, industries and academia have been designing the upcoming fifth-generation wireless system, known as 5G, since 2013 [2].
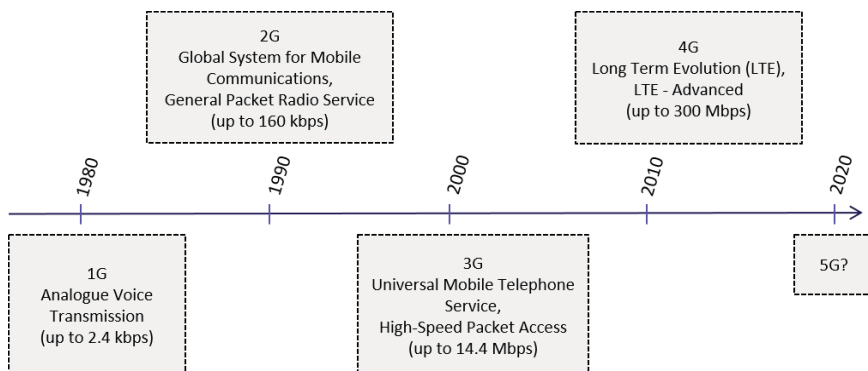
**Fig. I.1:** The evolution of mobile wireless systems.

3

# 1 Overview of 5G System

The 5G wireless communication systems are anticipated to fulfill the increasing demand for higher traffic and better mobile broadband services. Besides, the 5G networks aim to support a massive number of device connections. Overall, the 5G systems are seeking to support a large variety of use cases (Fig. I.2), such as:

- enhanced Mobile Broadband (eMBB) categorized as the evolution of today's human-centric broadband traffic with an improved spectral efficiency. In this regard, the 5G system is expected to accommodate a peak data rate up to 20 Gbits/s, and 100 Mbit/s data rate in broader area coverage cases (e.g., in urban and suburban areas) [3]. Its' application area covers both wide area coverage and hotspots.

- Ultra-Reliable Low-Latency Communications (URLLC) is the other use case which encompasses the transmission of a short packet with very high reliability (99.999%) and low latency. URLLC opens a wide range of use case including wireless control for the industrial production process, distributed automation in smart grid, safety in transportation, etc. [3].

- massive Machine Type Communication (mMTC) on the other hand aims towards accommodating a massive number of connected devices that may occasionally transmit with a low bit rate. The devices are expected to be low cost and have a longer operational lifetime, which is targeted to be above ten years.

Moreover, the 5G system are targeting to increase the capacity and the reliability of the wireless network as shown in Fig. I.2. To fulfill these targets, the 5G system explores different approaches:

- Bandwidth extension: One of the possible approaches for fulfilling the 5G system target is to increase the system bandwidth. However, the current terrestrial wireless system operating frequencies that span from several hundred MHz to a few GHz is nearly fully occupied. Therefore, the 5G networks are expected to adopt millimeter wave (mmWave) frequencies, which consist of a vast amount of unused spectrum. With such large available bandwidth, higher data transfer rates and connections of a large number of users can be achieved. Besides, the reliability of the network can also be improved by transferring redundant packets over a large unused spectrum. However, it is worth to mention that the usage of such frequencies will be limited by their detrimental propagation conditions which comprise large path loss, low diffractions around
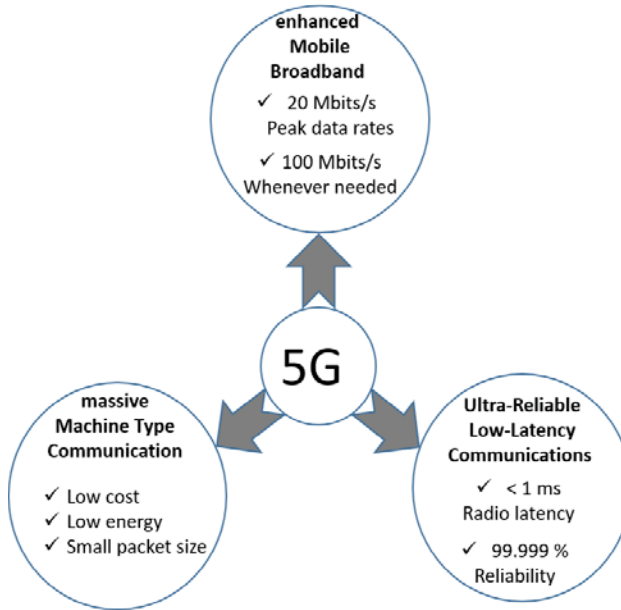
**Fig. I.2:** The 5G use cases and corresponding requirements.

obstacles and strong penetration loss through objects. Regardless of this limitation, the mmWave technologies have shown promising results towards ensuring the peak data rate target of the 5G system [4], [5].

- Multiple-Input Multiple-Output (MIMO) technology: The 5G capacity requirement can be achieved by increasing the spectral efficiency of the system using MIMO technology. It has also confirmed to be one of the key enablers for improving the system throughput and the reliability of the wireless networks, in the previous wireless communication system standards such as LTE [6]. Similarly, the MIMO technology is the main ingredient of the 5G systems for fulfilling stringent requirements. In that respect, the large-scale MIMO antenna system, known as massive MIMO, is considered as one of the most promising technologies of the upcoming 5G network [7]. Such availability of multiple antennas can enormously improve the spectral efficiency. However, it has a limitation regarding the channel estimation due to pilot contamination [8], [9], and also the architecture of antenna array increases the signal processing and hardware cost [10].

- Cell densification: Historically, cell densification (adding base stations) has been one of the vital components for improving the capacity of the cellular network and the cell edge users performance [11], [12], and

is also expected to play the most prominent role in the upcoming 5G mobile network. Cell densification, in small cells deployments, is an essential factor for fulfilling the 5G higher capacity requirements [13]. Small cells enable the reuse of the scarce spectrum across an area and decreasing the number of users competing per base station. These factors play a significant role in improving the capacity of the network. The potential of dense small cells deployments towards enhancing the network throughput performance has been confirmed by the work in [14]. However, this advantage has been hampered by the presence of strong inter-cell interference, which actually can to some extent be alleviated by using advanced inter-cell interference mitigation techniques [14].

# 2   5G Small Cells

It has been reported that around 80% of the mobile broadband traffic is consumed in a small geographical area such as indoor environments [11], and the need for better reliable connections and higher data rates are also growing continuously. Thereby, the need for a technology which comprises those characteristics is inevitable.

## 2.1   Improving broadband services in indoor environment

As discussed in the previous section, the 5G network is expected to provide better broadband services and high capacity. To accommodate these, 5G is adopting network densification as one of the main components. Moreover, the 5G network is expected to retain both macro cells and small cells. The work [14] indicates that dense small cells deployments play the most significant role to meet better broadband service and high capacity requirements of 5G. Besides that, using new spectrum bands and novel techniques for efficient utilization of available resources will contribute to reaching those requirements. These dense small cells deployments can be seen as a direct and extremely effective way to increase the network capacity.

However, dense small cells network introduces many challenges regarding the backhaul network, users mobility, and inter-cell interference. The backhaul network should be reliable and have sufficient capacity for handling massive traffic that comes from a large number of cells [15]. The presence of a large number of cells also poses challenges in supporting users mobility [16]. The work in [17], [18] investigated mobility schemes to address the challenge. Besides backhaul network and mobility challenges, inter-cell interference is also one of the major challenges in the dense deployment of small cells specifically in employing centimeter wave frequencies below 6 GHz. Such sub-6 GHz frequencies are envisioned as the operating band of the first deployment

phase of the 5G dense small cells network [19]. This is mainly due to their known propagation characteristics compared to mmWave frequencies which have a large amount of available bandwidth. However, given the scarcity of the available spectral resources in nearly full occupied sub-6 GHz bands, such small cells will be expected to operate using the same bandwidth. Besides, when the cells are small and densified, the distance between the neighboring cells become short. Due to these circumstances, inter-cell interference is the dominant factor affecting performance in dense small cell networks which is expected to be addressed using effective interference mitigation techniques.

**Inter-cell interference mitigation techniques**

Various mitigation techniques have been proposed to address the interference challenges via exploiting the available resource with respect to the time, frequency or space domain. These resources have been efficiently utilized, through coordination among the neighboring cells, to diminish the interference. Typically, techniques that rely on utilizing the frequency and time domains are based on partitioning the available resources among the neighboring cells. The resources partitioning is carried out, in such a way that, specific transmission resources are assigned to some cells for serving their users, without having any interference from other neighboring cells. Inter-cell interference coordination (ICIC) [20] and time-domain enhanced inter-cell interference coordination (eICIC) [21] techniques are examples of frequency and time domain resource partitioning, respectively. On the spatial domain, multiple transmit antennas have been used to decrease the interference using coordinated beamforming and coordinated multi-point transmission and reception techniques [22].

The techniques mentioned above are based on inter-cell coordination, and require the cells to be time-synchronized and coordinated when they are transmitting. To ensure these in dense small cells networks, a significant amount of information is indeed required to be exchanged among the cells through the backhaul network, and this will consequently increase the implementation expenditure (IMPEX) of the network. Besides, applying such techniques in the presence of large networks increases the complexity of managing the available resource. To alleviate these, the work in [23] proposes an interference mitigation scheme which relies on two consecutive steps. The first step is to divide the entire network into clusters considering that the interference between clusters is minimized. The second step is to mitigate the interference between cells grouped in the same cluster (i.e., intra-cluster) using inter-cell interference coordination.

An alternative to interference coordination schemes is to rely on the spatial domain resources with advanced receivers baseband signal processing [15]. Such techniques exploit the spatial domain resource, to suppress interference

using linear combining techniques (e.g., interference rejection combining), or cancel the interference using non-linear techniques (e.g., successive interference cancellation). Historically, such advanced receiver techniques used to be employed at the base station, because they require multiple antennas and extensive baseband signal processing capability. To employ these schemes at the user terminal has been expensive. However, recently the technologies are progressing, and the user terminals are employing more antennas and retain higher signal processing capability. To that end, the envisioned 5G system presented in [24] relies on the usage of advanced receivers, as major interference mitigation scheme for dense small cells networks. The advanced receivers are based on the interference rejection combining (IRC) technique that the interference suppression capability. The technique exploits the available resources on spatial domain, to suppress the interfering signals by projecting them over an orthogonal subspace relative to the desired signal. The computer simulation work in [25] shows that advanced receivers can significantly improve the network throughput in dense small cells networks. The performance of such receivers may be further improved with efficient utilization of the spatial resources using techniques such as rank adaptation algorithms. Such algorithms are used to find the spatial resource usage trade-off between increasing the spatial multiplexing gain or the receiver interference suppression capability. As a matter of fact, the work in [26] proposed interference aware rank adaptation schemes to decrease interference levels in interference limited scenarios, and their analysis using computer simulation showed that such schemes can improve the throughput performance in the 5G small cells network. However, further research is still required for validating the effectiveness of such those techniques (i.e., advanced receivers, rank adaptations) in real indoor small cells networks. It is also essential to evaluate whether advanced receivers can be a valid alternative to inter-cell interference coordination schemes ( i.e., the frequency reuse) in a practical dense small cells network.

## 2.2 Improving the reliability of the network in industry automation

The 5G system is targeting to support wireless connections with very high reliability and low latency. These will bring a great deal of improvement for a broad set of user applications, ranging from an industrial environment to control & automate the manufacturing process; vehicular communications to control drones; smart grid to control a large number of sensors and actuators [27].

For instance, in an industrial environment, highly reliable and low latency wireless communication can provide a considerable benefit towards monitoring and controlling the physical process, by offering a flexible communication

infrastructure [28]. This will improve the efficiency of the industrial production in respect to the traditional factory which is built based on wired communications [28]. Some of the current industrial automation is already using wireless technologies for providing a flexible infrastructure to speed up the manufacturing process. However, the existing wireless technologies do not provide satisfactory performance in terms of very high reliability and low latency requirements of the process control applications of the industry [29]. The work in [29] also reported that 5G would only be able to fulfill these requirements if there is a very high availability of wireless signal coverage in an industry hall environment. However, this would be very challenging due to the harsh propagation conditions of the environment.

In other words, a rough radio propagation condition is a limiting factor for increasing the reliability of the wireless network. The propagation is expected to be severe due to the concrete wall structure of indoor industrial buildings, and the presence of many propagation obstacles such as metallic machinery, robots, production line, etc. These will increase the radio propagation shadowing levels, which have a significant impact of the transmission reliability of the communication links. However, there is limited knowledge available in literature on characterizing the propagation conditions, and modeling the shadowing in connection with highly reliable industrial automation applications. Therefore, it is crucial to understand the propagation conditions of such environments and evaluate the capability of already existing models.

In such challenging environments, the reliability of the wireless network could also be improved using low-rate codes, or retransmission techniques. However, these techniques have their own limitation. First, using low-rate codes to improve the transmission reliability in poor channel conditions will increase the interference level in the networks due to the occupancy of more resources. Second, improving the reliability using retransmissions will increase the latency, and this will not be a favorable condition in latency-sensitive applications such as industrial automation. To enhance the reliability of the industrial environment, one can exploit the dense deployment of small cells networks [30]. Such availability of cells brings the abundance of links which can somehow lead to high interference in broadband services. On the other hand, it can be harnessed to improve the reliability using multi-connectivity schemes (where the receiver is connected through multiple communication paths/links) - to boost the received signal quality.

The reliability of a network can be improved by transferring the same data packets using available radio resources from multiple transmission points, which can be co-located at the same location or deployed at different locations. A variety of multi-connectivity techniques include single frequency network, coordinated multi-point transmission, and packet duplication which represents transmitting the same packets in a different carrier and combine them at Packet Data Convergence Protocol (PDCP) layer [31]. These multi-

connectivity techniques show a promising performance toward fulfilling the very high reliability and low latency requirements. The work in [32] investigated the potential of packet duplications using numerical analysis toward fulfilling the reliability requirements for URLLC services. Similarly, [33] showed the potential of transmitting the same data packets via independent paths towards improving reliability. According to their simulation results, multi-connectivity could play a significant role in enhancing the reliability in mixed services, where users are demanding a highly reliable link or enhanced broadband services. Overall, the studies indicate that multi-connectivity techniques can significantly boost the reliability of the wireless network. Therefore, these techniques can be used to improve the reliability of the industrial wireless system. However, there is still a lack of research towards investigating the potential of these techniques for industrial automation applications. It is also essential to identify a multi-connectivity approach that can provide better reliability performance in real indoor industrial environments.

# 3 Thesis objectives and scope

The main aim of this thesis is to demonstrate the feasibility and the potential of previously introduced techniques in real indoor small cells networks. To that end, various inter-cell interference mitigation techniques, such as advanced receivers (i.e., interference suppression receivers, successive interference cancelation ), maximum rank planning (a technique that utilizes spatial domain resources to combat interference), and interference coordination (i.e., frequency reuse), have been experimentally evaluated. Besides, the multi-connectivity techniques, that are employed to improve the reliability of wireless connections have been investigated.

Commonly, the potential of these techniques is evaluated in system-level simulations. The system level simulations are based on standard statistical channel models with geometrically regular scenarios. These abstractions provide a significant advantage to execute broad configuration parameters and different operating conditions quickly, and make the system-level simulations a crucial part of new concept validation. However, this approach has some known limitations. First, the real-world scenarios are geometrically irregular, and this will affect the position of the network nodes which have a significant impact on the network performance of the techniques. Second, the statistical channel models are generic, and they are not intended to accurately predict the channel conditions of any link, as it is in a real network deployment. Instead, they provide a statistical description of the environment. For instance, the work [34] investigated commonly used path loss channel model, known as WINNER II, in indoor office environments, and their analysis indicates

that such model does not predict the path loss of the selected links correctly. Due to those limitations, the system-level simulation cannot capture the full complexity of real operating conditions. Experiments on the field, on the other hand, can capture the real-world information. Such an experimental study, therefore, increases the level of accuracy and realism in the performance evaluation of wireless systems.

In indoor scenarios, the network topology (that describes all existing link channel characteristics among multiple network nodes) is affected by the existence of several indoor types of equipment, building irregularities, and ever-changing building structures and materials. These will significantly affect the radio propagation conditions and interference level. Indeed, the real radio propagation conditions will not be described adequately with channel models, and they will prominently affect the potential of previously introduced techniques. Hence, detailed research in this regard is of high importance. In this regards, several research questions have been formulated and addressed in this study:

- RQ1: Does the prominent performance of advanced receivers, towards coping inter-cell interference challange, can be seen in a real indoor dense small cells network?

- RQ2: To which extent interference mitigation techniques that rely on a spatial domain can be a valid/legitimate substitute to commonly used interference coordination scheme (i.e., frequency reuse) - for combating inter-cell interference in real channel conditions?

- RQ3: Do well known large-scale propagation models can accurately predict the severe propagation conditions of indoor industrial scenarios?

- RQ4: Can multi-connectivity techniques improve the reliability of wireless network in real indoor industrial scenarios, and which schemes can provide better reliability performance in such scenarios?

# 4 Employed validation methodology

Commonly, when new methods are proposed to improve technologies performance, they have to pass through an extensive analysis and testing in different operating conditions before they are considered to be a part of products or standards. The first evaluation of the new proposed technologies are usually based on analytical approach, and if the technologies show good performance, further steps of evaluation can be carried to validate the potential

of the technologies in real scenarios. The further steps of validation can be executed with computer simulations, or experiments in the real world environments. Notably, the computer-based analysis is agile and allows to simulate a large number of configuration parameters, which can mimic the real world behavior, and thus improve the accuracy level of analysis. In respect to that, most of the new wireless technologies are validated using computer-based system-level simulations [35]. The system-level simulators usually employ simplified models (i.e., statistical radio channel models), which are suitable to be implemented using software. However, such approaches may not adequately capture the complexity of the real world environments, such as the real radio propagation conditions of a given network. To fill this gap, in this thesis, the aforementioned 5G technologies have been experimentally studied.

The experimental study could be carried out on a full-blown 5G testbed (e.g., 5G Test Network Facilities [36]) which consists of the full wireless protocol stacks. However, developing such platforms is costly and requires a significant amount of resources; and this is out of the scope of this thesis objective. However, to meet the thesis objectives mentioned above, we considered a hybrid evaluation experimental methodology, where we utilized the system-level simulation approach and replaced the statistical radio channel model with real channel measurement data obtained from field measurements (the methodology will be further described in the next chapter). In this hybrid approach, the channel conditions of all communication links in a network (i.e., link path loss, shadowing level and multipath fading level) are not based on any models. Instead, the real channel characteristics of the links are measured, corresponding to given network topology and frequency, using a multi-node channel testbed (c.f. Paper A). The hybrid evaluation approach, however, will not grasp the full real-time behavior of the system and does also not employ large network deployments which are usually considered in system level simulations. However, to ensure a higher level of accuracy and realism in the hybrid evaluation, the channel conditions are based on extensive channel measurements that can sufficiently describe the multi-links channel characteristics of given network deployment. In doing so, such study offers additional insight into the potential behavior of the previously introduced technologies in real wireless network channel conditions.

## 5   List of Contributions

This thesis is organized as a collection of several publications. As a part of the main body of the thesis, the following publications, both authored and co-authored, have been included:

Paper A: Dereje A. Wassie, I. Rodriguez, G. Berardinelli, F. M. L. Tavares,

T. B. Sørensen, T. L. Hansen and P. Mogensen, "An Agile Multi-Node Multi-Antenna Wireless Channel Sounding System," *IEEE Access*, 2019.

Paper B: Dereje A. Wassie, G. Berardinelli, F. M. L. Tavares, O. Tonelli, T. B. Sørensen and P. Mogensen, "Experimental evaluation of interference rejection combining for 5G small cells," *IEEE Wireless Communications and Networking Conference (WCNC)*, 2015.

Paper C: Dereje A. Wassie, G. Berardinelli, D. Catania, F. M. L. Tavares, T. B. Sorensen and P. Mogensen, "Experimental Evaluation of Interference Suppression Receivers and Rank Adaptation in 5G Small Cells," *IEEE Vehicular Technology Conference (VTC2015-Fall)*, 2015.

Paper D: Dereje A. Wassie, G. Berardinelli, F. M. L. Tavares, T. B. Sorensen and P. Mogensen, "Experimental Verification of Interference Mitigation Techniques for 5G Small Cells," *IEEE Vehicular Technology Conference (VTC Spring)*, 2015.

Paper E: Dereje A. Wassie, G. Berardinelli, F. M. L. Tavares, T. B. Sorensen and P. Mogensen,"An Experimental Study of Advanced Receivers in a Practical Dense Small Cells Network," *Multiple Access Communications (MACOM) conference*, 2016.

Paper F: Dereje A. Wassie, I. Rodriguez, G. Berardinelli, F. M. L. Tavares, T. B. Sørensen, F. M. L. Tavares and P. Mogensen," Radio Propagation Analysis of Industrial Scenarios within the Context of Ultra-Reliable Communication," *IEEE Vehicular Technology Conference (VTC Spring)*, 2018.

Paper G: E. J. Khatib, Dereje A. Wassie, G. Berardinelli, I. Rodriguez and P. Mogensen, "Multi-Connectivity for Ultra-Reliable Communication in industrial scenarios," *accepted in IEEE Vehicular Technology Conference (VTC Spring)*, 2019.

Additionally, the following publications have been co-authored as a part of collaborative work with colleagues in Wireless Communication Networks (WCN) section:

Collaboration 1: G. Berardinelli and J. L. Buthler and F. M. L. Tavares and O. Tonelli and Dereje A. Wassie and F. Hakhamaneshi and T. B. Sørensen and P. Mogensen, "Distributed Synchronization of a testbed network with USRP N200 radio boards," *Asilomar Conference on Signals, Systems and Computers*, 2014.

Collaboration 2: G. Berardinelli, Dereje A. Wassie, N. H. Mahmood, M. G. Sarret, T. B. Sorensen and P. Mogensen, "Evaluating Full Duplex Potential in Dense Small Cells from Channel Measurements," *IEEE Vehicular Technology Conference*, 2016.

Collaboration 3: I. Rodriguez and E. P. L. Almeida and M. Lauridsen and Dereje A. Wassie and L. Chavarria Gimenez and H. C. Nguyen and T. B. Soerensen and P. Mogensen, "Measurement-based Evaluation of the Impact of Large Vehicle Shadowing on V2X Communications," *European Wireless Conference*, 2016.

An overview of all main contributions and collaboration works, and their related research topics are illustrated in Fig. I.3. Furthermore, the main contributions of this thesis can be summarized as follow:

- A hybrid experimental evaluation setup is developed to validate the potential of previously introduced techniques in real-world channel conditions. To support this, an agile multi-node channel sounder testbed platform is also developed.

- The performance of interference mitigation techniques that are based on receiver signal processing, and spatial domain resources, are experimentally verified in real indoor environments.

- Contribution to the understanding of the radio propagation in indoor industrial environments.

- Fnding the potential of multi-connectivity schemes towards improving the reliability of the wireless network in real industrial environments.

## 6  Thesis Outline

The overall contributions and main findings during this Ph.D. study are structured in six parts. Each part includes a short brief description of the background and a summary of the main findings (to guide the readers to understand how different topics and included articles are related to each other). The thesis is structured as follows:

- **Part I: Introduction -** This part is related to the current chapter, which presents the motivation of the work, describes the objectives and scope of the study, and explains the contributions and the outline of the thesis.
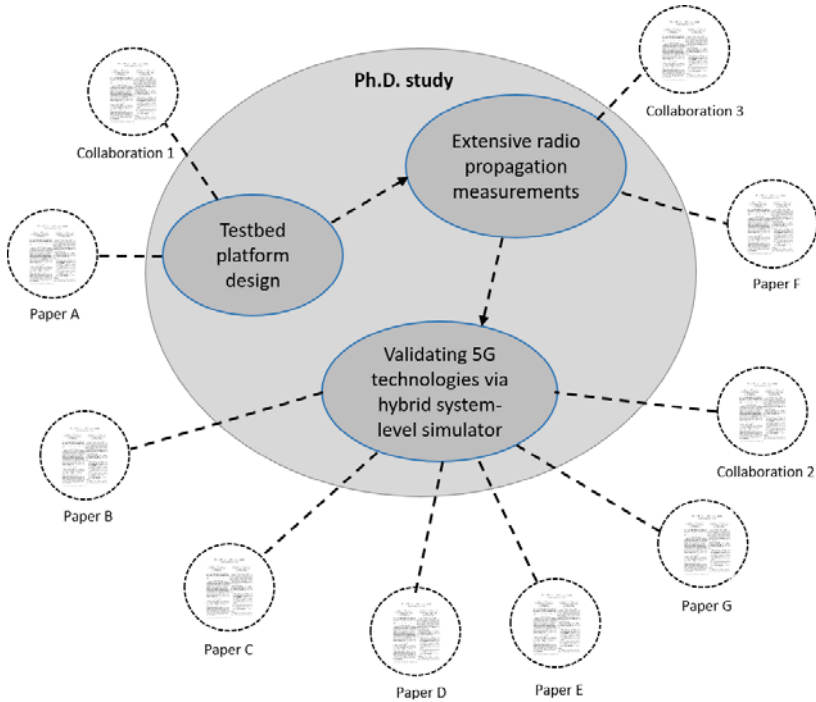
**Fig. I.3:** An overview of the contributions produced during this Ph.D. study.

- **Part II: Experimental Validation Methodology and Agile Multi-Node Channel Sounder -** This section presents a brief overview of the employed hybrid experimental approach, which is used to validate previously introduced technologies. The section is also dedicated to explaining the flexible multi-node channel sounder platform. Mainly, this part is adapted from paper A.

- **Part III : Proof-of-concept of Interference Mitigation Techniques in Indoor Small Cells Networks -** This part illustrates the potential of advanced receivers toward combating the inter-cell interference challenges in real indoor 5G small cells network. It also compares different interference mitigation schemes which relies upon the spatial domain and frequency domain resources. Overall, this section addresses the two main research questions (**RQ1** and **RQ2**) described above. The outcome of this study is included in paper B, C, D, and E.

- **Part IV : Radio Propagation and Multi-connectivity System Studies in Indoor Industrial Scenarios -** This part addresses the large-scale radio propagation characteristics study in indoor industrial scenarios, using

15

statistical radio propagation models. These models are also investigated towards their potential for predicting the severe industrial radio propagation level over industry hall environment. Additionally, this part discusses the experimental validation of multi-connectivity techniques promising potential, toward improving the reliability of wireless transmission in real industrial scenarios. Generally, this part addresses the third and fourth research questions (**RQ3** and **RQ4**) and is composed of paper F and G.

- **Part V : Conclusions -** This part describes the summary of the main findings and provides recommendations and topics which could be studied in the future.

# References

[1] *Future of internet - Innovation and investment in IP interconnection*, Liberty Liberty, may 2014.

[2] J. Thompson, X. Ge, H. C. Wu, R. Irmer, H. Jiang, G. Fettweis, and S. Alamouti, "5G wireless communication systems: prospects and challenges [guest editorial]," *IEEE Communications Magazine*, vol. 52, no. 2, pp. 62–64, February 2014.

[3] *Framework and overall objectives of the future development of IMT for 2020 and beyond*, International Telecommunication Union (ITU), February 2015.

[4] A. Ghosh, T. A. Thomas, M. C. Cudak, R. Ratasuk, P. Moorut, F. W. Vook, T. S. Rappaport, G. R. MacCartney, S. Sun, and S. Nie, "Millimeter-wave enhanced local area systems: A high-data-rate approach for future wireless networks," *IEEE Journal on Selected Areas in Communications*, vol. 32, no. 6, pp. 1152–1163, June 2014.

[5] S. G. Larew, T. A. Thomas, M. Cudak, and A. Ghosh, "Air interface design and ray tracing study for 5G millimeter wave communications," in *2013 IEEE Globecom Workshops (GC Wkshps)*, Dec 2013, pp. 117–122.

[6] M. B. Stefania Sesia, Issam Toufik, *LTE – The UMTS Long Term Evolution From Theory to Practice*. A John Wiley and Sons Ltd, 2011.

[7] F. Boccardi, R. W. Heath, A. Lozano, T. L. Marzetta, and P. Popovski, "Five disruptive technology directions for 5G," *IEEE Communications Magazine*, vol. 52, no. 2, pp. 74–80, February 2014.

[8] B. Hassibi and B. M. Hochwald, "How much training is needed in multiple-antenna wireless links?" *IEEE Transactions on Information Theory*, vol. 49, no. 4, pp. 951–963, April 2003.

[9] N. Jindal and A. Lozano, "A unified treatment of optimum pilot overhead in multipath fading channels," *IEEE Transactions on Communications*, vol. 58, no. 10, pp. 2939–2948, October 2010.

References

[10] Y. Zeng, R. Zhang, and Z. N. Chen, "Electromagnetic lens-focusing antenna enabled massive MIMO: Performance improvement and cost reduction," *IEEE Journal on Selected Areas in Communications*, vol. 32, no. 6, pp. 1194–1206, June 2014.

[11] V. Chandrasekhar, J. G. Andrews, and A. Gatherer, "Femtocell networks: a survey," *IEEE Communications Magazine*, vol. 46, no. 9, pp. 59–67, September 2008.

[12] M. Dohler, R. W. Heath, A. Lozano, C. B. Papadias, and R. A. Valenzuela, "Is the PHY layer dead?" *IEEE Communications Magazine*, vol. 49, no. 4, pp. 159–165, April 2011.

[13] X. Ge, S. Tu, G. Mao, C. X. Wang, and T. Han, "5G ultra-dense cellular networks," *IEEE Wireless Communications*, vol. 23, no. 1, pp. 72–79, February 2016.

[14] P. Mogensen, K. Pajukoski, E. Tiirola, E. Lähetkangas, J. Vihriälä, S. Vesterinen, M. Laitila, G. Berardinelli, G. W. O. D. Costa, L. G. U. Garcia, F. M. L. Tavares, and A. F. Cattoni, "5G small cell optimized radio design," in *2013 IEEE Globecom Workshops (GC Wkshps)*, Dec 2013, pp. 111–116.

[15] N. Bhushan, J. Li, D. Malladi, R. Gilmore, D. Brenner, A. Damnjanovic, R. T. Sukhavasi, C. Patel, and S. Geirhofer, "Network densification: the dominant theme for wireless evolution into 5G," *IEEE Communications Magazine*, vol. 52, no. 2, pp. 82–89, February 2014.

[16] J. G. Andrews, S. Buzzi, W. Choi, S. V. Hanly, A. Lozano, A. C. K. Soong, and J. C. Zhang, "What will 5G be?" *IEEE Journal on Selected Areas in Communications*, vol. 32, no. 6, pp. 1065–1082, June 2014.

[17] I. Hwang, B. Song, and S. S. Soliman, "A holistic view on hyper-dense heterogeneous and small cell networks," *IEEE Communications Magazine*, vol. 51, no. 6, pp. 20–27, June 2013.

[18] L. C. Gimenez, *Mobility Management for Cellular Networks: From LTE Towards 5G*. Aalborg University, 2017.

[19] M. Ding, D. Lopez-Perez, H. Claussen, and M. A. Kaafar, "On the fundamental characteristics of ultra-dense small cell networks," *IEEE Network*, vol. 32, no. 3, pp. 92–100, May 2018.

[20] G. Boudreau, J. Panicker, N. Guo, R. Chang, N. Wang, and S. Vrzic, "Interference coordination and cancellation for 4G networks," *IEEE Communications Magazine*, vol. 47, no. 4, pp. 74–81, April 2009.

[21] K. I. Pedersen, Y. Wang, S. Strzyz, and F. Frederiksen, "Enhanced inter-cell interference coordination in co-channel multi-layer LTE-advanced networks," *IEEE Wireless Communications*, vol. 20, no. 3, pp. 120–127, June 2013.

[22] D. Lee, H. Seo, B. Clerckx, E. Hardouin, D. Mazzarese, S. Nagata, and K. Sayana, "Coordinated multipoint transmission and reception in LTE-advanced: deployment scenarios and operational challenges," *IEEE Communications Magazine*, vol. 50, no. 2, pp. 148–155, February 2012.

[23] E. Pateromichelakis, M. Shariat, A. Quddus, M. Dianati, and R. Tafazolli, "Dynamic clustering framework for multi-cell scheduling in dense small cell networks," *IEEE Communications Letters*, vol. 17, no. 9, pp. 1802–1805, September 2013.

[24] P. Mogensen, K. Pajukoski, E. Tiirola, J. Vihriala, E. Lahetkangas, G. Berardinelli, F. M. L. Tavares, N. H. Mahmood, M. Lauridsen, D. Catania, and A. F. Cattoni, "Centimeter-wave concept for 5g ultra-dense small cells," in *2014 IEEE 79th Vehicular Technology Conference (VTC Spring)*, May 2014, pp. 1–6.

[25] F. M. L. Tavares, G. Berardinelli, N. H. Mahmood, T. B. Sorensen, and P. Mogensen, "On the potential of interference rejection combining in B4G networks," in *2013 IEEE 78th Vehicular Technology Conference (VTC Fall)*, Sept 2013, pp. 1–5.

[26] D. Catania, A. F. Cattoni, N. H. Mahmood, G. Berardinelli, F. Frederiksen, and P. Mogensen, "A distributed taxation based rank adaptation scheme for 5g small cells," in *2015 IEEE 81st Vehicular Technology Conference (VTC Spring)*, May 2015, pp. 1–5.

[27] E. Dahlman, G. Mildh, S. Parkvall, J. Peisa, J. Sachs, Y. Selén, and J. Sköld, "5G wireless access: requirements and realization," *IEEE Communications Magazine*, vol. 52, no. 12, pp. 42–47, December 2014.

[28] J. Lee, B. Bagheri, and H.-A. Kao, "Recent advances and trends of cyber-physical systems and big data analytics in industrial informatics," ResearchGate, 2014, keynote given at the 12th IEEE International Conference on Industrial Informatics (INDIN 2014), Porto Alegre, Brazil.

[29] O. N. C. Yilmaz, Y. P. E. Wang, N. A. Johansson, N. Brahmi, S. A. Ashraf, and J. Sachs, "Analysis of ultra-reliable and low-latency 5G communication for a factory automation use case," in *2015 IEEE International Conference on Communication Workshop (ICCW)*, June 2015, pp. 1190–1195.

[30] N. Brahmi, O. N. C. Yilmaz, K. W. Helmersson, S. A. Ashraf, and J. Torsner, "Deployment strategies for ultra-reliable and low-latency communication in factory automation," in *2015 IEEE Globecom Workshops (GC Wkshps)*, Dec 2015, pp. 1–6.

[31] D. Öhmann, *High Reliability in Wireless Networks Through Multi-Connectivity*. Deutsche Nationalbibliothek, 2017.

[32] J. Rao and S. Vrzic, "Packet duplication for URLLC in 5G: Architectural enhancements and performance analysis," *IEEE Network*, vol. 32, no. 2, pp. 32–40, March 2018.

[33] N. H. Mahmood, M. Lopez, D. Laselva, K. Pederesen, and G. Berardinelli, "Reliability oriented dual connectivity for URLLC services in 5G new radio," in *IEEE ISWCS 2018*, 2018, pp. 1–6.

[34] O. Tonelli, *Experimental analysis and proof-of-concept of distributed mechnisms for local area wireless network*. Aalborg University, 2014.

[35] M. Liu, P. Ren, Q. Du, W. Ou, X. Xiong, and G. Li, "Design of system-level simulation platform for 5g networks," in *2016 IEEE/CIC International Conference on Communications in China (ICCC)*, July 2016, pp. 1–6.

[36] "5G test network (5GTN) facilities," https://5gtn.fi/overview/, accessed: 2018-07-17.

**Part II**

# Experimental Validation Methodology and Agile Multi-Node Channel Sounder

# Experimental Validation Methodology and Agile Multi-Node Channel Sounder

This part of the thesis presents a brief overview of the experimental validation approach used in this thesis and the channel sounder platform. The sounder platform is designed for measuring the channel conditions of a given network layout (i.e., the channel characteristics of all links among the access points and users locations). The measured channel conditions are used in the hybrid system-level simulator for verifying the potential of the technologies studied in this Ph.D. project.

## 1 Motivation

As described in chapter I, the employed validation approach is based on a system-level simulation by substituting commonly used statistical channel models with the measured channel conditions of given network deployment. Such an approach is employed to increase the realism of the validation methodology since the channel models will not correctly estimate the channel condition of a given link as it is in real network deployment [2], [3]. From a validation point of view, the propagation conditions of any communication links in a given network layout have a significant impact on the performance of the wireless technologies. More accurate validation for the performance of the technologies can be achieved by using comprehensive information about the channel conditions of all the communication links of a network deployment. In this work, the validation methodology is based on measured conditions of all links in a given network deployment scenario. The sequential steps of the employed methodology are explained as follow:

1. Deployment scenarios selection: first, we select the scenarios where the measurements are to be taken. Then, we choose the measurement points which represent all possible $'N'$ locations of the access points and $'M'$ users. In fact, the measurement positions are selected considering to experience different propagation conditions (e.g., non-line-of-sight, line-of-sight, distances, obstacles).

2. Channel sounding: based on the deployment scenarios, extensive channel measurements are carried out to build $N \times M$ channel matrix which has complete information about the channel conditions of all existing links. The souding is performed using the multi-node channel sounder.

3. Offline processing: using the measured channel matrices, the performance estimation of previously introduced techniques is performed by the hybrid system level-simulation approach. Fig. II.1 illustrates the hybrid evaluation approach.
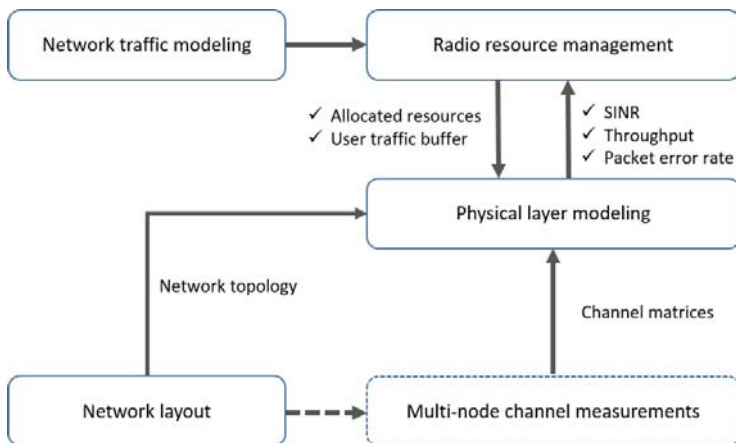


Fig. II.1: An overview of the hybrid system-level simulation approach.

During the offline process, the network layout entity emulates different possible network topologies (combination of access points and users) based on the deployment scenario. These and the channel matrices are then provided to the physical layer modeling for estimating the Signal-to-Interference Plus Noise Ratio (SINR). The SINR is calculated based on given physical layer parameters (i.e., resource blocks, bandwidth, frame structure, receiver type) and resource occupation of the network. The resource occupancy is provided by the radio resource management entity considering a given traffic model. Furthermore, the estimated SINR can be used to describe the reliability of the links, or it can be mapped to throughout using Shannon-Hartley formula to estimate the maximum achievable throughput over the links.

The channel matrices of a given network deployment contain the channel response of all the existing combinations of links in the network. The measured channel response of the links represents the full propagation effect of the environment such as path loss, shadowing, fading, etc. The whole channel matrices of all link combinations among a number of spatial positions (i.e., the access points and users locations) then describe the real channel conditions of the network deployment. These improve the capability of the validation methodology towards capturing the real word environment impact on the performance of the technologies.

In order to have a comprehensive understanding of the performance of the technologies in a given deployment environment, the channel matrices entry should contain a large number of network node spatial positions. For that, a large number of redeployments is required with commonly used channel sounder setup such as a vector network analyzer. Indeed, such setup is quite expensive and built from specialized hardware which is not easily reconfigurable. Besides, a large number of redeployments may impact the propagation conditions of the environment. On the other hand, a testbed platform composed of multiple transmitter and receiver nodes can measure all possible link combinations among distributed spatial positions without the need for many laborsome redeployments. The main aim of this part of the thesis is to present the design and development of an agile multi-node channel sounder testbed. The testbed features characteristics of easy reconfigurability (c.f. Paper A) to accommodate a wide range of wireless system experimental activities.

## 2 Included Article

This section of the thesis has been adapted from:

**Paper A: An Agile Multi-Node Multi-Antenna Wireless Channel Sounding System.**

This article presents the design of a flexible multi-node wireless channel sounder testbed, which was developed using software-defined radio (SDR) concepts. The testbed is built of 24 SDR devices (i.e., Universal Software Radio Peripheral) where each device consists of two radio frequency ports; this makes the testbed to feature a total of 48 antenna ports. The sounder system is developed using frequency domain sounding approach by utilizing Orthogonal Frequency Division Multiplexing (OFDM) modulation techniques.

## 3 Contributions

**Easy Reconfigurability**

The wireless channel sounder system presented in Paper A accommodates easy reconfigurability and quick proof-of-concept of new technologies. These are achieved by the usage of the SDR concepts which allow the baseband signal processing to be carried out using the software. Besides, the sounder system consists of twelve SDR testbed nodes where each node contains four radio frequency (RF) front ends. The RF front end supports different frequency configurations spanning from 1.2 GHz to 6 GHz, and the RF chain support transmission or reception configuration modes. These characteristics allow the testbed to accommodate different Multiple Input Multiple Output (MIMO) configurations (i.e., $2 \times 2$ or $4 \times 4$ MIMO setup). Also, the presence of multiple nodes and antennas per node can provide a possibility of understanding the propagation conditions of multiple links at the same time, as described in Paper A.

**Verification of the channel estimation approach and device calibration**

Commonly the SDR platforms are not purposefully designed for the usage of channel sounder applications. However, the work in Paper A demonstrated that with careful design and calibration, such devices could accurately estimate the channel conditions. In that respect, the study in Paper A confirms the sounder system channel estimation accuracy using known propagation conditions such as free space and deterministic channel emulator. The results indicated that the measured path loss using the sounder devices in line-of-sight conditions varies from the free space path loss via a standard deviation of less than 1 dB. Also, the potential of predicting fast fading condition was also verified using a deterministic channel emulator, and the results indicated that the sounder could resolve the fast fading components with a standard deviation of 5.7 ns.

**Toward measuring the channel conditions among a large number of spatial positions**

The sounder system is built using multiple software defined radio nodes. To accommodate the transmission and measurement acquisition among multiple testbed nodes, time and frequency division multiplexing schemes are employed. These allow measuring the channel response of multiple links at the same time and provide an ability to characterize a large number of links without laborsome redeployments. The study in Paper A indicated that with the multi-node sounder system (i.e., consists of 12 testbed nodes), the propagation conditions of a large number of links combinations among 24 spatially distributed positions are measured using only six redeployments of the twelve testbed nodes. The Paper also showed that a large set of chan-

nel measurement samples is essential to understand the overall propagation conditions of the given environment.

# References

[1] S. Cho, S. Chae, M. Rim and C. G. Kang, "System level simulation for 5G cellular communication systems," 2017 Ninth International Conference on Ubiquitous and Future Networks (ICUFN), Milan, 2017, pp. 296-299.

[2] W. H. Fan, L. Yu, Z. Wang and F. Xue, "The effect of wall reflection on indoor wireless location based on RSSI," 2014 IEEE International Conference on Robotics and Biomimetics (ROBIO 2014), Bali, 2014, pp. 1380-1384.

[3] M. Hassan-Ali and K. Pahlavan, "A new statistical model for site-specific indoor radio propagation prediction based on geometric optics and geometric probability," in IEEE Transactions on Wireless Communications, vol. 1, no. 1, pp. 112-124, Jan 2002.

[4] N. Chiurtu, B. Rimoldi and E. Telatar, "On the capacity of multi-antenna Gaussian channels," Proceedings. 2001 IEEE International Symposium on Information Theory (IEEE Cat. No.01CH37252), Washington, DC, 2001.

References

# Paper A

## An Agile Multi-Node Multi-Antenna Wireless Channel Sounding System

Dereje Assefa Wassie, Ignacio Rodriguez, Gilberto Berardinelli,
Fernando M. L. Tavares, Troels B. Sørensen, Thomas L. Hansen
, Preben Mogensen

# Abstract

*The upcoming $5^{th}$ generation (5G) wireless technology application areas bring new communication performance requirements, mainly in terms of reliability and latency, but also in terms of radio planning, where further detailed characterization of the wireless channel is needed. To address these demands, we developed an agile multi-node multi-antenna wireless channel sounding system, using multiple software defined radio (SDR) devices. The system consists of 12 testbed nodes which are controlled from a centralized testbed server. Each node features a control host computer and 2 multi-antenna universal software radio peripheral (USRP) boards. By managing the transmission and reception of reference signals among all the distributed testbed nodes, the system can measure the channel conditions of all multiple independent radio links. At the same time, the distributed architecture of the testbed allows a large number of spatially distributed locations to be covered with only a few redeployments of the testbed nodes. As a consequence of this, the system favors the collection of a large number of distributed channel samples with limited effort within a short dedicated measurement time. In this paper, we detail the general testbed design considerations, along with the specific sounding signal processing implementations. As further support to the system design, we also include the results from different verification and calibration tests, as well as a real measurement application example.*

# 1  Introduction

In the last three decades, wireless communication systems have evolved from the $1^{st}$ generation to the $4^{th}$ generation, with the primary aim of improving user cellular broadband services. The upcoming $5^{th}$ generation (5G) systems are expected also to enhance the wireless connection capabilities towards connecting things. Wireless connected things in the context of 5G are envisioned to be employed in new application areas, e.g., smart factories, smart grids, and health-care, as prominent examples. Apart from new communication requirements in terms of latency and reliability, these new areas entail new and unconventional deployment scenarios [1]. These scenarios, including, for example, deployments in deep underground, inside factory clutter, at low antenna height or at different frequency bands, may be quite different from the typical urban/rural outdoor and indoor cases [2]. As a result, different propagation conditions may apply, which brings the need for further detailed characterization of the wireless channel. For example, with 5G applied to automation in the factories of the future (Industry 4.0) [3, 4], a process controller may need to communicate simultaneously, and wirelessly with sensors and actuators, which are deployed in different locations, in a very robust and reliable manner. Therefore, not only the outage due to channel fading on the

single link becomes of interest, but, also the outage of the composite channel considering multiple simultaneous links.

Known sounding approaches for characterizing the radio channel distortion (i.e., channel fading) [5] include direct radio-frequency pulse excitation, transmission of multi-tone reference signals, frequency sweeping, or transmission of a spread spectrum waveform with a sliding correlator at the receiver. The implementations of such systems have typically been built using specialized and/or very expensive equipment (e.g., spectrum analyzer, wideband signal generator, vector network analyzer, etc.) [6–9]. As an alternative, there have been other more cost-effective and flexible implementations which are based on the software defined radio (SDR) concept. With SDR, the baseband signal processing of the radio frequency (RF) signals is handled by software, rather than using specialized hardware. This offers a high degree of flexibility, and the prominent benefit of ease of reconfigurability and rapid prototyping. On the downside, compared to the specialized systems, SDR systems are limited, among other aspects, in frequency range, transmission bandwidth, and receiver dynamic range.

A large number of channel sounding systems have been reported in the literature [10]. By design, each of the systems considers a very specific implementation and frequency range of operation. Table A.1 presents a list of some SDR-based channel sounder systems presented in the recent literature [11–18]. The focus here is on channel sounder systems operating at frequency below 6 GHz, since this is the spectrum range of interest for our design. The considered designs are built on universal software radio peripheral (USRP) platforms [19]. For comparison, Table A.1 includes sounding method, carrier frequency, transmitter (TX) - receiver (RX) synchronization method, and main specific measurement features. As it is described in the table, most of the designs support limited frequency ranges and low transmission bandwidth. Also, they are built with a relatively low number of transmitter and receiver nodes, if not only one of each. This limits, practically, the ability to characterize a large number of links, as required for proper statistical outage characterization, due to the needed number of laborsome redeployments. Similarly, the limited number of nodes also restricts the ability to characterize the composite radio channel, considering multiple simultaneous links, due to the inevitable change from redeploying nodes.

The design goal of the testbed presented in this paper is to overcome some of these limitations, by applying a distributed multi-node multi-antenna approach. The testbed consists of 12 testbed transceiver nodes equipped with 4 antennas, and uses a multi-tone channel sounding method to measure, all the 2112 independent radio links between the nodes, within a single measurement snapshot. The radio channel sounder is developed using the NI LabVIEW communications system design suite [20], and NI USRP-R2953 boards [21], supporting a wide range of carrier frequencies, spanning from

**Table A.1:** SDR USRP-based channel sounding systems for below 6 GHz.

| Reference | Sounding Method | Software Platform | Carrier Frequency | Clock Synchronization | Main Specific Features |
|---|---|---|---|---|---|
| [11] | spread-spectrum sliding correlation | GNU Radio | 2.4-2.5 GHz 4.9-5.9 GHz | via RF cable | 4 MHz RF bandwidth, single TX and RX, covers short distances. |
| [12] | multi-tone, reference signal-based | GNU Radio | 2.4 GHz | not specified | RX estimates channel impulse response of a packet transmitted from a IEEE 802.11b access point with a time resolution of 125 ns. |
| [13] | frequency sweep | LabVIEW | not specified | via HW reference time | 20 MHz RF bandwidth, single TX and RX. |
| [14] | sliding correlation & multi-tone | GNU Radio | 1 MHz-6 GHz | via GPS | 8-20 MHz RF bandwidth, 6 TXs and single RX. |
| [15] | multi-tone, OFDM-based | not specified | 5.9 GHz | via GPS-disciplined rubidium clocks | Single TX and RX, support of up to 4x4 MIMO with 15 MHz RF bandwidth. |
| [16] | multi-tone, reference signal-based | GNU Radio | 2.4-2.5 GHz | not specified | 2 MHz RF bandwidth, estimation based on IEEE 802.11a waveform. |
| [17] | multi-tone, OFDM-based | not specified | 1.2-6 GHz | not specified | Built from 2 X310 USRPs which support 20-100 MHz RF bandwidth. |
| [18] | correlation-based | LabVIEW & GNU Radio | 5.8 GHz | not specified | 2 nodes, measures fast channel variations with the support of 93 MHz RF bandwidth. |

31

1.2 to 6 GHz, with up to 40 MHz of RF channel bandwidth.

As compared to the existing systems, the multi-node and multi-antenna sounder system presented in this paper has a distinctive feature towards measuring multiple channel links, thus generating not only more samples, but also a consistent set of samples for statistical channel characterization. Also, by virtue of the employed SDR devices, the system supports larger frequency spans and transmission bandwidth as compared to most of the existing systems. However, achieving accurate channel measurement across multiple links using the SDR devices presents several challenges. First, typically, SDR devices have somewhat limited specifications in relation to the requirements for channel sounding, particularly concerning phase noise, long-term stability, and dynamic range. Second, the presence of multiple nodes arises challenges toward managing and automating the system. Therefore, this paper introduces the overall system design as well as the specific implementation parameters, which have been carefully selected to overcome these challenges. It should be noted that, in any case, the overall design principles of the sounder are extensible to other specific implementations based on devices with different capabilities. Further, this paper shows how statistical radio channel characterization can be enhanced when using the multi-node sounding system in conjunction with appropriate measurement procedures.

The paper organized as follows. In Section II, we describe the architecture and design of the wireless channel sounding system. In Section III, we detail the reasoning behind the selection of each of the specific implementation parameters. Section IV presents the results from the verification and calibration tests. In Section V, we illustrate the advantages of using our multi-node setup in actual field tests. Finally, the conclusions and future work are presented in Section VI.

## 2 System Design

The conceived distributed sounding system is comprised of multiple cost-effective testbed nodes, each of them built from two SDR boards connected to a host computer through high-speed PCI Express (PCIe) interface, as illustrated in Figure A.1. Each board consists of two full-duplex transmitter and receiver channels. Within each node, the board clocks are synchronized in a master/slave configuration by using the 10 MHz clock signal provided by the master, ensuring synchronous transmission or reception, over the 4 radio frequency transceiver antenna ports. Our primary aim is to design a system which can measure the composite channel of multiple links among different nodes deployed at different locations, capturing the overall radio propagation effect of a given environment within the coherence time of the channel. Achieving such a system design has some associated challenges, mainly re-

lated to managing the multiple testbed nodes for having a consistent set of channel measurements, and to coping with the limitations of SDR devices to ensure an accurate channel estimation.
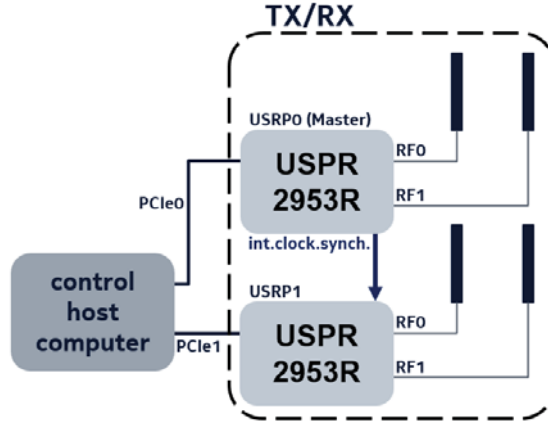


**Fig. A.1:** Testbed node architecture with 1 control host computer and 2 synchronized SDR transceiver boards (4 fully-synchronous RF ports in total).

One of the primary challenges using multiple testbed nodes is how to automatize the system in order to minimize the effort of controlling the testbed nodes and set the different operational parameters. To that end, we employ the general control system architecture presented in Figure A.2, where each of the individual testbed nodes is connected to the main control testbed server by means of a local Ethernet network. The connection is based on TCP/IP sockets to make sure that the testbed server controls multiple testbed nodes with high reliability. In order to measure the composite radio channel, we propose a time division multiplexing (TDM) scheme where one testbed node transmits at a time, in order to discriminate the channel measurements of different links. During the channel measurement operation, the testbed server assigns a single testbed node to transmit the sounding reference signals (e.g., pilot signals which are known to both transmitter and receiver) in a specific time interval, whereas the other nodes are receiving and demodulating the reference signals for estimating the radio channel response. This procedure is repeated in a time-interleaved fashion until each node has transmitted the reference signals, and the channel response between all possible combinations of the testbed nodes are measured.

The testbed nodes are required to be time-synchronized to control the proposed TDM operation, and ensure consistent channel measurements among multiple testbed nodes. This is achieved by pre-synchronizing all testbed nodes at the beginning of each run by employing a proprietary Network Time System (NTS) protocol [22]. NTS is a robust, virtually fail-safe, client/server
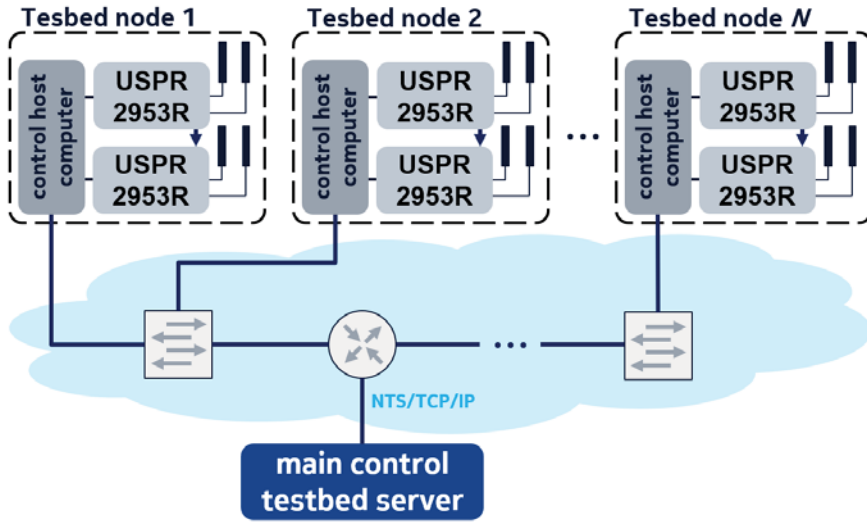
**Fig. A.2:** Ethernet-based general control system architecture.

software, operating as background service and ensuring that the testbed node clock is aligned with the clock of the main control testbed server. By using such protocol, a very tight and stable time-alignment in the order of 1-2 ms is achieved over Ethernet. This constitutes an increased level of accuracy as compared to standard Network Time Protocol (NTP) which typically delivers synchronizations in the order of tens of milliseconds [23].
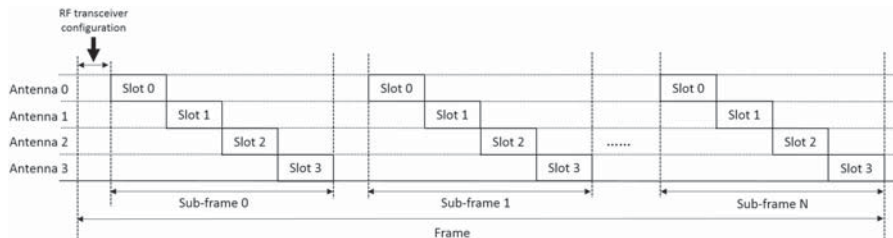


**Fig. A.3:** TDM frame structure considering $N$ sub-frames (with 4 time slots each) and their corresponding re-synchronization/re-configuration periods.

Once the general multi-node TDM control scheme is in place, the next challenge is the management of the multi-link measurement (e.g., 4x4 channel links) between each pair of testbed nodes. Two different schemes were considered for managing the transmission of the reference signals over the 4 antenna ports at each testbed node: TDM, or frequency-division multiplexing (FDM). In the TDM approach, the reference signal is transmitted in a time-interleaved fashion over multiple antenna ports [24]. By contrast, in

the FDM approach, the antenna ports map the reference signal over orthogonal frequency interleaved patterns which span the entire available bandwidth [25]. The FDM approach has an advantage in decreasing the time duration of the reference signal transmission per testbed node, compared to the TDM approach. However, for a fixed bandwidth used for the reference signals transmission, the FDM approach decreases the maximum resolution of the channel response estimation in the frequency domain, which will further decrease the maximum channel delay that can be estimated. Therefore, the design solution presented in this paper, is to use the TDM approach for managing the transmission of the reference signals over the multiple antenna ports.

The overall time frame structure of the channel sounder system, resulting from applying the TDM scheme for multi-node and multi-antenna transmission management, is shown in Figure A.3. A frame accounts for the time duration required for the transmission and acquisition of the reference signals between all possible combinations among the testbed nodes, including the time required for configuring the RF transceiver channels of the testbed nodes. A frame consists of $N$ sub-frames, where $N$ equals to the number of testbed nodes in the system. During one sub-frame duration, only one testbed node is transmitting the reference signals, while all others are receiving them. At the same time, each sub-frame is divided into 4 time slots, accommodating the TDM transmission of the reference signals over the four antenna ports of an individual testbed node.

Note that the millisecond accuracy achievable with the aforementioned NTS solution sets restrictions on the time slot duration, which should be sufficiently long to ensure a synchronization time margin for correct measurements. An extended time slot duration translates to an extended frame duration. Since a proper characterization of the composite channel subsumes such channel to remain static within a frame, the applicability of the channel sounder may be restricted to static environments, or to environments whose coherence time is estimated to be significantly larger than the frame duration. These facts will be further discussed in the following section.

The combination of NTS protocol and control over Ethernet to provide the baseline synchronization to the TDM testbed measurement operation scheme was carefully selected. Other control alternatives were explored during the design phase, but their performance was proven to be significantly worse. For example, keeping the local area architecture and using a dedicated WiFi network instead of Ethernet links, the synchronization accuracy dropped to approximately 20 ms on average, reaching even 100 ms in some of the tests. Another alternative would have been to distribute a locally generated high precision clock reference synchronization signal among all the nodes. This solution may reach accuracies at sub-millisecond level and therefore enable the possibility of characterizing composite channels with limited coherence

time. However, in a cost-effective distributed measurement system, as the one presented in this paper, its implementation would be rather complex and expensive if built over rubidium clocks or optical cables; or quite limited in measurement distance range if built over RF clock distribution cables [10, 26]. GPS-based synchronization was not an option either. The testbed is designed for reliable indoor use in deployment scenarios associated to some of the new 5G application areas, e.g., in deep indoor clutter conditions within factories, where GPS signals are, in general, not available. By using an Ethernet cabled control network instead, we achieve a good trade-off between synchronization accuracy and measurement distance range, as we are able to span our distributed measurement system over several hundreds of meters by deploying a small switch-based network [27].

We have, until now, discussed the design solutions regarding the challenge of coordinating multiple testbed nodes with the aim of collecting consistent channel measurement samples using SDR devices. However, the SDR devices present some limitations regarding long-term clock stability, phase noise, and receiver dynamic range, which may distort the channel measurements if they are not properly addressed. In order to cope with such limitations, all testbed nodes are re-synchronized during the RF transceiver configuration (cf. Figure A.3) before a new node begins its transmission to cope with the long-term clock instability. Further, we propose to transmit a large number of repeated similar reference signals in each time slot, to increase the receiver dynamic range by coherently averaging received reference signals. To cope with the phase noise, we consider sufficient sub-carrier spacing in our multi-tone sounding reference signal. All these design aspects will be discussed in detail in the coming section.
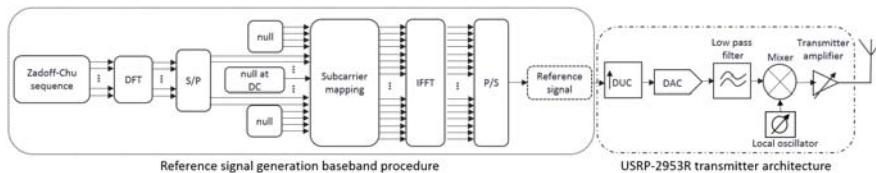


**Fig. A.4:** Transmitter chain for reference signal generation.

We would like to highlight that, by using the proposed distributed architecture and frame design, the testbed could be easily upgraded to include real data transmissions among the nodes by replacing the sounding reference signals with any other customized signal carrying data. Also, the system allows for live demonstration of network algorithms for e.g. interference coordination, which are based on instantaneous mapping of the real-world measurements to relevant key-performance indicators (KPIs). Similarly, it enables the usage of hybrid simulations, where the obtained measurements

can replace standard channel models used for system-level analysis [28, 29]. We see these two aspects as positive design-enabled benefits that also make a difference with respect to the systems reviewed in the previous section.

# 3   System Implementation

In this section, we discuss the applied signal processing procedures at both transmitter and receiver side for accurate estimation of the channel response using the SDR platforms. Besides, the section illustrates the implementation-specific aspects, including the system parameter numerology selected as a reference for our multi-node multi-antenna sounding setup.

## 3.1   Reference signal generation

The reference signals used for channel estimation are built by mapping Zadoff-Chu (ZC) sequences  [30] over Orthogonal Frequency Division Multiplexing (OFDM) symbols. ZC sequences are selected thanks to their property of having constant amplitude over the dual time/frequency domain.  A constant time domain amplitude allows using a limited power back-off at the transmitter for counteracting signal distortions due to e.g.  digital clipping and non-linear power amplifier response, translating to a higher transmit power. A flat frequency domain response translates to zero autocorrelation, which improves channel estimation and time synchronization.  ZC sequences are also used by many radio standards, including the uplink of 3GPP long-term evolution (LTE) [31].

The block diagram of the reference signal transmission is shown in Figure A.4.  A ZC sequence is converted to frequency domain via Discrete Fourier Transform (DFT), and the resultant vector is mapped over the set of subcarriers which represents the transmission bandwidth. Zeros are padded over the edges of the bandwidth to limit the out-of-band spectral interference. Also, the direct current (DC) subcarrier is nulled for circumventing the DC signal leakage.  The baseband time domain signal is finally generated via Inverse Fast Fourier Transform (IFFT). Such transmitter architecture allows preserving the flat frequency response of the original ZC sequence in the bandwidth of interest.  The time domain amplitude of the signal may still have minor fluctuations, which appears due to the mismatch between ZC sequence length and IFFT size. This will be further discussed in the next section.

The generated baseband reference signal is then streamed to the RF board via the PCIe connector. The board up-samples the digital signal and converts it to an analog RF signal for transmission over the antenna. Four antennas are employed in each testbed node, and the transmission of the reference signals

over each antenna is performed in a time-interleaved fashion as discussed in the above. In order to discriminate the different antenna links for channel estimation, two reference sequences are employed, where one of the sequences is mapped to the first antenna port (first time slot in the sub-frame), and the other sequence is mapped to the other three antenna ports (second, third and fourth time slots). Then, at the receiver side, the signal transmitted over the first antenna port is identified via cross-correlation using the first reference sequence, whereas the other slots are identified based on the predefined TDM sub-frame structure. The use of a difference sequence for the first, resolves any ambiguities with respect to the antenna transmitted sequence.

One reference signal is transmitted over an OFDM symbol, and repeated a large number of times to fit a predefined time slot duration. Such redundancy offers a margin for the time synchronization between transmitter and receiver nodes. Transmitting repeated identical symbols per time slot allows the receiver processing to benefit from signal cyclicity. As explained later, this also provides a prominent advantage for estimating the frequency offset at the receiver side, by observing the phase shift of consecutive repeated OFDM symbols. Also, we can benefit from the transmission of consecutive repeated OFDM symbols to increase the receiver dynamic range of the SDR platform, by exploiting coherent averaging [32] over an assumed static channel.
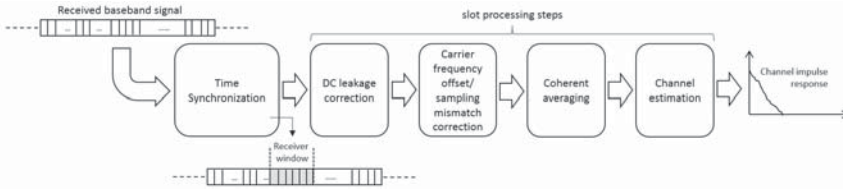


**Fig. A.5:** Baseband processing operations at receiver side.

## 3.2 Receiver processing

The aforementioned lack of a tight synchronization may rise challenges concerning frequency instability and residual time misalignment between the transmitter and receiver boards. To address these challenges, and ensure accurate channel estimation using SDR devices, the receiver digital signal processing shown in Figure A.5 is employed.

At the receiver end, the node receives the RF signal on each antenna ports and down-converts it to a complex digital baseband signal (I/Q signals) using the SDR RF boards. The I/Q signals are streamed to the host PC, where the digital baseband signal processing is carried out. First, the time synchronization is performed using cross-correlation between the received signal and a copy of the transmitted reference signal, to find the position of the first use-

ful sample of the received signal. Then, DC leakage cancellation, correction
of the carrier frequency offset and sampling clock mismatch are performed
in each time slot. Afterward, a coherent averaging can eventually be car-
ried out to increase the receiver dynamic range, before channel estimation is
performed. Such steps are described in more detail below.

**Time synchronization**
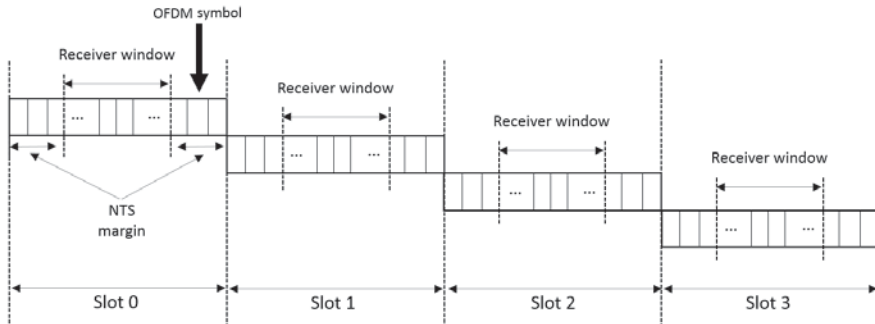


**Fig. A.6:** Sub-frame structure with possible receiver window position.

The NTS protocol enables a first synchronization among the nodes with
accuracy in the order of a millisecond, as described in the previous section.
While this may suffice for aligning the nodes at level of a slot interval, fur-
ther refinements are needed to identify the antenna port mapped over that
slot, and to enable a proper time alignment at OFDM symbol level for correct
channel estimation. Cross-correlation between the received sequence and the
transmitted one is therefore performed. A first cross-correlation operation
is applied for identifying the first slot in a sub-frame. This computation is
carried out using the first reference sequence, which was mapped to the first
antenna port/time slot. As a result, the first antenna port is identified and
OFDM-level symbol alignment for channel estimation is also achieved. To
accommodate an error margin of the NTS time synchronization, the receiver
window spans only a subset of the repeated OFDM symbols within the time
slot, as shown in Figure A.6. The receiver window for the following slots is
identified by using the known TDM time frame structure, given the periodic-
ity of the system. The size of the receiver window is dimensioned according
to the time slot duration, the symbol duration, and the error margin of the
NTS time synchronization protocol.

**DC leakage**

To reduce device cost and the power consumption, SDR receivers are com-
monly based on a direct-conversion, or zero intermediate frequency, archi-

tecture, where the received radio frequency signal is converted directly to baseband. Such receiver suffers from the "direct current", caused by the local oscillator leakage. To reduce its impact, we implemented a basic DC leakage cancellation using a notch filter in the frequency domain. Note that the DC subcarrier was blanked at the transmitter.

**Carrier frequency offset**

Since transmitter and receiver are not sharing the same oscillator, carrier frequency offset may affect the performance of the sounding system. To deal with the carrier frequency offset, we employ the maximum likelihood estimation (MLE) scheme proposed in [33]. The scheme estimates the frequency offset by observing the phase shift of the subcarriers between consecutive repeated OFDM symbols, and use the estimated values to counter-rotate the subcarrier phase accordingly.

**Sampling clock mismatch drift**

Besides the carrier frequency offset, the lack of a common reference clock at the transmitter and receiver induces a sampling frequency mismatch. That leads to a drift in the time synchronization between the consecutively transmitted OFDM symbols. To overcome this, a cross-correlation in the time domain is applied to estimate the timing offset of each received symbol, in relation to an arbitrary chosen received reference symbol. Assuming that the drift within a symbol is small, the offset/drift is corrected on a per symbol basis, by correspondingly counter-rotating the sub-carrier phases in the frequency domain [34].

**Coherent averaging**

Typically, the SDR device receiver dynamic range is limited (i.e., the employed SDR platform receiver dynamic range is ideally 86 dB, considering a 14 bit resolution of the ADC [21]). This may represent a limitation for the sounding system capability in measuring large path losses. To increase the receiver dynamic range, we employ coherent averaging of several consecutive received symbols, assuming that frequency offset and sampling clock mismatch have been properly corrected, and the channel is static during the receiver window. This allows reducing the noise power while maintaining constant the useful signal power. For instance, with 1000 consecutive symbols being averaged, the sounding system dynamic range can be increased up to 30 dB, due to the resulting processing gain of the coherent averaging [32]. Note that such gain in terms of dynamic range can not be achieved in case the scenario is dynamic within the receiver window. The stationarity prop-

erties of the channel therefore affect the size of the receiver window used for coherent averaging.

**Channel estimation**

The channel frequency response is estimated using a least square estimator, over the sub-carrier positions, where the ZC sequence is mapped. The frequency response of the DC sub-carrier is computed by interpolating the response of the neighboring sub-carriers. The channel impulse response can in principle be computed using an IDFT operation, on the estimated channel frequency response. However, this operation leads to low resolution and side lobe leakage effects, that are exacerbated by the relatively low bandwidth of the testbed. To overcome these limitations, we apply parametric channel modeling [35], which works by fitting a sum-of-spikes representation of the channel impulse response to the observed signal. The superfast line spectral estimation (SF-LSE) algorithm [36] is used for estimating the parameters (model order, delays, and coefficients) of the parametric channel model. This type of method is known as a super-resolution approach, because it allows the multipath components to be estimated with a higher delay resolution, than the reciprocal of the bandwidth, as is approximately the case when using the IDFT. The parametric approach also avoids the presence of sidelobes as in the case of IDFT operation.

## 3.3 System Configuration and System Parameters

The main parameters of the sounding system are summarized in Table A.2, where we highlight both the general configuration parameters and the reference numerology which has been used in the activities described in Sections 4 and 5.

The implemented sounding system consists of 12 SDR testbed nodes, each of them with the physical configuration displayed in Figure F.3. The specific trolley-based implementation, complemented by an uninterruptible power supply (UPS), facilitates a quick and easy redeployment of the nodes during the measurement. The antenna configuration per testbed node of 2 antennas at two different heights (0.25 and 1.75 m) is chosen with the target of using the system for characterizing the channel at different spatial positions (e.g, different heights) at given physical locations. Carrier frequency-wise, the main goal of our activities was the evaluation of radio propagation at two ISM bands (e.g, 2.45 and 5.8 GHz). Therefore, for this reference implementation of the testbed, the carrier frequencies configured were 2.3 and 5.7 GHz, as they were the closest frequency allocations possible ensuring interference avoidance with/from other coexisting radio systems. Moreover, the spacing between antennas is dimensioned to be larger than half of a wavelength at

**Table A.2:** Reference configuration of the multi-node multi-antenna channel sounder.

| Parameter | General Design | Reference Configuration |
|---|---|---|
| Number of testbed nodes | N | 12 |
| Antenna configuration per node | 4x4 MIMO, fully flexible | 2x2 MIMO @ 2 antenna heights |
| Carrier frequencies | 1.2–6 GHz | 2.3 GHz / 5.7 GHz |
| Sounding signal | multi-tone | OFDM |
| Reference sequence | flexible | Zadoff-Chu (ZC) |
| Sampling rate | flexible, max. 40 MS/s | 40 MS/s |
| Sub-carrier spacing | flexible | 39.06 kHz |
| Length of the reference sequence | flexible | 601 |
| FFT size | depends on sampling rate and reference sequence size | 1024 |
| Symbol duration | depends on sub-carrier spacing | 25.6 $\mu$s |
| Signal bandwidth | depends on reference sequence length and sub-carrier spacing, max. 40 MHz | 24 MHz |
| Temporal resolution | depends on signal bandwidth | 41.66 ns (* improved by SF-LSE) |
| Slot duration | depends on symbol duration and number of symbols transmitted | 25.6 ms (1000 symbols) |
| Receiver dynamic range | 86 dB (14 bit resolution) | 115.5 dB (900 symbols) |
| Receiver window reference level | flexible, max. 0 dBm, min. –25 dBm | –25 dBm |
| Transmit power per branch | flexible, depends on carrier frequency, max. +10 dBm | +6.4 dBm @ 2.3 GHz<br>+5.2 dBm @ 5.7 GHz |
| Antenna type | flexible | Vertical dipoles, 2 dBi peak gain<br>1.28 dBi effective gain @ 2.3 GHz<br>0.39 dBi effective gain @ 5.7 GHz |
| Cable type | flexible | 1 m long RF flex coaxial cables<br>2.4 dB @ 2.3 GHz<br>3.3 dB @ 5.7 GHz |
| Maximum measurable path loss | depends on transmit power, receiver window reference level, receiver dynamic range, antenna type and cable type | 134.7 dB @ 2.3 GHz<br>129.9 dB @ 5.7 GHz |
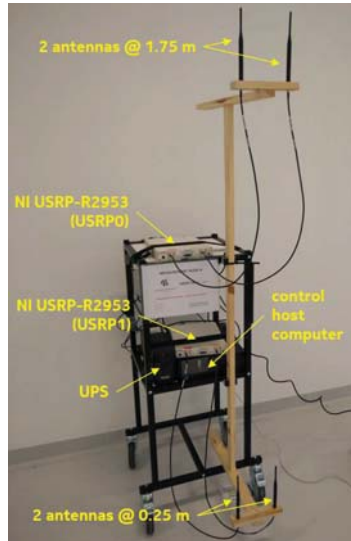
**Fig. A.7:** Testbed node physical setup. Trolley-based implementation considering a distributed antenna configuration with 2 antennas at two different heights (0.25 and 1.75 m).

the lower frequency (6.52 cm), aiming to de-correlate the set of measurement samples from each antenna at both frequencies of operation.

As per the general system design considerations given in Section 2, the number of sub-frames in the TDM frame structure (cf. Figure A.3) is set equal to the number of testbed nodes available for measurement. Every testbed node is assigned a single transmission sub-frame, which allows for the broadcast of the reference signals over its 4 antenna ports in 4 consecutive time slots. Simultaneously, the other 11 sub-frames are used for reception. Before the testbed nodes are allocated a sub-frame for transmission or reception, the configuration of the RF transceivers channel is carried out, and also re-synchronization of the testbed nodes clock to keep the clock timing stability of the system. These operations are performed within a 10 ms interval. Considering a predefined time slot duration of 25.6 ms, the sub-frame duration is set to be 4x25.6 ms = 102.4 ms. Overall, the transmission and reception of the reference signals among all 12 testbed nodes are performed over one full frame duration of approximately 1.35 s. Such frame execution will be carried out per single deployment of the tested nodes, enabling the collection of 12x11x4x4 = 2112 independent link samples. Thus, considering a number of re-deployments, a large number of spatially distributed channel measurement links can be effectively collected within a short period of time.

The specific sounding implementation employs ZC reference sequences mapped over OFDM symbols. In this case, the reference sequence length is chosen to be 601 samples, which are mapped over the center of the band-

width. We consider a FFT size of 1024 and we set a 40 MHz sampling rate, leading to a 39.06 kHz sub-carrier spacing. The resulting baseband signal was shown to have minor envelope fluctuations, not larger than 2 dB. The signal presents an overall bandwidth of 24 MHz, which translates into a time resolution of 1/24 MHz = 41.66 ns. However, in practice, this resolution can be improved by means of SF-LSE, as detailed in Subsection 3.2. The sub-carrier spacing is sufficiently large for coping with the phase noise of the employed SDR devices. Given the 1/39.06 kHz ≈ 25.6 $\mu$s symbol duration, 1000 symbols can be mapped over the 25.6 ms slot. This large number of symbols allows us to increase the dynamic range of the receiver by 29.5 dB, considering 900 effective symbols per receiver window (cf. Figure A.6) are used for coherent averaging, and the remaining received symbols are used as error margin (1.25 ms) for counteracting the possible NTS time synchronization misalignment. By configuring the reference level of the receiver window (which fixes the RX gain to a proportional value to the specific expected signal input level) to its minimum value of -25 dBm, and applying coherent averaging, we are able to increase the sensitivity of the measurement system from -111 dBm to -140.5 dBm. The output TX power is set to +6.4 dBm at 2.3 GHz and +5.2 dBm at 5.7 GHz. It was verified that these levels avoid the appearance of non-linear distortion effects, thanks to the limited envelope fluctuations of the signal.

To ensure the consistency of different measurement samples across multiple SDR devices, a thorough calibration of the devices is performed during the implementation of the system. Figure A.8 shows the result from a back-to-back test with two RF ports from two different boards. Due to hardware imperfections, the normalized amplitude response exhibits a slight attenuation over the considered measurement bandwidth (24 MHz). Such behavior is observed for the different boards at both considered carrier frequencies, with an average maximum variation of 0.5 dB among all carried tests. To ensure that such variation does not affect the quality of the channel estimation, we performed an extensive individual calibration measurement among all RF ports from all sounder devices, at both frequencies of interest - in both TX and RX mode, and then used the results to compensate for the device-specific variations during the receiver data processing procedures. The results from the calibration test across all SDR devices indicated a similar average TX power and RX gain performance at both frequencies of operation, with a standard deviation of 1.3 and 1.6 dB, respectively.

All other physical elements considered in the implemented setup were also calibrated (cf. Figure F.3). The Wanshih Electronic WSS007 dual-band dipole antennas, with 2 dBi peak gain at both frequency bands according to specifications [37], exhibited a quasi-isotropic mean effective gain of approximately 1.28 dBi at 2.3 GHz and 0.39 dBi at 5.7 GHz in an anechoic chamber calibration measurement. The attenuation introduced by the coaxial cables
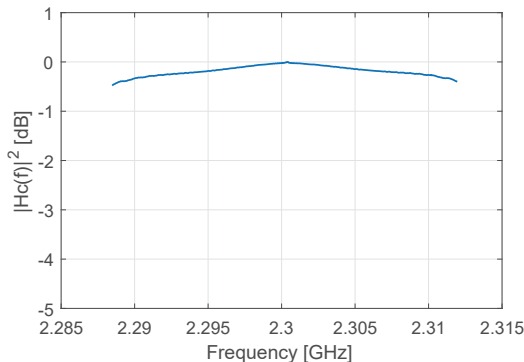
**Fig. A.8:** Normalized frequency amplitude response of two interconnected RF ports from two different USRP boards at 2.3 GHz.

interconnecting the different RF ports to the antennas was also measured, finding values of 2.4 and 3.3 dB at 2.3 and 5.7 GHz, respectively. Altogether, the reference configuration of the testbed implemented allows for maximum link loss measurements of 134.7 dB at 2.3 GHz and 129.9 dB at 5.7 GHz, ensuring sufficient measurement dynamic range to cover TX-RX distances in the range of a few hundred meters, even in dense clutter conditions.

# 4  System Verification

To validate the proposed SDR USRP-based channel sounding procedures and demonstrate the measurement capabilities of the system, we performed different verification tests. These tests had two different aims: 1) to verify the accuracy of the system in terms of channel impulse response estimation; and 2) to verify the accuracy of the system in terms of measured received power to perform path loss estimation. All tests were done with the reference configuration detailed in Section 3 and summarized in Table A.2.

## 4.1  Channel Impulse Response

The objective of the first test is to verify the sounder system capability of estimating resolvable temporal multipath components (taps) accurately. This test has also the aim of confirming the potential of the employed channel estimation approach (i.e., superfast line spectral estimation, SF-LSE), in comparison with the commonly used IDFT-based estimation. The test measurement was conducted by using a standard multi-tap channel emulator, connected between two RF ports of two different boards belonging to different testbed nodes, one acting as the TX and the other as RX.
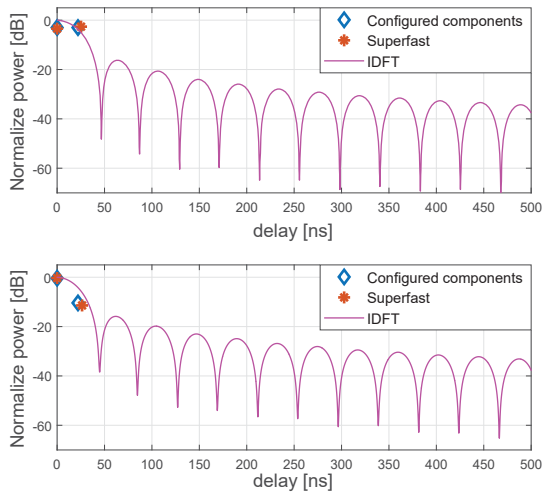
**Fig. A.9:** Results of the channel impulse response verification test with channel emulator configured with two taps with equal amplitude (above), and 10 dB difference in amplitude (below).

We tested two cases. First, the channel emulator was configured to emulate two multipath components with equal power and separated by 22 ns. In the other case, the second multipath component was configured to be 10 dB lower than the first component. Figure A.9 displays the results from the two tests. Both plots illustrate the configured multipath components (blue diamonds), and the estimated components using the standard IDFT operation (magenta lines) and the SF-LSE approach implemented in our system (red stars). In both cases, by using the superfast parametric approach, we can resolve correctly the two multipath components in both delay (with $\pm 5$ ns deviation) and amplitude (with a maximum deviation of 0.97 dB). This result demonstrates the capability of the SF-SLE in resolving taps that are separated by delays below the temporal resolution set by the signal bandwidth (41.66 ns), thus achieving an effective increase of the temporal resolution.

For further verification, we also tested the case where the channel emulator is configured with a reference standard channel model. We selected the ITU-R indoor office channel model (Channel A) [38], with a fixed power delay profile and larger excess delay compared to the previous cases. The 6-tap configuration of the model is as follows: relative delay of 0, 50, 110, 170, 290 and 310 ns, and average power of 0, -3, -10, 18, -26 and -32 dB. The results from this test are presented in Figure **??**. Similarly to the previous case, the figure depicts the original channel model taps and the estimated taps using both the SF-LSE approach and the IDFT operation. In this case,

once again, the IDFT operation is not able to resolve the taps, due to the side lobe leakage. On the contrary, the superfast parametric channel modeling approach can resolve the configured taps with a standard deviation of 5.7 ns in delay and 0.5 dB in amplitude. Still, one can notice the presence of an extra component at around 220 ns delay, that also corresponds to a sidelobe of the IDFT estimation. This is a processing artifact limitation of the SF-LSE algorithm in estimating low energy components with high accuracy. However, given the low energy of the artificial component, the impact of such inaccuracies on the channel estimation quality is minimal. This ratifies the capability of the sounder of accurately estimating the channel impulse response, and supporting even super-resolution techniques.
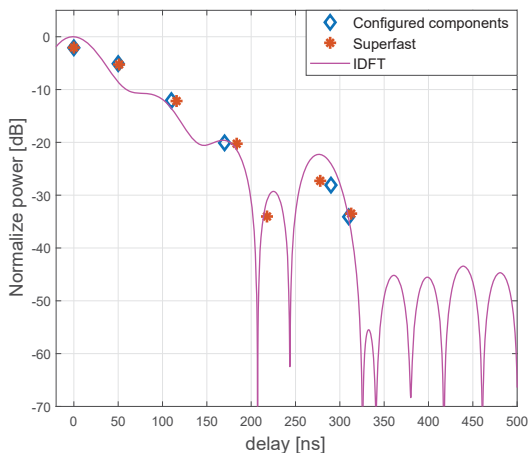


**Fig. A.10:** Results of the channel impulse response verification test with channel emulator configured with the 6-tap ITU-R indoor office channel model (Channel A).

## 4.2 Received Power and Path Loss

The second test aims at verifying the accuracy of the sounding system in performing power measurements and path loss estimation. In order to test that, we performed a line-of-sight (LOS) over-the-air measurement in a large open space where free space conditions apply. The measurement was performed by deploying one of the testbed nodes at a fixed location, and second one at a variant distance (2.5, 5, 7.5, 10.0, 12.5, 15 and 20 m).

Figure A.11 shows the power measurement test results in terms of path loss (PL) as a function of the distance between nodes for both configured carrier frequencies (2.3 and 5.7 GHz), considering the two different antenna heights configurations (0.25 and 1.75 m) applied at both transmitter and re-
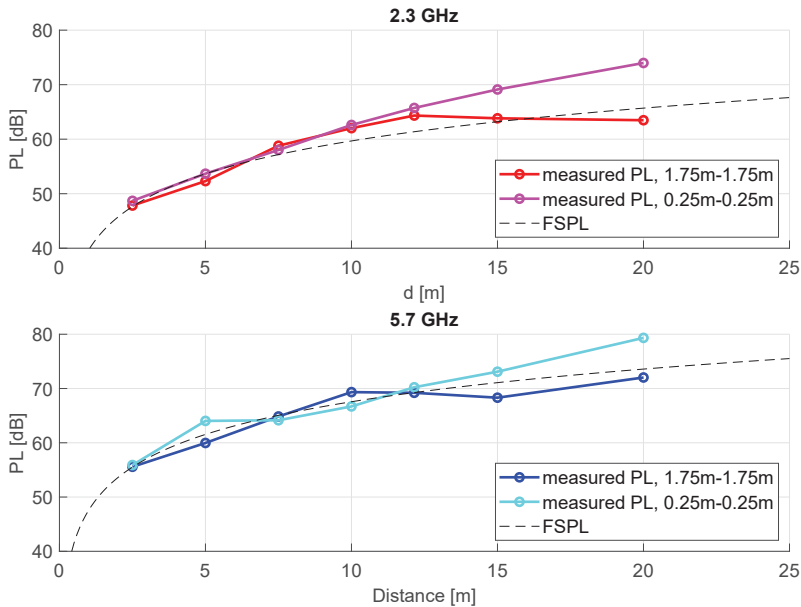
**Fig. A.11:** Results of the path loss verification test in line-of-sight free space conditions for two antenna height configurations (higher link at 1.75 m, and lower link at 0.25 m) at both configured testbed carrier frequencies (2.3 and 5.7 GHz).

ceiver nodes. Each of the PL values was estimated by integrating the received power over the operational bandwidth, and averaging the results from all the individual 8 links at a given position (e.g., to average fast-fading effects by taking into account all possible links between the two nodes at each particular height). Each of the individual link measurements is independently calibrated in the receiver data processing stage, accounting for any device-specific deviations, as it was explained previously in Section 3.3 (i.e., subtracting the average measured RX power from the calibrated RF port-specific TX power, and compensating by the also calibrated RF port-specific RX gain imperfections, effective antenna gains and cable losses at the particular frequency of operation). The results indicate that the measured PL follows the free space path loss (FSPL) reference [39], with standard deviations of 0.79 and 0.82 dB for 2.3 and 5.7 GHz, respectively, for the case where the antennas are mounted at a 1.75 m height. In the case of the lower antenna configuration (antennas mounted at 0.25 m), a similar behavior is observed for the short distances, while for distances larger than the theoretical breakpoints (6 m at 2.3 GHz, and 15 m for 5.7 GHz), an increase in PL is observed due to the effect of the ground reflection.

Overall, these test results are very well aligned with the expected behavior as a function of distance range, carrier frequency, and antenna height. This

endorses the measurement capabilities of our sounder in performing accurate power estimation and therefore an accurate path loss characterization.

# 5 Experimental Results

Until now, we have detailed the different design, implementation and verification aspects of our multi-node multi-antenna channel sounder. In this section, we demonstrate the agility of our system for effectively collecting large data sets of measurement data without the need for an excessive number of laborsome redeployments. By using our proposed measurement system in a given scenario, we can simultaneously collect samples at multiple distributed spatial locations, allowing for an accurate statistical characterization of the composite radio channel.

In order to illustrate the above-mentioned, we present the results from a field test performed in an industrial setting. The selected scenario (Smart Production Lab, at the Department of Mechanical and Manufacturing Engineering, Aalborg University) is closely related to those considered in the 5G new application areas described in the introduction (i.e. factory automation). The measurements were performed at 24 selected locations which were approximately uniformly spatial-distributed across the facility, based on a visual inspection and considering potential deployment positions of controllers, sensors, and actuators in such industrial automation scenario. The size of the facility is 20x40x6 m. Such dimensions imply a maximum possible measurement distance of approximately 45 m, which is well within the measurement distance range capabilities of the system. To illustrate the type of factory clutter explored in the measurements, a picture of the scenario and the associated floor plan with the measurement locations are displayed in Figure A.12. Further details about the scenario and the measurement campaign can be found in [40].

To measure all the 24x23 = 552 possible links between these 24 spatial positions using a standard approach (e.g., with a single fixed transmitter and a mobile receiver) requires a large number of redeployments (i.e., more than 200) which translates also into a big effort in terms of overall measurement collection time. By using our multi-node multi-antenna system, with 12 nodes, we were able to reduce the effort to only 6 redeployments, with an approximated total measurement time of approximately 3 h (considering the time spent in the initial deployment, measurement collection at the two considered carrier frequencies and the different redeployments). The initial deployment of the 12 nodes and the Ethernet control network takes approximately 1 h. After the first measurement snapshot, each of the 5 remaining redeployments was carefully planned to minimize the number of changes in node positions needed to sweep all the possible spatial combinations. In each

redeployment, a maximum number of 8 nodes (and their associated Ethernet control cables) was moved, resulting in an average redeployment time of approximately 20 min. It should be highlighted that such fast re-deployment time is partly achieved by the use of the UPS units in each of the nodes; as they allow a smooth transition between measurement points without the need of powering the nodes off and thus, without the need of manually re-booting and re-configuring the USRP boards.
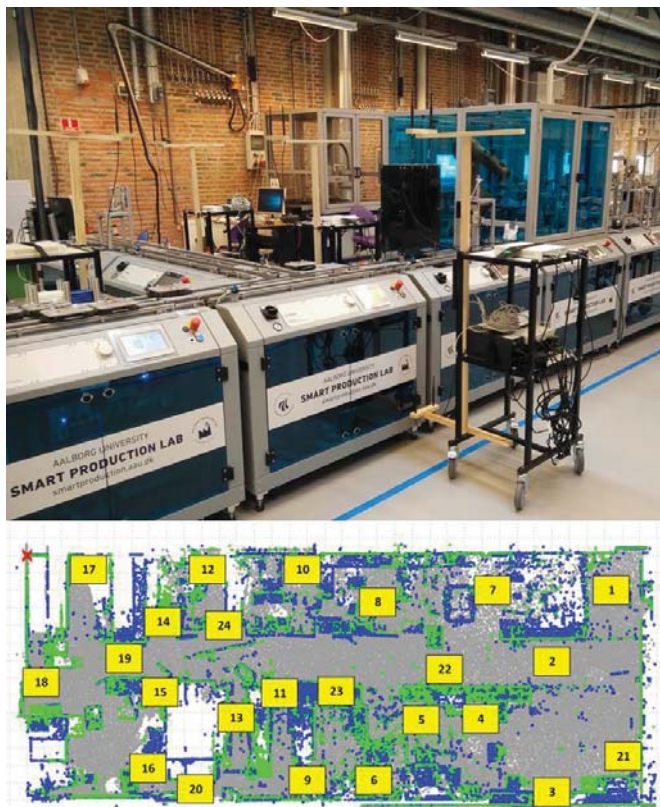


**Fig. A.12:** Overview of the industrial measurement scenario: testbed nodes deployed at some of the measurement positions (above), and measurement positions indicated over a plane-cut of a 3D laser scan of the industrial facility (below).

Considering the 24 measurement locations and the 4 different spatial positions of the antennas at each node, we collected a total number of 24x23x4x4 = 8832 samples. With such large number of independent samples, obtained in a spatially-distributed manner, it is possible to get a deep insight into the overall radio propagation behavior across the industrial scenario, statistically characterizing the channel at levels close to the $10^{-4}$ percentile. Those levels (and lower) are typically the percentiles at which the effects of rare events

are captured in the tails of the channel distributions, and thus it is of great importance to have enough relevant empirical data to characterize them. If radio network planning is done based on channel distributions derived from empirical sets with limited number of samples, there is a risk of being inaccurate, experiencing significant deviations in the radio signal availability and reliability predicted for a given scenario.
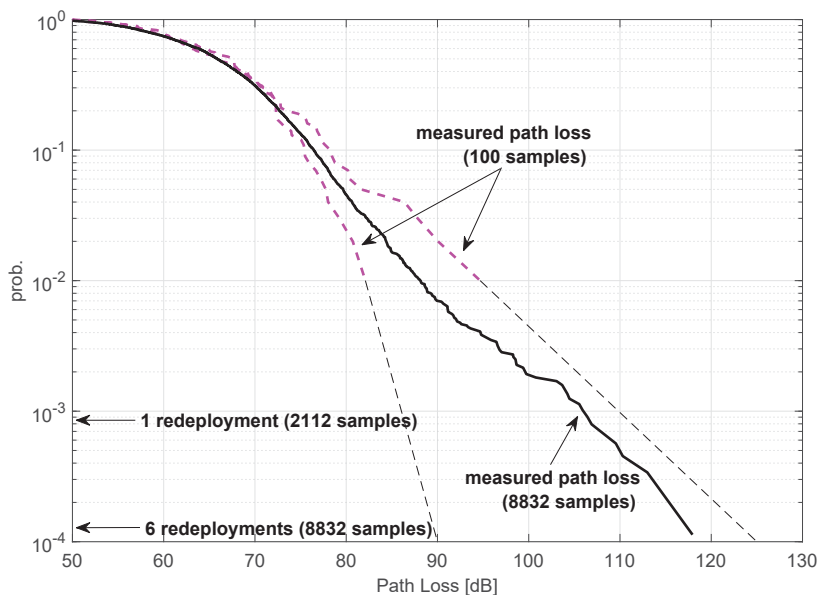


**Fig. A.13:** Empirical complementary cumulative distribution functions of measured path loss in an industrial production lab facility at 2.3 GHz.

In order to illustrate this fact, we display three different empirical channel distributions in terms of 2.3 GHz measured path loss in Figure A.13. The two first distributions (thick dashed magenta lines) are obtained by randomly and independently selecting a low number of samples from our measurement (i.e. 100 samples), while the remaining (thick solid black line) considers the full data set of 8832 samples. We have selected such cases for brevity, to illustrate the extreme cases of the above-discussed. In this case, the distributions based on the low number of samples, result in a $\pm 6$ dB deviation from the distribution extracted from the large measurement data set at the $10^{-2}$ percentile, representative of the 99% of signal availability. Moreover, by extending the tails of the distributions (thin dashed black lines) based on the low number of samples, as is typically done to get an indication of the behavior at lower percentiles [41], it is possible to observe the considerable deviation from the more reliable distribution computed over all samples. In the path loss pessimistic case, at the $10^{-4}$ percentile (99.99% signal availability), the deviation

is still bounded by the previous error (+6 dB). However, in the optimistic case, this deviation can be as much as 30 dB from the "sample truth". Clearly, if radio network planning for the wireless factory (which should be robust and reliable), relied on models, or empirical evidence deviating this much, the integrity of the factory automation would be at risk.

The described activity confirms the unique capability of our multi-node multi-antenna channel sounder in characterizing radio propagation in potentially large and complex scenarios with limited human effort. This paves the way for an agile characterization of relevant scenarios for future 5G systems.

# 6 Conclusions and Future Work

We have presented a distributed multi-node multi-antenna channel sounder based on universal software radio peripheral (USRP) boards. Our flexible design is meant to measure all channel links among all the nodes in the system, generating large sets of measurement samples useful for characterization of radio propagation in a given environment with limited human effort. In particular, the current setup of the sounder consists of 12 nodes with up to 4x4 multiple input multiple output (MIMO) antenna capabilities, and is able to measure up to 2112 independent radio links per deployment in $\sim$1.35 seconds. The major challenges for the design of the channel sounder are related to testbed management, synchronization of the nodes, overcoming non-idealities of the SDR hardware and signal processing design for accurate channel estimation. These have been thoroughly discussed in the paper, along with our proposed solutions. System verification and preliminary experimental results have also been presented.

Our future research activities target the usage of the multi-node multi-antenna channel sounder for an extensive evaluation of radio propagation in diverse scenarios in light of the novel 5G use cases. Also, the possibility of further improving the system performance will be pursued. In particular, synchronization solutions such as Precision Time Protocol (PTP) are to be explored, given their promise of significantly reducing the residual timing errors, translating to significantly shorter frame duration and therefore the possibility of tracking time-varying channels.

# 7 Acknowledgments

# References

[1] 3GPP TS 22.261, "Service Requirements for the 5G System, Stage 1 (Release 16)," v.16.5.0 (2018-09).

[2] 3GPP TR 38.901, "Study on channel model for frequencies from 0.5 to 100 GHz (Release 14)," v.14.3.0 (2017-12).

[3] B. Chen, *et al.*, "Smart Factory of Industry 4.0: Key Technologies, Application Case, and Challenges," *IEEE Access*, vol. 6, pp. 6505-6519, Dec. 2017.

[4] B. Holfeld, *et al.*, "Wireless Communication for Factory Automation: An Opportunity for LTE and 5G Systems," *IEEE Communications Magazine*, vol. 54, no. 6 , pp. 36-43, Jun. 2016.

[5] J. D. Parsons, D. A. Demery and A. M. D. Turkmani, "Sounding techniques for wideband mobile radio channels: a review," *IEE Proceedings I - Communications, Speech and Vision*, vol. 138, no. 5, pp. 437-446, Oct. 1991.

[6] C. Holloway, *et al.*, "Attenuation of radio wave signals coupled into twelve large building structures," National Institute of Standards and Technology (NIST), Technical Note 1545, Aug. 2008.

[7] J. Austin, *et al.*, "A spread spectrum communication channel sounder," *IEEE Transactions on Communications*, vol. 45, no. 7, pp. 840-847, Jul. 1997.

[8] MEDAV, RUSK channel sounder [Online] Available: http://www.channelsounder.de/medavdocs/RUSK-MIMO-Produktinfo-E_W701WI.096_.pdf [Accessed Oct. 2018].

[9] P. Pajusco, N. Malhouroux-Gaffet, and G. El Zein, "Comprehensive Characterization of the Double Directional UWB Residential Indoor Channel," *IEEE Transanctions on Antennas and Propagation*, vol. 63, no. 5, pp. 1129-1139, Mar. 2015.

[10] George R. MacCartney Jr., and Theodore S. Rappaport, "A Flexible Millimeter-Wave Channel Sounder With Absolute Timing," *IEEE Journal on Selected Areas in Communications*, vol. 35, no. 6, pp. 1402-1417, Jun. 2017.

[11] M. Gahadza, M. Kim, and J. Takada, "Implementation of a Channel Sounder using GNU Radio Opensource SDR Platform," *IEICE Technical*, vol. 108, no. 446, pp. 33-37, Mar. 2009.

[12] D. Maas, *et al.*, "Channel Sounding for the Masses: Low Complexity GNU 802.11b Channel Impulse Response Estimation," *IEEE Transactions on Wireless Communications*, vol. 11, no 1, pp. 1-8, Jan. 2012.

[13] A. Merwaday, *et al.*, "USRP-based indoor channel sounding for D2D and multi-hop communications," In Proc. Annual IEEE Wireless and Microwave Technology Conference (WAMICON), pp. 1-6, Jul. 2014.

[14] M. N. Islam, *et al.*, "A wireless channel sounding system for rapid propagation measurements," In Proc. IEEE International Conference on Communications (ICC), pp. 5720-5725, Jun. 2013.

[15] R. Wang, *et al.*, "A real-time MIMO channel sounder for vehicle-to-vehicle propagation channel at 5.9 GHz," In Proc. IEEE International Conference on Communications (ICC), pp. 1-6, Jul. 2017.

[16] H. W. H. Jones, P. A. Dmochowski, and P. D. Teal, "Channel Sounding with Software Defined Radio," In Proc. 16th Electronics New Zealand Conference (ENZCon), Nov. 2009.

[17] H. Boeglen, *et al.*, "An SDR based channel sounding technique for embedded systems," In Proc. 11th European Conference on Antennas and Propagation (EUCAP), pp. 3286-3290, May. 2017.

[18] N. H. Fliedner, D. Block, and U. Meier, "A Software-Defined Channel Sounder for Industrial Environments with Fast Time Variance," In Proc. 11th international Symposium on Wireless Communications Systems (ISWCS), Aug. 2018.

[19] Ettus Research, Universal Software Radio Peripheral [Online] Available: https://www.ettus.com/product [Accessed Oct. 2018].

[20] National Instruments, LabVIEW Communications System Design Suite [Online] Available: http://www.ni.com/en-us/shop/select/labview-communications-system-design-suite [Accessed Oct. 2018].

[21] National Instruments, USRP-R2953 Software Defined Radio Reconfigurable Device [Online] Available: http://www.ni.com/en-us/support/model.usrp-2953.html [Accessed Oct. 2018].

[22] Softros Systems, Network Time System [Online] Available: https://nts.softros.com/ [Accessed Oct. 2018].

[23] D. Mills, "Network Time Protocol Version 4: Protocol and Algorithms Specification," IETF, RCF-5905, Jun. 2010.

[24] D. R. Smith, *Digital Transmission Systems*, Springer, 2004.

[25] S. Weinstein, and P. Ebert, "Data Transmission by Frequency-Division Multiplexing Using the Discrete Fourier Transform," *IEEE Transactions on Communication Technology*, vol. 19, no. 5, pp. 628-634, Oct. 1971.

[26] L. Talbi, and J. Lebe, "Broadband 60 GHz Sounder for Propagation Channel Measurements Over Short/Medium Distances," *IEEE Transactions on Instrumentation and Measurement*, vol. 63, no.2, Feb. 2014.

[27] M. J. Castelli, *LAN Switching first-step*, Cisco Press, Jul. 2004.

[28] D. A. Wassie, *et al.*, "An Experimental Study of Advanced Receivers in a Practical Dense Small Cells Network," In Proc. 9th International Workshop on Multiple Access Communications (MACOM), Nov. 2016.

[29] O. Tonelli, "Experimental analysis and proof-of-concept of distributed mechanisms for local area wireless networks," Ph.D. dissertation, Dept. Electronic Systems, Aalborg University, Denmark, 2014.

[30] Y. Wen, W. Huang, and Z. Zhang, "CAZAC sequence and its application in LTE random access," In Proc. IEEE Information Theory Workshop (ITW), pp. 544-547, Mar. 2007.

[31] H. Holma, and A. Toskala, *LTE for UMTS: OFDMA and SC-FDMA Based Radio Access*, Wiley, 2009.

[32] R. G. Lyons, *Understanding Digital Signal Processing*, 2nd Edition, Prentice Hall PTR, 2004.

[33] P. H. Moose, "A technique for orthogonal frequency division multiplexing frequency offset correction," *IEEE Transactions on communication*, vol. 42, no. 10, pp. 2908-2914, Oct. 1994.

[34] J. H. Yooh, and V. K. Wei, "On synchronizing and detecting multi-carrier CDMA signals", In Proc. 4th IEEE International Conference on Universal Personal Communications (ICUPC), Nov. 1995.

[35] B. Yang, *et al.*, "Channel estimation for OFDM transmission in multipath fading channels based on parametric channel modeling," *IEEE Transactions on Communications*, vol. 49, no. 3, pp. 467-479, Mar. 2001.

[36] T. L. Hansen, B. H. Fleury, and B. D. Rao, "Superfast line spectral estimation," *IEEE Transactions on Signal Processing*, vol. 66, no. 10, pp. 2511-2526, Feb. 2018.

[37] Wanshih Electronic, WSS007 Dual Band Antenna [Online] Available: http://www.wanshih.com.tw/products_3.php?sgid=2&gid=131 [Accessed Oct. 2018].

[38] ITU-R Rec. M.1225-0, "Guidelines for Evaluation of Radio Transmission Technologies for IMT-2000," (02/97).

[39] H. T. Friis,"A Note on a Simple Transmission Formula," *Proceedings of the IRE*, vol. 34, no. 5, pp. 254-256, May. 1946.

[40] D. A. Wassie, *et al.*, "Radio propagation analysis of industrial scenarios within the context of ultra-reliable communication," In Proc. 87th Vehicular Technology Conference (VTC2018-Spring), Jun. 2018.

[41] P. C. F. Eggers, M. Angjelichinoski, and P. Popovski, "Wireless Channel Modeling Perspectives for Ultra-Reliable Low Latency Communications," Submitted to *IEEE Transactions on Wireless Communications*, Jan. 2018 [Online] Available: https://arxiv.org/abs/1705.01725v2 [Accessed Oct. 2018].

# Part III

# Proof-of-concept of Interference Mitigation Techniques in Indoor Small Cells Networks

# Proof-of-concept of Interference Mitigation Techniques in Indoor Small Cells Networks

This chapter presents the experimental validation of interference-mitigation techniques (i.e., advanced receivers) toward dealing with the harmful effect of inter-cell interference, in real indoor 5G small cells deployment.

## 1    Motivation

The upcoming 5G mobile networks are envisioned to accommodate data traffic demands that are expected to be tremendously higher than what the current mobile networks are serving [1]. The 5G networks are expected to adopt the deployment of massive numbers of small cells to attain large traffic demands [2]. The deployment of 5G dense small cells is anticipated to be random and uncoordinated, as observed in the deployment of femtocells in the previous generation of cellular networks [3]. Also, small cells deployments decrease the distance between neighboring cells. Due to these circumstances, inter-cell interference is the primary limiting factors to the network throughput improvement, in the 5G small cells networks that are expected to operate in the sub-6 GHz frequencies band.

Commonly, the inter-cell interference problem is tackled by partitioning the available resources (i.e., frequency domain) among neighboring cells. For instance, partitioning the frequency resource for assigning a part of spectrum chunk at each cell may not be a reasonable approach due to the presence of a large number of cells. Plus, the available spectrum below 6 Hz is already scarce and applying such techniques in the presence of a massive number of cells become more challenging. Due to those circumstances, other mitigation

techniques (i.e., advanced receivers, maximum rank planning) which rely on spatial domain resource are expected to be suitable solutions.

## Advanced receivers

The usage of advanced baseband processing at the receiver showed noticeable potential toward combating inter-cell interference [4]. To that end, the 5G dense small cells concept addressed in [5] considers the usage of Interference Rejection Combining (IRC) as an essential interference mitigation technique. The principle of the IRC receivers is based on utilizing the degrees of freedom of the MIMO transceivers for suppressing the strongest interferers, using a minimum mean square error detector. Such a technique does not require cells coordination which is difficult to apply in the presence of dense cells deployment. Due to this, the IRC receiver becomes a good candidate in the uncoordinated 5G small cells deployment. The work [6] showed the usage of the advanced receiver for interference management in the 5G dense small cell scenarios, and it demonstrated the significant potential of such techniques toward dealing with the interference challenges using a computer simulation. One of the primary goals of this project is to evaluate the potential of advanced receivers, towards being a good candidate in the 5G uncoordinated deployment of small cells, based on measured channel conditions of indoor environments.

## Maximum Rank Planning

Similar to the previous generation of cellular networks, MIMO antenna techniques are also considered as the essential element for attaining the throughput performance targeted by 5G. Indeed, MIMO antennas are used for transmitting independent data stream in parallel utilizing spatial multiplexing techniques, resulting in increased throughput. On the other hand, limiting the maximum number of the spatial stream that can be transmitted in a network would increase the interference suppression capability of IRC receiver [7]. Such interference management scheme that relies on the spatial domain could be employed to further improve the interference suppression resilience capability of the entire network. In this project, the Maximum Rank Planning (MRP) technique that limits the spatial stream in a network, is experimentally evaluated, and compared with static Frequency Reuse Planning, using real channel conditions of indoor 5G small cells networks.

## Rank Adaptation

Rank adaptation algorithm should be applied to effectively utilize the benefit of the advanced receiver for suppression interference. Rank adaptation is used for finding a balance on the usage of spatial domain resource for

spatial multiplexing gain or interference resilience. The MRP scheme introduced in above limits the maximum number of desired spatial streams that can be employed in a network, on the other hand, rank adaptation selects the number of streams that can be transmitted at each node based on instantaneous interference conditions. Rank adaption is necessary to control interference dimensions in a given network, that helps to improve the interference suppression performance of IRC receiver. The work in [5] investigated the promising benefit of rank adaptation algorithms for hindering the inter-cell interference problem. Their analysis showed that an efficient rank adaption algorithm, which considers the interference level of a given network, can further improve the interference resilience capability of IRC receiver.

Moreover, there is a lack of investigation towards validating the potential of those techniques (i.e., advanced receivers, maximum rank planning, rank adaptation) in real indoor 5G small cells deployments. Hence, this chapter presents the proof-of-concept of such techniques in real environments using the experimental methodology described in Chapter II.

## 2 Objectives

The objectives of this chapter are the following:

- Investigate advanced receivers effectiveness in dealing with inter-cell interference in a real uncoordinated dense small cells deployment.

- Evaluate the potential of combining advanced receivers and frequency reuse techniques to deal with the interference problem in the unplanned deployment of small cells.

- Examine interference mitigation techniques that rely on the spatial domain being a valid/legitimate substitute to commonly used frequency reuse scheme for combating inter-cell interference in real network deployment channel conditions.

## 3 Included Articles

The articles that make the main body of this part of the thesis are the following:

**Paper B: Experimental Evaluation of Interference Rejection Combining for 5G small cells**

This article presents the potential advantage of advanced receivers (i.e., interference rejection combining) in real deployment scenarios, using the experimental methodology presented in the previous chapter. For the experimental

activity, a multi-node channel sounder testbed, that consists of 8 SDR network nodes was used. The testbed network presented in this article was built based on the techniques discussed in Paper A, and also multiple SDR devices and software components have been used. The employed testbed network and the experimental results are discussed in the article in great detail.

### Paper C: Experimental Evaluation of Interference Suppression Receivers and Rank Adaptation in 5G Small Cells

This article addresses the potential benefit of rank adaptation algorithms (that are used for balancing the spatial multiplexing and interference resilience gains of the MIMO technologies) towards improving network throughput. In particular, the interference-aware rank adaption technique and successive interference cancelation receiver have been investigated. The study was carried out using an SDR testbed network that is similar to the one used in Paper B.

### Paper D: Experimental Verification of Interference Mitigation Techniques for 5G Small Cells

As of articles, B and C, the SDR testbed network is used to evaluate the benefit of maximum rank planning (which limits the maximum number of streams that can be transmitted in the network) and frequency reuse planning techniques towards decreasing the inter-cell interference. This article discusses the network throughput performance results of these techniques that are evaluated using real-world channel measurements.

### Paper E: An Experimental Study of Advanced Receivers in a Practical Dense Small Cells Network

In order to increase the performance of interference suppression receivers, a sufficient number of transceivers antennas are required. This article presents the experimental study of the interference suppression receivers with different MIMO antenna configurations. The work presented in this article also investigated the performance of the receivers with several sets of deployed access points. The experimental validation was carried out using the testbed featuring 12 SDR testbed nodes and $4 \times 4$ MIMO configuration while in the previous papers $2 \times 2$ MIMO configuration and lower number of nodes were employed.

## 4 Main Findings

**The benefit of advanced receivers in real indoor small cells deployment scenarios**

The included articles in this part of the thesis demonstrate how advanced receivers can significantly improve the network throughput performance in real indoor small cells network. The performance evaluations are carried out based on the measured channel conditions obtained from the real-world experimental analysis. The usage of the advanced receivers such as interference rejection combining (IRC) shows better throughput improvement compared to a maximum ratio combining techniques (known as MRC, which treats the interference as noise [8]). In particular, the IRC receiver performance gain is significantly higher in a situation where dominant interferer cells are observed (c.f., Paper B). This is mainly observed in the open hall indoor environment where there are not any walls that may decrease the interferers level coming from neighboring cells. On the other hand, in a condition where the interferers levels are comparable, the IRC performance gain is lower compared to prior condition. The reasoning behind is that, in dominant interferer conditions, the IRC receiver is able to suppress the strongest interferer, and results in higher performance gain. In the situation where the interferers levels are comparable, IRC is able to suppress only some the interferers; the numbers of interferers that can be suppressed depends on the available spatial degrees of freedom. On the contrary, MRC receiver adds the interferers as a noise power. Note that, such better performance of IRC receiver is obtained while the neighboring cells are time synchronized, and the receivers are able to estimate interference covariance matrix adequately.

Also, Paper E confirmed that the IRC receiver with $4 \times 4$ MIMO antenna configuration significantly improved the network throughput compared to the receiver with $2 \times 2$ MIMO in a real uncoordinated 5G small cells network. The enhanced network throughput is observed due to the use of higher spatial degrees of freedom. Such performance demonstrates that the use of advanced receivers with adequate MIMO antenna configurations can combat sufficiently interference challenge in uncoordinated small cells deployment. This learning indicates the operators can deploy dense small cells in uncoordinated fashion without using detailed network planning. The interference introduced due to this can be dealt with using advanced receivers. The uncoordinated deployment approach will decrease the dense small cells network planning complexity that will rise due to the presence of a large number of cells.

The performance results in Paper D showed that the use of MRP technique offered extra degrees of freedom to the IRC receiver for suppressing interferers, results in better throughput gain compared to FRP scheme. For instance, the use of MRP provided 30% outage throughput gain over the use of FRP in moderate traffic load conditions (i.e., 50% cells activity). Such gain

is observed due to certain factors. First, the moderate traffic load condition decreases the number of active interferers in a given frame, and this increases the presence of a dominant interferer. Second, the use of MRP technique limits the maximum number of transmission streams in a network. Due to these circumstances, the IRC receiver gains extra degree of freedom for suppressing the dominant interferer. Furthermore, a noticeable improvement on the outage network throughput is also observed when the IRC receiver is used with interference aware rank adaptation technique (c.f. Paper C). The rank adaptation enables each cell to select the number of transmitting streams depending on the incoming interferers level instead of limiting the maximum number of transmission streams in a network. When the cell experiences strong interference, the number of transmitting streams decreased from 2 to 1 to enable the capability of the IRC receiver to suppress interferers. Such an approach helped the outage cells to enhance their throughput performance in the interference limited scenario. In general, experimental studies verified that that advanced receivers bring significant gain in peak and median throughput, also, the outage throughput of IRC is further improved with the use of interference rank adaption. Therefore, from these learnings, one can conclude that advanced receivers could be a viable alternative to frequency planning schemes, considering supporting system design is provided.

In addition, combining IRC receiver with frequency reuse can also be employed to improve the outage throughput performance without significantly limiting the achievable peak throughput, as observed in Paper B. Such an approach brings reasonable trade-off among the network throughput and fairness. This learning indicates that combing different interference mitigations techniques can further enhance the overall network performance.

# References

[1] J. G. Andrews, S. Buzzi,W. Choi and S. V. Hanly, A. Lozano, A. C. K. Soong and J. C. Zhang, "What Will 5G Be?," in IEEE Journal on Selected Areas in Communications, vol. 32, no. 6, pp. 1065-1082, June 2014.

[2] O. Galinina, A. Pyattaev, S. Andreev, M. Dohler and Y. Koucheryavy, "5G Multi-RAT LTE-WiFi Ultra-Dense Small Cells: Performance Dynamics, Architecture, and Trends," in IEEE Journal on Selected Areas in Communications, vol. 33, no. 6, pp. 1224-1240, June 2015.

[3] J. G. Andrews, H. Claussen, M. Dohler, S. Rangan and M. C. Reed, "Femtocells: Past, Present, and Future," in IEEE Journal on Selected Areas in Communications, vol. 30, no. 3, pp. 497-508, April 2012.

[4] N. Bhushan, J. Li, D. Malladi, R. Gilmore, D. Brenner, A. Damnjanovic, R. T. Sukhavasi, C. Patel and S. Geirhofer, "Network densification: the

dominant theme for wireless evolution into 5G," in IEEE Communications Magazine, vol. 52, no. 2, pp. 82-89, February 2014.

[5] P. Mogensen, K. Pajukoski, E. Tiirola and J. Vihriala, E. Lahetkangas, G. Berardinelli, F. M. L. Tavares, N. H. Mahmood, M. Lauridsen and D. Catania and A. F. Cattoni., "Centimeter-Wave Concept for 5G Ultra-Dense Small Cells," 2014 IEEE 79th Vehicular Technology Conference (VTC Spring), Seoul, 2014, pp. 1-6.

[6] Fei Hu, "Opportunities in 5G Networks: A Research and Development Perspective," CRC Press, April 2016.

[7] F. M. L. Tavares, G. Berardinelli, N. H. Mahmood, T. B. Sørensen and P. Mogensen, "Inter-cell interference management using maximum rank planning in 5G small cell networks," 2014 11th International Symposium on Wireless Communications Systems (ISWCS), Barcelona, 2014, pp. 628-632.

[8] F. M. L. Tavares, G. Berardinelli, N. H. Mahmood, T. B. Sørensen, P. Mogensen, "On the potential of Interference Rejection Combining in Beyond 4G networks, in Proc. IEEE VTC2013-Fall, September 2013.

References

# Paper B

Experimental Evaluation of Interference Rejection Combining for 5G small cells

Dereje Assefa Wassie, Gilberto Berardinelli, Fernando M. L. Tavares, Oscar Tonelli, Troels B. Sørensen, Preben Mogensen

# Abstract

*The Interference Rejection Combining (IRC) receiver can significantly boost the network throughput in scenarios characterized by dense uncoordinated deployment of small cells, as targeted by future 5th generation (5G) radio access technology. This paper presents an experimental study on the potential benefit of IRC receiver in real deployment scenarios. The study is carried out using a software defined radio (SDR) testbed network with four cells, each featuring one Access Point (AP) and one User Equipment (UE) with two antennas. The testbed network was placed in an indoor office and open hall scenarios, respectively. In each scenario, the cells were arranged to characterize the propagation in different spatial configurations. Using the obtained propagation data, we analysed the cases of closed and open subscriber group for the respective scenarios, to compare the achievable throughput with IRC and Maximum Ratio Combining (MRC) receivers. Different frequency reuse schemes were also considered. The throughput results confirm the effectiveness of the IRC receiver in improving the network throughput with respect to the MRC receiver, under the assumption of single stream (rank 1) transmission. Results show average gains up to around 40% and outage gains up to 70% over the MRC receiver. The combination of the IRC receiver and frequency reuse achieves a favourable trade-off between the network throughput and fairness. Overall, due to the direct propagation, the open hall open subscriber group scenario is benefiting the most from the ability of the IRC receiver to cancel a strong dominant interferer.*

# 1 Introduction

A novel 5th Generation (5G) radio access technology (RAT) is expected to be introduced in the mass market around 2020 to cope with the exponential increase of the data traffic demand [1]. Recent studies on heterogeneous networks have revealed that the enormous capacity requirements of 5G can be achieved by deploying a large number of small cells, operating over a dedicated portion of the spectrum [2]. The same spectrum may be shared by the neighbour cells, which inherently increases inter-cell interference levels, and causes significant impact on the cell's throughput performance.

The traditional approaches for mitigating inter-cell interference are based on planned frequency reuse or distributed spectrum sharing mechanisms. The main principle of such approaches is to assign statically or dynamically orthogonal spectrum chunks to neighbour cells that may experience significant mutual interference [3].

The usage of advanced baseband processing at the receiver has also been proved to be effective in mitigating inter-cell interference. In particular, the 5G concept presented in [4] relies on the usage of Interference Rejection Combining (IRC) receivers as main interference mitigation technique. The princi-

ple of the IRC receivers is to exploit the degrees of freedom of the Multiple Input Multiple Output (MIMO) transceivers, for projecting the significant interfering signals over an orthogonal subspace, with respect to the desired signal, thus diminishing their detrimental impact. The benefits of IRC receivers in improving the network throughput in dense small cells networks have been assessed with system level simulations in [5].

However, besides simulation studies, there is an increasing interest by both industry and academia for a more tangible evidence of the effectiveness of interference mitigation techniques in realistic small cell deployments. Software defined radio (SDR) testbeds represent a flexible and cost-effective paradigm for an agile experimentation of wireless research concepts. In that respect, our previous experimental work has been mainly focused on the validation of a known spectrum sharing algorithm [6].

In this paper, we evaluate the potential benefits of IRC receivers in a real deployment scenario, using a SDR testbed network. The testbed network has been developed with Universal Software Radio Peripheral (USRP) hardware [7], and the ASGARD software platform [8]. The testbed setup is extensively described, as well as the adopted deployments and the experimental results. Our main aim is to obtain insights on the effective capabilities of the IRC receivers in a real network deployment.

The rest of the paper is structured as follows. First, we describe the usage of IRC in 5G small cells networks in Section II, and the setup of the testbed in Section III. In Section IV, we present and analyse the experimental results. Finally, we resume the conclusions in Section V, and state the future work.

## 2   On the usage of IRC in 5G

The aim of this section is to introduce the usage of the IRC receivers in the 5G small cells concept envisioned in [1], in order to justify the target of our experimental activities.

MIMO antenna techniques are considered as a fundamental feature for achieving the data rate performance targeted by 5G  [2]. It is well known that MIMO provides multiple spatial degrees of freedom (DoFs). The desired throughput can be increased by transmitting independent information streams in parallel using spatial multiplexing technology [9]. On the other hand, the spatial DoFs can be used to enforce the receiver resilience towards inter-cell interference by means of IRC receivers, at the cost of limiting the number of data streams. In case of $N$ transmit/receive antennas, up to $N$ independent streams can be sent without any interference resilience, or up to $N-1$ interfering streams can be suppressed in the case of the transmission of a single stream. In other words, while frequency reuse solutions exploit the frequency orthogonality for separating interfering cells, IRC receivers rely on

the 'spatial orthogonality' among independent spatial streams to enhance the interference suppression capabilities [5]. As mentioned in the introduction, suppressing inter-cell interference is of fundamental importance for ultra-dense deployment of small cells operating over the same spectrum.

The IRC receiver operation requires an accurate estimate of the interference covariance matrix (ICM) [10]. Such ICM can be computed from an estimate of the channel responses of the significant interfering streams. Current RATs, such as Long Term Evolution (LTE) and Long Term Evolution - Advanced (LTE-A), have not been designed for supporting an efficient computation of the ICM. The LTE/LTE-A frame structure only allows to estimate the ICM based on long term statistics on the interfering streams, leading to poor IRC performance [11]. The problem is exacerbated in case of low traffic aggregation (as expected in 5G due to the low number of users per cell), leading to a large burstiness level which may lead to highly unpredictable interference patterns among neighbor cells. This compromises a reliable ICM estimate. Moreover, in case of Time Division Duplex (TDD) mode also cross-link interference may appear in case of uncoordinated switching point between neighbour cells, e.g. User Equipment (UE) to UE, and Access Point (AP) to AP.

The 5G frame structure envisioned in [4] is designed instead with the aim of supporting an efficient ICM estimation in TDD mode, thus improve the IRC capabilities. The frame is based on Orthogonal Frequency Division Multiplexing (OFDM) modulation, and consists of a control part followed by a data part. The first symbol of the data part is dedicated to the reference sequence (RS) used for channel estimation purpose.

The possibility of a straightforward estimate of the ICM is enabled by specific design choices. First, it is assumed all the network nodes (APs and UEs) are using the same frame format, are time aligned, and transmitting their RSs in the same OFDM symbol; in case such RSs are orthogonal in the code domain, it is possible then for every receiver to estimate the channel responses of both desired and instantaneously interfering streams. This allows to estimate the ICM for the interferers that are instantaneously active in that frame. Further, it is assumed that the transmission direction, uplink or downlink, remains constant within the frame (i.e., no transmission switching point within the frame); as a consequence, the computed ICM can be used for tuning the IRC receiver for the detection of the entire frame. At each frame, a new ICM is computed depending on the instantaneously active interferers, and used for rejecting them. The principle is shown in Figure B.1. Note that, in [4] the frame duration is set to be very short (0.25 ms) in order to cope with the expected traffic burstiness and reduce the latency. For further details, we refer to [4].
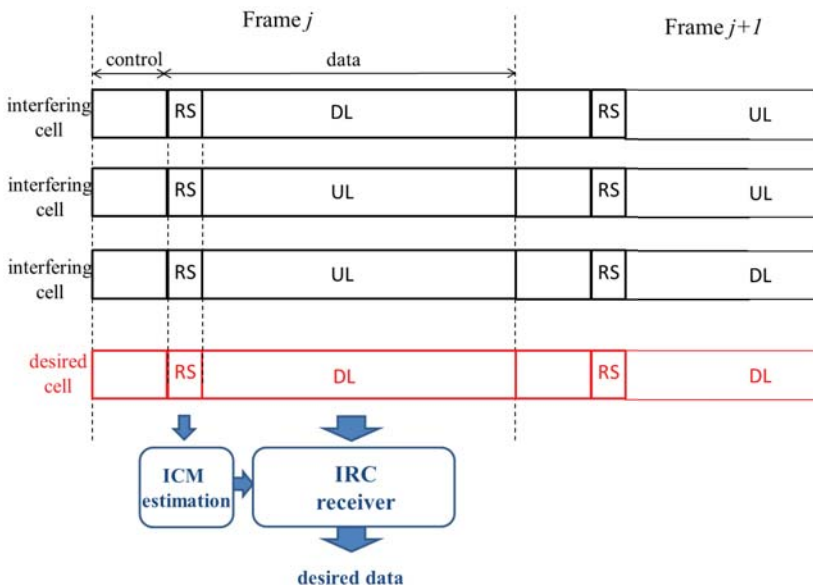
**Fig. B.1:** 5G frame structure optimized for IRC receivers.

# 3 Testbed setup

The goal of the presented testbed setup is to verify the potential of the IRC receivers in improving the network throughput in real interference limited scenarios, provided a system design which enables an efficient estimation of the ICM. In that respect, a full-blown live execution of the envisioned 5G concept is out of our current scope; the testbed rather aims at estimating the ICM in each cell, and derive from it the potential IRC performance. In other words, we are not aiming here at being fully compliant with the envisioned 5G system design, but rather at emulating the same ability of estimating the ICM supported by the envisioned 5G frame structure. The ICM can be computed upon estimation of the channel responses of desired and interfering cells in real deployment scenarios based on their transmitted RSs.

The testbed setup presented in this work is an extension of our previous experimental activity [12], which validates inter-cell interference coordination schemes in real-world deployment scenarios; there, the testbed was built considering a single antenna configuration.

The current testbed consists of 8 SDR nodes featuring a $2 \times 2$ MIMO configuration. Each node can be configured as AP or UE, and consists of an Intel I7 host PC connected through Gigabit Ethernet to an USRP N200 boards. Such board is in turn connected to another USRP N200 board through the

MIMO cable, which ensures synchronous transmission. As shown in Figure E.1, the equipment for each node is located on a movable trolley. The USRP N200 boards are equipped with the XCVR2450 daughterboard, a dual-band transceiver operating over 2.4 GHz and 5 GHz bands. In our setup, the USRP N200 boards are used only as radio-frequency front end, while the entire baseband processing runs on the host PC. The 8 nodes are arranged in 4 cells, featuring 1 AP and 1 UE each. We assume that each cell is operating in rank 1 mode, i.e. a single data stream mapped over the two antennas by a $2 \times 1$ fixed precoding matrix.



**Fig. B.2:** MIMO Transceiver Testbed Node.

The two USRP N200 boards at each node are transmitting their RSs in a frequency interleaved fashion; at the receiver side, the channel frequency response is computed over the positions where the RSs are allocated, and then linearly interpolated in order to obtain a response across the entire transmit bandwidth. We assume a transmit power of 10 dBm per antenna, and a transmission bandwidth of 3.125 MHz.

The estimation of the channel responses from multiple nodes can be obtained by executing a Time Division Duplex (TDD) pattern where only one node at a time is transmitting in a certain time slot, while all the others are receiving. Such TDD pattern subsumes time synchronization among the nodes, which can be achieved by relying on the Network Time Protocol (NTP). The accuracy of the NTP is in the order of tens on milliseconds, and poses a con-

straint on the duration of each time slot. In our testbed, the slot duration of the TDD frame is set to 0.2 seconds. With 8 nodes in the network, a TDD pattern of 8 time slots is then required for estimating the entire $8 \times 8$ complex channel matrix, with a total duration of 1.6 seconds. Note that each of the entries of the channel matrix has the dimension of the $2 \times 2$ MIMO configuration. The estimated channel matrices at each node, are then sent through a backhaul network (Ethernet or WiFi) to a centralized server, which log them for offline analysis. During the post processing, desired and interfering channels are fed as an input to a Signal-to-Interference plus Noise (SINR) estimator. The described procedure allows to emulate the capability of estimating both desired, and interfering streams provided by our envisioned 5G frame structure.

Different SINR estimators are used depending on the selected receiver. Besides the aforementioned IRC receiver, for the sake of comparison, we also consider the Maximum Ratio Combining (MRC) receiver, which maximizes the power of the desired signal, but is unaware of the inter-cell interference. Further details on the used detectors can be found in [5]. Based on the calculated SINR we derive the maximum achievable throughput using the Shannon-Hartley formula, assuming the highest order modulation being 256QAM (maximum spectral efficiency of 8 bits/s/Hz).

We also consider two options for the division of the spectral resources. In frequency reuse one mode, the entire transmission bandwidth is assigned to all the cells. In frequency reuse two mode, the bandwidth is divided in two chunks, and each chunk is preassigned to each cell, in a way that the cells that are expected to generate strong mutual interference, are transmitting over orthogonal resources.

We place the four cells in the two different scenarios depicted in Figure D.3 and Figure B.4, both located at Aalborg University premises.

Scenario A is a typical indoor office deployment, with two pairs of adjacent rooms separated by a corridor. We consider a single cell in each room, operating in Closed Subscriber Group (CSG) mode, i.e. each UE is connected to the AP in the same room. A number of redeployments of the nodes in the same scenario is considered in order to obtain a large set of performance results. Further, we assume that each node can be configured as AP or UE at each experimental trial, such that several interference patterns can be obtained for each physical deployment of the nodes. Moreover, in order to experience different propagation conditions, results are collected over 40 carrier frequencies spanning over the 4.91 GHz - 6 GHz range of the XCVR2450 daughterboard.

Scenario B is an open hall, where APs and UEs are all located in line of sight. We assume here that, at each deployment, the APs are always placed in proximity of the walls, while the UEs are located in random positions within the hall area. Open Subscriber Group (OSG) mode is considered for

Scenario B, i.e. each UE connects to the AP for which it measures the highest received power. In case an AP is connected to multiple UEs, the bandwidth is equally shared among them. APs that are eventually not serving any UE, are assumed to be inactive.

The measurement campaigns in both scenarios were run during night hours, to ensure a steady environment.
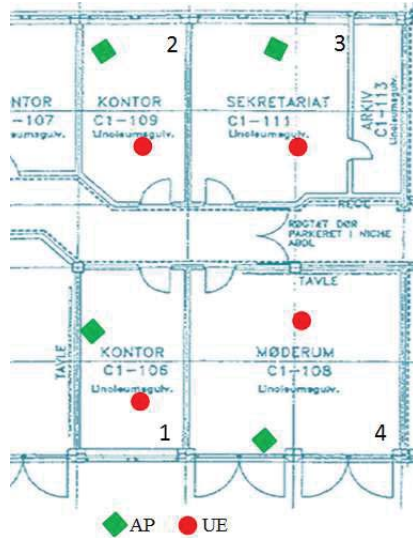


**Fig. B.3:** Indoor office scenario and one possible deployment is depicted.

# 4 Performance Evaluation

In this section, we present the performance results of our experimentation. As mentioned above, the throughput results are obtained by Shannon mapping, assuming the SINR computed upon estimation of both desired and interfering channels. The SINR is computed for both MRC and IRC receivers. We also apply frequency reuse techniques. Statistics are collected out the multiple deployments and trials at different carrier frequencies.

Figure B.5 shows the Empirical Cumulative Distribution Function (ECDF) of the cell downlink throughput for the indoor office scenario. Note that the throughput is scaled from the measurement bandwidth (3.125 MHz) to the transmission bandwidth of our envisioned 5G concept (200 MHz) [1]; this is done with the aim of obtaining insights on the potential of the presented techniques for 5G, circumventing the limitations of the used hardware. In addition, Table B.1 presents the key performance indicators (KPIs), and the relative gains of IRC over MRC receiver for different frequency reuse sche-

**Fig. B.4:** Open hall scenario and one possible deployment is depicted.

mes. Outage (5%-tile), average and peak data rate (95%-tile) are extracted from the plot. The gain of IRC receiver over MRC receiver is significant when frequency reuse 1 (R1) is adopted, up to 36.01% for the outage data rates. By using a $2 \times 2$ antenna configuration with single stream transmission, the IRC receiver is indeed able to use the extra degree of freedom, to suppress one interfering cell. The deployments that lead to a situation of a dominant interfering cell, are benefiting from the usage of an IRC receiver, while the MRC performance is severely compromised. Nonetheless, the IRC gain tends to diminish for the average and the peak data rates. This is due to the cells that, given the specific deployment and propagation conditions, are perceiving a lower interference level, e.g. there is not a dominant interfering cell, but multiple cells with milder interfering levels. In this case, the relative impact of an interference suppression receiver on the throughput performance is lower. Such trend is further exacerbated in the case of frequency reuse two (R2). In general, the usage of frequency reuse two improves the outage for both MRC and IRC receivers at the expense of the reduction of half maximum throughput. While the gain of the IRC receiver over the MRC receiver in terms of outage data rate is approximately the same of the frequency reuse one case, the gain in terms of average data rate is significantly lower. Further, there is no gain for the peak data rate. The usage of orthogonal frequency chunks reduces in most of the cases the probability of having one strong interfering

cell, and hence the benefit of the IRC receiver. However, it is worth to notice that the combination of the IRC receiver with frequency reuse two leads to a situation where in a most of the cases all the cells obtain the same thoughput, thus enhancing the fairness.
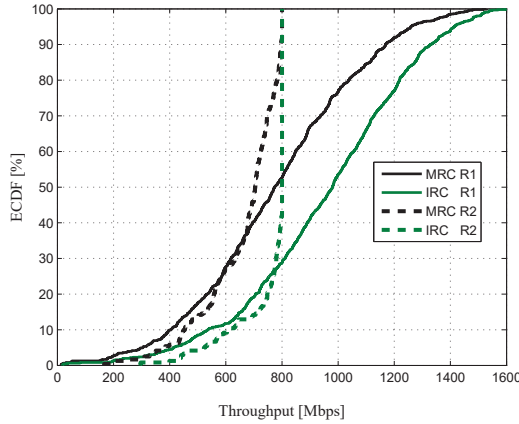


**Fig. B.5:** ECDF of the throughput for both receiver types (MRC and IRC) and different frequency reuse schemes for an Indoor office scenario.

**Table B.1:** Throughput [Mbps] for both receiver types (MRC and IRC) and different frequency reuse schemes - indoor office scenario.

| R1 | | | |
|---|---|---|---|
|  | MRC | IRC | Gain (IRC over MRC) |
| Outage | 304.60 | 414.30 | 36.01 % |
| Average | 779.96 | 954.40 | 22.36 % |
| Peak | 1260.00 | 1416.00 | 12.38 % |

| R2 | | | |
|---|---|---|---|
|  | MRC | IRC | Gain (IRC over MRC) |
| Outage | 384.50 | 522.00 | 35.76 % |
| Average | 662.83 | 755.19 | 13.93 % |
| Peak | 800.00 | 800.00 | 0.00 % |

Figure B.6 illustrates the performance results for the open hall scenario,
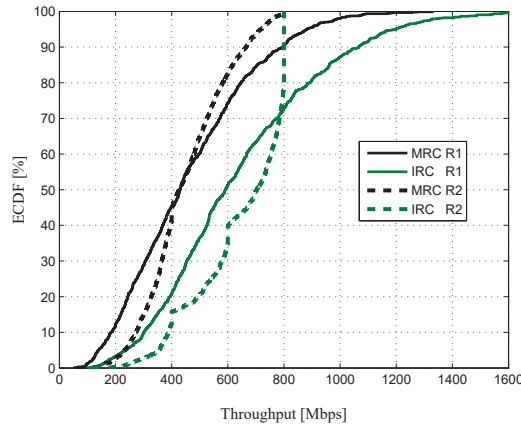
**Fig. B.6:** ECDF of the throughput for both receiver types (MRC and IRC) and different frequency reuse schemes for Open Hall scenario.

**Table B.2:** Throughput [Mbps] for both receiver types (MRC and IRC) and different frequency reuse schemes - open hall scenario.

| R1 | | | |
|---|---|---|---|
| | MRC | IRC | Gain (IRC over MRC) |
| Outage | 140.60 | 237.30 | 68.78 % |
| Average | 459.58 | 642.18 | 39.73 % |
| Peak | 883.00 | 1200.00 | 35.90 % |

| R2 | | | |
|---|---|---|---|
| | MRC | IRC | Gain (IRC over MRC) |
| Outage | 231.10 | 357.80 | 54.82 % |
| Average | 451.05 | 644.55 | 42.90 % |
| Peak | 720.30 | 800.00 | 11.06 % |

while the KPIs and the relative gains of IRC over MRC receiver, are outlined in Table B.2. In such scenario, the overall interference level is higher due to the absence of walls, i.e. all the potential interferers are in line of sight. This justifies the overall lower throughput with respect to the indoor office scenario. Nonetheless, the relative gains of the IRC receiver over the MRC receiver are higher (see Table B.2), up to 68.78 % in terms of outage data

rate for frequency reuse one. Such result can be explained by looking at the distribution of the Dominant Interference Ratio (DIR) in Figure B.7, defined as the ratio between the power of the strongest interferer, and the rest of the interferers perceived at each UE. The DIR can be expressed as:

$$DIR = \frac{P_I(1)}{\sum\limits_{k=2}^{N_k} P_I(k) + \sigma^2} \qquad (B.1)$$

where $P_I$ denotes the set of $N_k$ interferers signal power sorted according to the received signal strength and $\sigma^2$ is the noise power. From Figure B.7, it is clear that the DIR is higher in the open hall case, especially in the upper part of ECDF, thus favouring the IRC receiver. Such counterintuitive behaviour is due to the OSG operational mode, which allows multiple UEs to connect to the same AP. As a consequence, the number of interfering APs can be lower than in CSG mode, thereby enhancing the probability of the presence of a dominant interferer to be suppressed by the IRC receiver. Furthermore, when frequency reuse two is employed, some steps are visible on the trend of IRC receiver performance curve as shown in Figure B.6. This is due to OSG operational mode, where UEs are connected to the same AP and shared the available resources. On the other hand, IRC receiver provides considerable gain with respect to MRC receiver in terms of outage and average data rate as shown in Table B.2.



**Fig. B.7:** ECDF of the DIR for both Indoor Office and Open Hall scenarios.
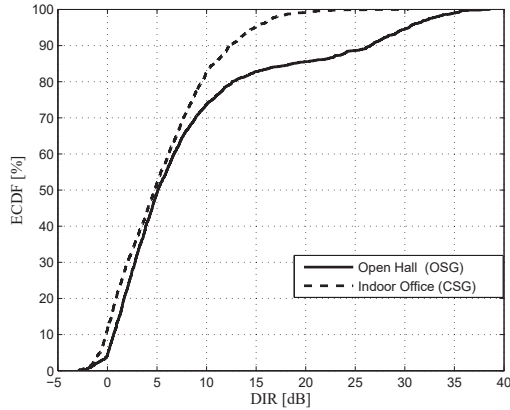
# 5 Conclusions and future work

In this paper, we evaluated the potential benefits of the IRC receiver in real small cell deployment scenarios, where the network throughput performance is mainly limited by the inter-cell interference. Our experimental setup consists of eight SDR nodes with $2 \times 2$ MIMO configuration, arranged in four neighbor cells. The experimental results in indoor office and open hall scenarios have shown the effectiveness of the IRC receiver in improving the network throughput with respect to the interference unaware MRC receiver. Such gain is particularly visible in the outage data rates, with up to 70% gain in the case of open hall scenario. The combination of IRC receiver and frequency reuse can improve the fairness in the network at the expense of a reduction of the maximum data rate.

Furthermore, the experimental results confirm the ability of the IRC receiver in rejecting the strongest interferers in SDR testbed network. Further studies will evaluate the performance of IRC receiver in a large network setup, e.g. from 8 to 16 cells, as well as higher order MIMO configurations ($4 \times 4$). In addition, further techniques such as rank adaptation and dynamic uplink/downlink scheduling will be experimentally investigated.

# References

[1] P. Mogensen, K. Pajukoski, E. Tiirola, E. Lähetkangas, J. Vihriälä, S. Vesterinen, M. Laitila, G. Berardinelli, G. W. O. D. Costa, L. G. U. Garcia, F. M. L. Tavares, and A. F. Cattoni, "5g small cell optimized radio design," in *2013 IEEE Globecom Workshops (GC Wkshps)*, Dec 2013, pp. 111–116.

[2] P. Mogensen, K. Pajukoski, B. Raaf, E. Tiirola, E. Lähetkangas, I. Z. Kovács, G. Berardinelli, L. G. U. Garcia, L. Hu, and A. F. Cattoni, "B4g local area: High level requirements and system design," in *2012 IEEE Globecom Workshops*, Dec 2012, pp. 613–617.

[3] G. W. O. Costa, A. F. Cattoni, I. Z. Kovacs, and P. E. Mogensen, "A fully distributed method for dynamic spectrum sharing in femtocells," in *2012 IEEE Wireless Communications and Networking Conference Workshops (WCNCW)*, April 2012, pp. 87–92.

[4] P. Mogensen, K. Pajukoski, E. Tiirola, J. Vihriala, E. Lahetkangas, G. Berardinelli, F. M. L. Tavares, N. H. Mahmood, M. Lauridsen, D. Catania, and A. F. Cattoni, "Centimeter-wave concept for 5g ultra-dense small cells," in *2014 IEEE 79th Vehicular Technology Conference (VTC Spring)*, May 2014, pp. 1–6.

[5] F. M. L. Tavares, G. Berardinelli, N. H. Mahmood, T. B. Sorensen, and P. Mogensen, "On the potential of interference rejection combining in b4g networks," in *2013 IEEE 78th Vehicular Technology Conference (VTC Fall)*, Sept 2013, pp. 1–5.

[6] O. Tonelli, G. Berardinelli, F. M. L. Tavares, A. F. Cattoni, I. Z. Kovacs, T. B. Sorensen, P. Popovski, and P. E. Mogensen, "Experimental validation of a distributed algorithm for dynamic spectrum access in local area networks," in *2013 IEEE 77th Vehicular Technology Conference (VTC Spring)*, June 2013, pp. 1–5.

[7] "Ni usrp: Software defined radio platform,," http://www.ni.com/usrp/, accessed: 2014-07-17.

[8] "The asgard software radio,," http://asgard.lab.es.aau.dk, accessed: 2014-07-17.

[9] L. Zheng and D. N. C. Tse, "Diversity and multiplexing: a fundamental tradeoff in multiple-antenna channels," *IEEE Transactions on Information Theory*, vol. 49, no. 5, pp. 1073–1096, May 2003.

[10] M. Lampinen, F. D. Carpio, T. Kuosmanen, T. Koivisto, and M. Enescu, "System-level modeling and evaluation of interference suppression receivers in lte system," in *2012 IEEE 75th Vehicular Technology Conference (VTC Spring)*, May 2012, pp. 1–5.

[11] Y. Ohwatari, N. Miki, T. Asai, T. Abe, and H. Taoka, "Performance of advanced receiver employing interference rejection combining to suppress inter-cell interference in lte-advanced downlink," in *2011 IEEE Vehicular Technology Conference (VTC Fall)*, Sept 2011, pp. 1–7.

[12] O. Tonelli, I. Rodriguez, G. Berardinelli, A. F. Cattoni, J. L. Buthler, T. B. Sorensen, and P. Mogensen, "Validation of an inter-cell interference coordination solution in real-world deployment conditions," in *2014 IEEE 79th Vehicular Technology Conference (VTC Spring)*, May 2014, pp. 1–5.

References

# Paper C

Experimental Evaluation of Interference Suppression Receivers and Rank Adaptation in 5G Small Cells

Dereje Assefa Wassie, Gilberto Berardinelli, Davide Catania, Fernando M. L. Tavares, Troels B. Sørensen, Preben Mogensen

*The layout has been revised.*

# Abstract

*Interference suppression receivers are one of the key components in 5th Generation (5G) dense small cells concept that are expected to deal with the ever-increasing problem of inter-cell interference. In this paper, we evaluate the capabilities of interference suppression receivers with respect to traditional frequency reuse schemes in real network scenarios using a software defined radio (SDR) testbed. The experimentation is carried in an indoor office and open hall scenarios. In particular, we study to what extent the interference suppression receiver is an alternative to frequency reuse techniques. To this end we evaluate the Interference Rejection Combining (IRC) and Successive Interference Cancellation (SIC) receivers and different rank adaptation approaches. Each node in our software defined radio (SDR) testbed features a $2 \times 2$ MIMO transceiver built with the USRP N200 hardware by Ettus Research. Our experimental results confirm that interference suppression receivers can be a valid alternative to frequency reuse, by achieving nearly the same outage and high peak throughput performance.*

# 1 Introduction

The data traffic demand is expected to increase exponentially in the upcoming years and this brought industry and academia to investigate novel paradigms for a 5th generation (5G) radio access technology (RAT). An ultra-dense deployment of small cells is foreseen as a cost effective solution for coping with the data traffic demand. However, the existing RAT standards are not well designed for such type of deployment. In this respect, a novel 5G RAT concept optimized for small cells networks operating over the centimetre wave spectrum region (below 30 GHz) has been proposed in [1].

Inter-cell interference is the main performance limiting factor in such ultra-dense small cells deployments. The traditional approaches for dealing with the inter-cell interference are based on static or dynamic frequency reuse schemes. However, static frequency reuse planning may be unrealistic in the case of uncoordinated deployment of small cells and dynamic frequency reuse requires significant signalling overhead. Therefore, the usage of advanced receivers with interference suppression capabilities has been investigated as an alternative approach. While frequency reuse schemes aim at avoiding interference by assigning orthogonal spectrum resources to neighbor cells, advanced receivers exploit the Multiple Input Multiple Output (MIMO) antenna transmission capability for suppressing a number of interfering streams.

In previous works, we have investigated the potential of Interference Rejection Combining (IRC) receivers in improving the throughput with respect to the inter-cell interference unaware Maximum Ratio Combining (MRC) re-

ceivers in a network of small cells, using system level simulations [2] and experimentally using a testbed network [3].

In this paper, we evaluate the performance of interference suppression receivers with respect to traditional frequency reuse techniques in real deployment scenarios using a software defined radio (SDR) testbed network. Our aim is verifying that interference suppression receivers are a valid alternative to frequency reuse techniques. In this evaluation, different rank adaptation approaches are also investigated. Our SDR testbed network is built on the Universal Software Radio Peripheral (USRP) hardware [4] by Ettus Research, and the ASGARD software platform [5], developed at Aalborg University.

The paper is organised as follows. Section II presents our current vision on a 5G robust air interface. The testbed setup is discussed in Section III, while Section IV presents the results of the experimentation. Finally, conclusions and future work are recalled in Section V.

## 2 Robust Air Interface for 5G

In this section, we introduce the major aspects of the proposed 5G RATs concept in [1]: the usage of interference suppression receivers and the benefits of rank adaptation, in order to substantiate the target of our experimentation.

### 2.1 The usage of interference suppression receivers in 5G

A dense uncoordinated deployment of small cells may lead to situations where neighboring cells generate significant mutual interference, thus affecting their throughput performance. The usage of interference suppression receivers may overcome this problem. In particular, IRC receiver exploits the degrees of freedom (DoF) of Multiple Input Multiple Output (MIMO) transceivers, for projecting the significant interfering signals over an orthogonal subspace with respect to the desired signal, thus reducing their detrimental impact [6]. Moreover, the IRC receiver exploits the MIMO spatial DoFs at the expense of limiting the number of the transmitted streams, i.e. in the case of $N$ transmit and receive antennas, up to $N$ spatial streams can be transmitted without any resilience to inter-cell interference or instead $N - K$ interfering streams can be suppressed in the case of $K$ desired streams.

However, the IRC receivers require an accurate estimate of the interference covariance matrix (ICM) [7] in order to efficiently perform their role. In that respect, a novel frame structure for 5G has been proposed in [1], which grants a reliable estimate of the ICM at each frame. The proposed frame structure is designed for Time Division Duplex (TDD) mode, based on the Orthogonal Frequency Division Multiplexing (OFDM) modulation scheme in both uplink and downlink. It consists of a control part and data part. The beginning of

the data part the reference sequences (RSs) are included for channel estimation purposes. Moreover, in order to cater for a straightforward estimation of ICM, it is assumed all the network nodes are using the same frame format, are time aligned, and transmitting orthogonal RSs in the code domain to estimate the channel responses for both desired and instantaneously interfering signals. This enables IRC to suppress the instantaneously active interferers. Further details are discussed in [1].

The successive Interference Cancellation (SIC) receiver is also considered as a part of the 5G small cells concept to deal with inter-cell interference [1]. In a SIC receiver, first a data stream is successfully detected and then it is subtracted from the received vector to reduce its impact on the undetected data stream as stated in [6]. The SIC receiver requires information about the interfering signal transmission format (particularly, the used Modulation and Coding Scheme (MCS) as well as transmission rank) [8]. However, providing this information requires a very complex and costly inter-cell control channel. In this respect, we use the SIC receiver to deal with inter-stream interference since the information for detecting the desired stream is available at the receiver. Therefore, a joint IRC+SIC receiver is considered, where the IRC receiver is responsible for suppressing inter-cell interference while the SIC receiver is responsible for cancelling inter-stream interference.

## 2.2 Rank adaptation

In the absence of interference, MIMO system can exploit their spatial DoFs to reach higher peak throughputs. Conversely, in more severe interference conditions the DoFs can instead be used to suppress interference. This process is referred to as rank adaptation, as it aims to find a trade-off related to the number of utilized spatial streams. A simple known approach is based on the cell's capacity, called Selfish Rank Adaptation (SRA). In the SRA approach, each cell selects the transmission rank which maximizes its own channel capacity given its estimated Signal to Interference plus Noise Ratio (SINR) situation. However, the rank adaptation decision of one cell may harm the performance of its neighboring cells because the total number of interfering streams affects the performance of the IRC receiver. Therefore, an interference aware rank adaptation solution helps diminishing this negative effect, thus improving the overall performance of the network.

For example, the Victim-aware Rank Adaptation (VRA) concept proposed in [9] also attempts to maximize the cell capacity but in addition to that it also considers the potential harm it may cost to its neighboring cells. Therefore, the VRA approach will not opt for higher transmission ranks if there is limited benefit in doing so. The potential harm in the neighbor cells is evaluated by considering the capacity of the incoming interference over noise. Ideally, one should consider the outgoing interference but such metric requires a

large inter-node signaling burden. Therefore, in a distributed version of the algorithm the outgoing interference is assumed to be equal to the incoming interference. This gives an idea of the instantaneous perceived interference level. The incoming interference can be estimated from the RS, given the aforementioned frame structure. Furthermore, the working paradigm of the proposed victim-aware rank adaptation is based on a taxation mechanism that introduces a tax to discourage the selection of higher transmission ranks in the presence of high interference level. Therefore, each node selects the transmission rank $k$ which maximizes the utility function $\Pi_k$ defined as follows:

$$\Pi_k = C_k - \underbrace{kW_kC_I}_{\text{Taxation for rank k}} \tag{C.1}$$

where $C_k$ is the estimated capacity for rank $k$, $W_k$ is a weight function of rank $k$ which measures the level of discouragement and $C_I$ is the capacity of the incoming interfering channels. Further details regarding the operation of the algorithm are discussed in [9].

## 3 Testbed setup

In this section, we present the SDR testbed setup, which is used to verify the performance of interference suppression receivers with respect to frequency reuse planning schemes in a real interference limited scenarios. The testbed consists of 8 SDR nodes which can be configured as Access Points (APs) or User Equipments (UEs). Each node is composed of a host PC and 2 USRP N200 boards. The PC is connected to one of the boards trough Gigabit Ethernets and the boards are linked with a MIMO cable (provided by Ettus), as shown in Figure E.1. The MIMO cable ensures synchronous transmission by the two boards. In addition, the USRP N200 boards are equipped with the XCVR2450 daughterboard, a dual-band transceiver operating over 2.4 GHz and 5 GHz bands. In the testbed setup, the USRP N200 boards are used only as radio-frequency front end, while the entire baseband processing runs on the host PC. The software has been entirely written with the ASGARD software platform.

The 8 nodes are grouped in four cells, each cell featuring 1 AP and 1 UE. The four cells are deployed in two different scenarios depicted in Figure C.2 and Figure C.3, both located at Aalborg University premises.

Scenario A is an open hall, where all APs and UEs are placed in line of sight. The APs are always placed in proximity of the walls, while the UEs are located in random positions within the hall area. In this scenario, Open Subscriber Group (OSG) mode is considered, i.e. each UE affiliated to the AP for which it measures the highest received power. In the case where multiple
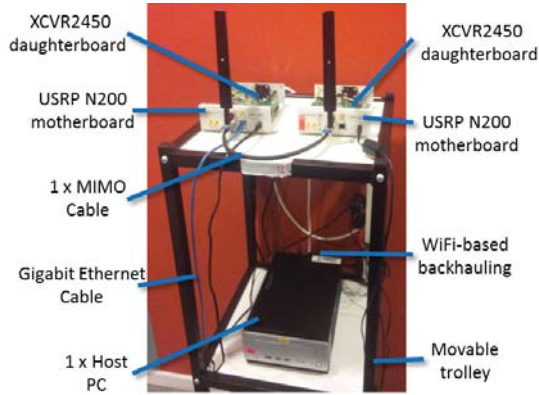
**Fig. C.1:** MIMO Transceiver Testbed Node

UEs are associated to an AP, the bandwidth is equally shared among them. In addition, APs which are not serving any UE are set to be inactive. Moreover, a number of redeployments of nodes is considered for the sake of collecting a large set of performance results.
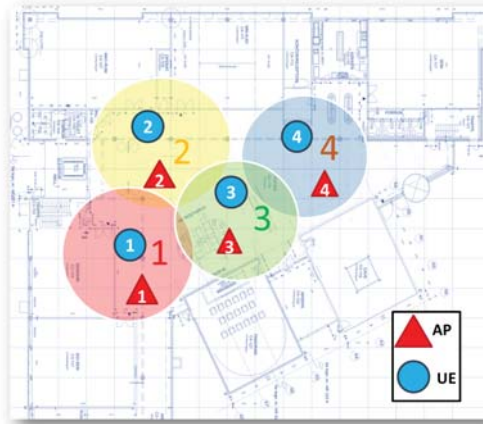


**Fig. C.2:** Open Hall scenario. One possible deployment is depicted.

Scenario B is a typical indoor office deployment, with two pairs of adjacent rooms separated by a corridor. We consider a single cell in each room, operating in Closed Subscriber Group (CSG) mode, i.e. each UE is affiliated to the AP in the same room. In this scenario, we assume that each node can be configured as AP or UE at each experimental trial, such that several interference conditions can be obtained for each physical deployment of the

nodes.
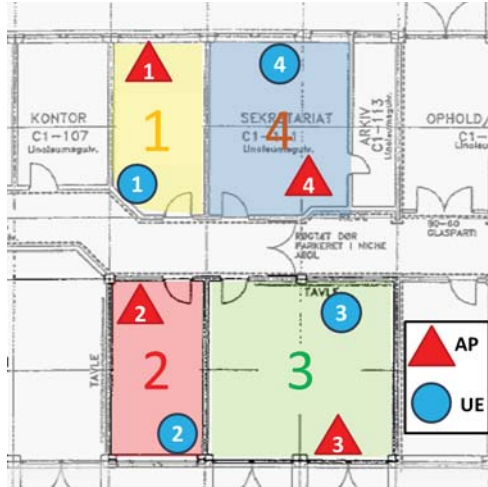


**Fig. C.3:** Indoor office scenario. One possible deployment is depicted.

The experimentation only assumes downlink data transmission with 3.125MHz bandwidth, considering 10dBm transmit power per antenna. The experimental results are obtained over 40 carrier frequencies spanning over the 4.91 GHz - 6 GHz range of the XCVR2450 daughterboard in order to experience different propagation conditions. Furthermore, the testbed operates in *channel sounding mode* similar to our previous activities ( [10], [3], [11]), where use the testbed as a tool for estimating the channel responses among every couple of nodes in the network, and emulate their throughput performance offline. The two USRP N200 boards at each node are transmitting RSs in a frequency interleaved fashion; at the receiver side, the channel frequency response is computed over the positions where the RSs are allocated, and then linearly interpolated in order to obtain a response across the entire transmission bandwidth. Time Division Multiplexing (TDM) pattern is employed for collecting the estimation of the channel response from multiple nodes: only one node at a time is transmitting in a specific time slot while the others are receiving. Time synchronization among the nodes can be attained by relying on the Network Time Protocol (NTP). The accuracy of the NTP is in the order of tens on milliseconds, and introduces a limitation on the duration of each time slot. In our testbed, the slot duration of the TDM frame is set to 0.2 seconds and the total duration of the TDM frame is 1.6 seconds for estimating the entire $8 \times 8$ complex channel matrix. Note that each of the entries of the channel matrix has the dimension of the $2 \times 2$ MIMO configuration. The estimation of the channel matrices is carried on at each node, are then sent through a backhaul network (Ethernet or WiFi) to a centralized server, which

log such matrices for offline analysis.

During offline analysis, the estimated channel matrices for the desired and interfering channels are fed as an input to a SINR estimator, and different SINR estimators are used according to the selected receivers. The maximum achievable throughput is calculated using the Shannon-Hartley formula at a given estimated SINR condition, assuming the highest order modulation being 256QAM (maximum spectral efficiency of 8 bits/s/Hz).

In order to test the operation of the discussed interference suppression receivers in combination with rank adaptation approaches, we consider low load and high load conditions to represent both low and high interference level situation. The low load condition is modelled by introducing a 50% probability that a certain AP is active in a given frame. Similarly, the high load condition assumes that all the APs are active at each frame.

# 4 Performance Evaluation

In this section, we present the performance results of our experimentation, obtained using our SDR testbed setup. The interference suppression receivers and frequency reuse planning scheme are evaluated in the two different scenarios presented in the previous section. The performance results are presented in terms of Empirical Cumulative Distribution function (ECDF) of the cells downlink throughput and the key performance indicators are expressed in-terms of outage (5%-tile), median (50%-tile) and peak (95%-tile) data rates. The throughput of each cell is obtained by mapping their calculated SINR to Shannon rate, and the bandwidth is scaled from the operational bandwidth of the USRP N200 boards to the 200 MHz bandwidth which is targeted by our envisioned 5G concept for cm-waves [1].

For verifying whether the interference suppression receivers represent a valid alternative to frequency reuse planning schemes, we compare the downlink throughput performance of interference suppression receivers with a *baseline configuration* which employs an interference unaware MRC receiver, selfish rank adaptation and the frequency reuse scheme which provides, for each study case, the best outage performance between the reuse 1 (FR1) and reuse 2 (FR2) options. On the other hand, the configurations featuring advanced receivers include IRC and IRC+SIC processing and assume FR1 and both selfish and victim-aware rank adaptation. The victim-aware rank adaptation is evaluated with two set of weights 'W1=[0, 0.1]' and 'W2=[0, 0.5]'. The first weight leads to an aggressive approach which favours slightly higher rank (in our evaluation it favours rank 2 since we have a maximum of 2 streams due to the 2x2 MIMO antenna configuration) and the second one leads to a conservative approach which favours rank 1 by applying a high taxation for rank 2.

## 4.1 Scenario A - Open Hall (OSG)

In this Scenario, selfish rank adaptation is assumed for both the baseline and the interference suppression receivers configurations. Moreover, the baseline configuration considers FR2, since it can be shown to provide the best outage performance in this scenario, while the interference suppression receivers arrangements include both IRC and IRC+SIC approaches.

Figure D.4 shows the average cell throughput ECDFs of different configurations, while Table C.1 presents the outage, median and peak data rates which have been extrapolated from the plot in high load situation. The figure depicts that the interference suppression receivers outperform the baseline configuration, and receivers achieve more than 50% of the peak data rate gain with respect to the baseline configuration as indicated in Table C.1. On the other hand, IRC+SIC receiver performance is slightly better than the IRC-only receiver due to the SIC receiver capability of cancelling the inter-stream interference in case of rank 2 transmission.
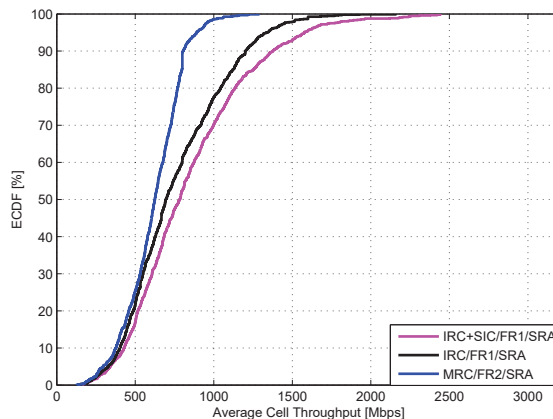


**Fig. C.4:** Cell throughput ECDFs - Scenario A- high load.

**Table C.1:** Scenario A- Key performance indicators [in Mbps] and performance gains over the baseline configuration -high load

| Configuration | Outage | Median | Peak |
|---|---|---|---|
| MRC/FR2/SRA | 294.4 | 624.8 | 890.7 |
| IRC/FR1/SRA | 331.0 (+12.4%) | 694.4 (+11.1%) | 1342.0 (+51.0%) |
| IRC+SIC/FR1/SRA | 341.8 (+16.1%) | 783.5 (+25.4%) | 1579.0 (+77.3%) |

From results in this scenario, one can conclude that interference suppres-

sion receivers can be legitimate substitutes to frequency reuse planning schemes for mitigating the inter-cell interference.

## 4.2 Scenario B - Indoor Office (CSG)

In this scenario, the number of interfering APs is expected to be higher compared with scenario A, since all APs are active due to CSG operational mode while in scenario A some of the APs may be inactive in case they don't have affiliated UEs. Hence, the usage of frequency reuse planning may guarantee better outage data rate.

Similarly to scenario A, we also consider FR2 for the baseline configuration and selfish rank adaptation for both the baseline and the interference suppression receivers configurations. In addition, victim-aware rank adaptation is also assumed in this scenario, given its potential of providing better outage throughput performance with respect to selfish rank adaptation [9].

The average cell throughput ECDFs of interference suppression receivers and the MRC receiver with FR2 configuration are depicted in Figure C.5, while Table C.2 reports the corresponding extracted key performance indicators in-terms of outage, median and peak data rates in high load situation. Both the figure and the table show that the outage throughput performance of IRC and IRC+SIC receivers with selfish rank adaptation is worse compared with the baseline configuration, though their median and peak data rates are much higher.



**Fig. C.5:** Cell throughput ECDFs - Scenario B- high load.

The outage data rate performance of interference suppression receivers is improved when using victim aware rank adaptation as shown in Figure C.5. Two schemes are used for the victim aware rank adaptation, based on
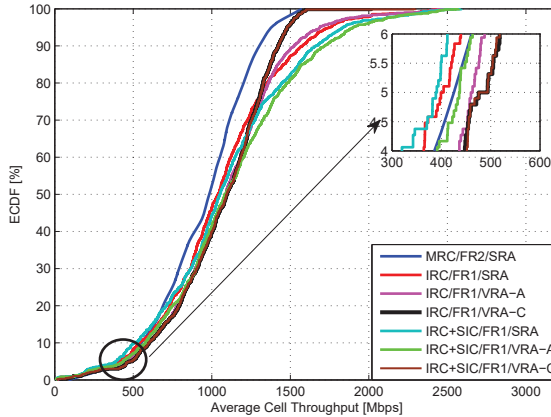
**Table C.2:** Scenario B- Key performance indicators [in Mbps] and performance gains over the baseline configuration -high load

| Configuration | Outage | Median | Peak |
|---|---|---|---|
| MRC/FR2/SRA | 426.9 | 978.8 | 1370.0 |
| IRC/FR1/SRA | 404.5 (-5.2%) | 1041.0 (+6.4%) | 1690.0 (+23.5%) |
| IRC/FR1/VRA-A | 463.4 (+8.5%) | 1087.0 (+11.1%) | 1747.0 (+27.5%) |
| IRC/FR1/VRA-C | 475.8 (+11.5%) | 1095.0 (+12.0%) | 1480.0 (+8.0%) |
| IRC+SIC/FR1/SRA | 390.9 (-8.4%) | 1052.0 (+7.4%) | 1839.0 (+34.0%) |
| IRC+SIC/FR1/VRA-A | 437.4 (+2.5%) | 1082.0 (+10.5%) | 1902.0 (+39.0%) |
| IRC+SIC/FR1/VRA-C | 475.8 (+11.5%) | 1095.0 (+12.0%) | 1480.0 (+8.0%) |

the set of weights specified above, aggressive victim-aware rank adaptation (VRA-A) which corresponds to weight 'W1' and conservative victim-aware rank adaptation (VRA-C) which corresponds to weight 'W2'. Both VRA-C and VRA-A provide outage data rate higher or nearly equal to the baseline configuration as reported in Table C.2. Table C.2 indicates that interference suppression receivers with VRA-A achieve up to 39% of peak data rate gain and acceptable outage performance. Moreover, the main difference between the two victim-aware rank adaptation approaches is mainly noticeable on the peak data rate; VRA-C introduces high taxation on the higher rank and limits the peak throughput, while VRA-A provides higher peak data rate and reasonable outage performance.

However, as shown in Table C.3, in low load situation interference suppression receivers grant higher outage data rate with respect to MRC receiver with FR2 configuration, even in case a selfish rank adaptation.

**Table C.3:** Scenario B- Key performance indicators [in Mbps] and performance gains over the baseline configuration -low load.

| Configuration | Outage | Median | Peak |
|---|---|---|---|
| MRC/FR2/SRA | 531.0 | 1240.0 | 1600.0 |
| IRC+SIC/FR1/SRA | 568.2 (+7.0%) | 1651.0 (+33.1%) | 3200.0 (+50.0%) |
| IRC+SIC/FR1/VRA-A | 609.1 (+15.0%) | 1705.0 (+37.5%) | 3200.0 (+50.0%) |
| IRC+SIC/FR1/VRA-C | 684.2 (+29.0%) | 1483.0 (+20.0%) | 3200.0 (+50.0%) |

Scenario B results also confirm that interference suppression receivers can be a valid possible choice, though in high load condition victim aware rank adaptation is required for a reasonable outage data rate.

# 5  Conclusions and future work

In this paper, we presented an experimental investigation on the usage of interference suppression receivers in a real small cells network scenarios. Our experimental setup is based on a SDR testbed which is composed of the USRP N200 hardware by Ettus Research and a host PC running the ASGARD software platform, and each node features a $2 \times 2$ MIMO configuration. The experimental results in an open hall scenario have shown that using interference suppression receivers it is possible to obtain higher outage data rate (+16%) with respect to frequency reuse. Similar performance is also obtained in an indoor office scenario with the usage of victim-aware rank adaptation. Interference suppression receivers with aggressive victim-aware rank adaptation also attain up to 39% gain in terms of peak data rates and reasonable outage performance.

Our future work will focus on the extended investigation on interference suppression receivers and different rank adaptation approaches in a larger testbed setup (e.g., eight cells). The testbed setup will also feature a higher order MIMO configuration ($4 \times 4$), and thus provide higher degrees of freedom for interference suppression as well as for the selection of the transmission rank.

# References

[1] P. Mogensen *et al.*, "5G small cell optimized radio design," *Globecom, International workshop on emerging techniques for LTE-Advanced and Beyond 4G*, 2013.

[2] F. M. L. Tavares, G. Berardinelli, N. H. Mahmood, T. B. Sørensen, and P. Mogensen, "On the potential of interference rejection combining in B4G networks," *IEEE 78th Vehicular Technology Conference, VTC2013-Fall*, 2013.

[3] D. A. Wassie, G. Berardinelli, F. M. L. Tavares, O. Tonelli, T. B. Sørensen, and P. Mogensen, "Experimental evaluation of interference rejection combining for 5G small cells," *accepted to IEEE Wireless Communications and Networking Conference, WCNC2015*, 2015.

[4] "Ettus research," http://www.ettus.com.

[5] "The ASGARD software radio," http://asgard.lab.es.aau.dk.

[6] J. Choi, *Optimal Combining and detection Statistical Signal Processing for Communications*. Camberidge University Press, 2010.

[7] Y. Ohwatari, N. Miki, T. Asai, T. Abe, and H. Taoka, "Performance of advanced receiver employing interference rejection combining to supress inter-cell interference," *IEEE Vehicular Technology Conference, VTC2011-Fall*, 2011.

[8] N. Bhushan *et al.*, "Network densification: The dominant theme for wireless evolution into 5G," *IEEE Communication Magazine*, 2014.

References

[9] D. Catania, A. Cattoni, N. H. Mahmood, G. Berardinelli, P. Frederiksen, and p. Mogensen, "A distributed taxation based rank adaptation scheme for 5G small cells," *accepted to IEEE 81st Vehicular Technology Conference, VTC2015-Spring*, 2015.

[10] O. Tonelli, G. Berardinelli, F. M. L. Tavares, A. F. Cattoni, I. Z. Kovács, T. B. Sørensen, P. Popovski, and P. Mogensen, "Experimental validation of a distributed algorithm for dynamic spectrum access in local area networks," *IEEE 77th Vehicular Technology Conference, VTC2013-Spring*, 2013.

[11] D. A. Wassie, G. Berardinelli, F. M. L. Tavares, T. B. Sørensen, and P. Mogensen, "Experimental verification of interference mitigation techiques for 5G small cells," *accepted to IEEE 81st Vehicular Technology Conference, VTC2015-Spring*, 2015.

# Paper D

## Experimental Verification of Interference Mitigation techniques for 5G Small Cells

Dereje Assefa Wassie, Gilberto Berardinelli, Fernando M. L. Tavares, Troels B. Sørensen, Preben Mogensen

# Abstract

*Inter-cell interference is the main performance limiting factor in the dense deployment of small cells targeted by the upcoming 5th Generation (5G) radio access technology. In this paper, we present an experimental evaluation of inter-cell interference mitigation techniques in a real indoor office deployment with four cells, where each cell features one Access Point (AP) and one User Equipment (UE). In particular, we compare traditional Frequency Reuse Planning (FRP) with the recently proposed Maximum Rank Planning (MRP) technique, which relies on the degrees of freedom offered by the multi-antenna transceivers for suppressing a number of interfering streams. Different receiver types are also considered, namely Interference Rejection Combining (IRC) and the interference unaware Maximum Ratio Combining (MRC). Each node in our software defined radio (SDR) testbed features a $2 \times 2$ MIMO transceiver built with the USRP N200 hardware by Ettus Research. The experimental results in a fully loaded network reveal the capability of the MRP technique to achieve higher throughput performance than FRP for 90% of the cases when IRC receivers are used. Lower network loads lead to further performance improvements for MRP.*

# 1 Introduction

The exponential increase of the data traffic demand which is foreseen in the upcoming years has brought industry and academia to investigate novel paradigms for a 5th generation (5G) radio access technology (RAT). It is agreed that the most feasible solution for boosting the network capacity is cell densification, i.e. an ultra-dense deployment of small cells with limited coverage is targeted by 5G. Candidate spectrum resources for 5G are both in the cm-wave region (below 30 GHz), and in the mm-wave region (above 30 GHz). A cm-wave concept for 5G has been proposed, for instance in [1]. It is well known that inter-cell interference is the main performance limiting factor in ultra-dense small cells deployments operating at cm-wave frequencies. In that respect, interference management techniques are of fundamental importance in such scenarios.

The traditional approaches for mitigating the inter-cell interference are based on static or dynamic frequency reuse. Recently, the usage of advanced receivers such as Interference Rejection Combining (IRC) has also been considered as a solution for dealing with the inter-cell interference. While frequency reuse techniques aim at avoiding interference among neighbor cells by assigning to them orthogonal spectrum resources, IRC receivers rely on the spatial degrees of freedom offered by the Multiple Input Multiple Output (MIMO) antenna transmission for suppressing a number of interfering streams at the expense of a reduction of the spatial multiplexing gain. In

particular, the Maximum Rank Planning (MRP) concept has been recently proposed as a solution for boosting the interference suppression capability of the entire network [2].

Interference mitigation approaches either based on frequency reuse or advanced baseband processing have been studied and evaluated by system level simulations, addressing their specific pros and cons in different load and deployment scenarios. However, the experimental evidence of novel communication concepts in a real network is emerging as a pressing requirement for assessing their effective potential, by overcoming the ambiguities due to the typically simplified models taken in simulation. In that respect, our previous experimental activities have been focused on the validation of an interference coordination solution [3], as well as on the usage of IRC receivers in a small cells network [4].

This paper focuses on the performance evaluation of the aforementioned interference mitigation techniques in a software defined radio (SDR) testbed network with four cells, with particular emphasis on the novel MRP concept. Our testbed is based on the Universal Software Radio Peripheral (USRP) hardware [5] by Ettus Research, and the ASGARD software platform [6], developed at Aalborg University. Our aim is to obtain a tangible evidence of their effective potential in a real network.

The paper is structured as follows. Section II recalls the interference mitigation techniques targeted by our experimental activity. The testbed setup is presented in Section III, while Section IV presents the results of the experimentation. Finally, conclusions are drawn in Section V.

## 2 Inter-cell Interference Management in 5G

An uncoordinated deployment of small cells may lead to situations where neighbor cells generate significant mutual interference, thus affecting their throughput performance. The most established solution for avoiding inter-cell interference is frequency reuse, i.e. splitting the available bandwidth in a number of orthogonal chunks, and assigning them to the cells which are (or are expected to be) mutually affected by their own transmissions. The price to pay for such interference avoidance approach is a reduction of the maximum achievable throughput since cells may utilize only part of the available resources for avoiding interference to the neighbors. Frequency reuse solutions may be static or dynamic. In the static case, the spectrum resources are assigned in a grid of cells according to their topology, forcing neighbor cells to operate over different portions of the spectrum, and reusing the same portion in cells located at a sufficient physical distance. In dynamic frequency reuse, the spectrum chunks are assigned at each cell depending on the effective estimated interference rather than being pre-allocated. For the

rest of the paper, we will restrict our focus on static frequency reuse, often referred as Frequency Reuse Planning (FRP).

The usage of IRC receivers may partly overcome the necessity of inter-ference avoidance in small cells since it enables some degree of interference suppression. In particular, IRC exploits the degrees of freedom (DoF) of the MIMO transceivers, for projecting the significant interfering signals over an orthogonal subspace with respect to the desired signal, thus diminishing their detrimental impact [7]. In order to efficiently perform their duties, IRC receivers require a supportive system design which allows a reliable estimate of the interference covariance matrix (ICM) [8]. In [1], a novel frame structure for 5G has been proposed, which allows to estimate the ICM at each frame, thus allowing IRC to suppress the instantaneously active interferers.

While the usage of IRC allows neighbor cells to operate over the same bandwidth, the interference suppression capabilities can only be exploited by limiting the number of desired spatial streams, thus also leading to a throughput reduction. In other terms, in the case of $N$ transmit and receive antennas, up to $N$ spatial streams can be transmitted without any robustness to the inter-cell interference; by limiting the number of desired streams to $N - K$, with $1 \leq K \leq N - 1$, up to $K$ interfering streams coming from the neighbor cells can be suppressed. A rank adaptation algorithm takes care of balancing the trade-off between spatial multiplexing gain and interference resilience by selecting the number of streams (referred as transmission *rank*) to be transmitted depending on the instantaneous interference conditions. For instance, selfish solutions for the rank adaptation select the number of streams which is expected to maximize the throughput of the cell regardless of the impact on the neighbors, and may not represent the best solutions for boosting the overall the network performance. On the other hand, altruistic approaches may require significant signaling overhead among the neighbor cells.

The MRP technique has been proposed in [2] as a novel inter-cell interfer-ence management approach which limits the maximum number of streams that can be transmitted in the network. This is meant to ensure some degrees of freedom for interference suppression at each cell. Figure D.1 depicts the working principle of MRP and compares it with traditional FRP in a simple scenario with two neighbor cell operating in downlink. Each cell contains one Access Point (AP) and one User Equipment (UE), equipped with $2 \times 2$ MIMO transceivers. In Figure D.1a, both cells are transmitting with rank 2 over the entire available bandwidth $B$. Due to the physical location of the devices, UE 1 is expected to receive significant interference from AP 2. Since cells are using their MIMO DoF for spatial multiplexing, they do not have any inter-ference rejection capability, and the throughput performance of cell 1 may be significantly affected by the inter-cell interference. MRP forces all the cells to limit their transmission rank to 1 (Figure D.1b). As a consequence, UE 1 can
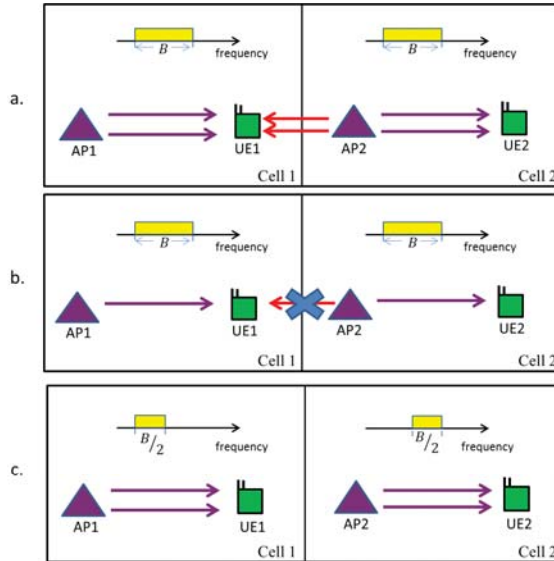
**Fig. D.1:** Example of MRP and FRP working principle.

use its extra degree of freedom for suppressing the interfering stream coming from cell 2, at the expenses of halving the maximum achievable throughput of cell 2 but providing fairness in the network. The case of FRP is depicted in Figure D.1c. Here, both cells are assigned half of the available bandwidth. Since they are operating over orthogonal chunks, interference is avoided and they can use the MIMO DoF for spatial multiplexing gain. Due to the limited spectrum resources, the maximum achievable throughput is also halved.

It is not straightforward to determine which technique performs the best, since their performance may depend on the particular scenario/topology or activity level of each cell. As observed in [2], MRP is expected to outperform FRP in scenarios characterized by the presence of a strong dominant interferer, while FRP is more advantageous in the case of a number of interferers with comparable power level. Note that MRP is more simple than FRP since it only sets the maximum rank to be used in the entire network, while FRP requires indexing the frequency chunk to be used at each cell. The comparison of static FRP and MRP in a real scenario is the main object of the experimental activity in this paper.

## 3 Testbed setup

In this section, we describe the SDR testbed setup which is used for the performance evaluation of the aforementioned interference mitigation tech-

niques. The current testbed consists of 8 SDR nodes, that can be configured as AP or UE and feature $2 \times 2$ MIMO. Each node consists of an Intel I7 host PC connected through Gigabit Ethernet to an USRP N200 boards, which is in turn connected to another USRP N200 board through the MIMO cable (provided by Ettus), which ensures synchronous transmission. As shown in Figure E.1, the equipment for each node is located on a movable trolley, in order to ease the node re-deployment. The USRP N200 boards are equipped with the XCVR2450 daughterboard, a dual-band transceiver operating over 2.4 GHz and 5 GHz bands. In our setup, the USRP N200 boards are used only as radio-frequency front end, while the entire processing executes on the host PC. Our software has been entirely written with the ASGARD software platform. The 8 nodes are arranged in four cells, featuring 1 AP and 1 UE each. We only assume downlink data transmission.



**Fig. D.2:** MIMO Transceiver Testbed Node

The experiment is run in the scenario depicted in Figure D.3, consisting of four neighbor rooms located at Aalborg University premises. It is a typical indoor office deployment, with two pairs of adjacent rooms separated by a corridor. We consider a single cell per room, operating in Closed Subscriber Group mode, i.e. each UE is connected to it's affiliated AP in the same room. A number of redeployments of the nodes in the same scenario is considered in order to obtain a large set of performance results. Further, we assume that each node can be configured as AP or UE at each experimental trial, such that
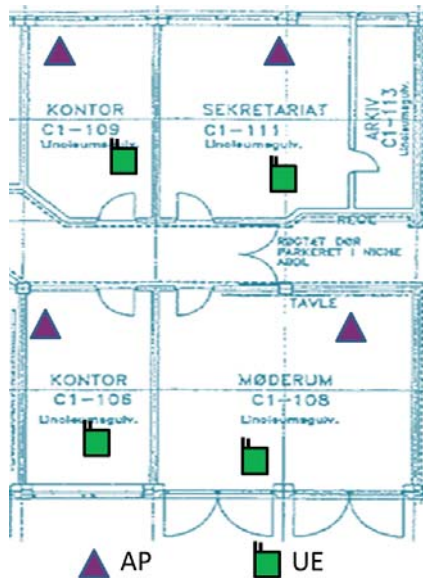
**Fig. D.3:** Indoor office scenario. One possible deployment is depicted.

several interference patterns can be obtained for each physical deployment of the nodes. Moreover, in order to experience different propagation conditions, results are collected over 40 carrier frequencies spanning over the 4.91 GHz - 6 GHz range of the XCVR2450 daughterboard. We assume a transmit power of 10 dBm per antenna, and a transmission bandwidth of 3.125 MHz.

As already done in our previous activities ( [3], [4]), we assume the testbed to operate in *channel sounding mode*. In other terms, we are not aiming at a full live execution of our system, but we use the testbed as a tool for estimating the channel responses among every couple of nodes in the network, and emulate their throughput performance offline. The two USRP N200 boards at each node are transmitting reference sequences in a frequency interleaved fashion; at the receiver side, the channel frequency response is computed over the positions where the reference sequences are allocated, and then linearly interpolated in order to obtain a response across the entire transmission bandwidth. The estimation of the channel responses from multiple nodes can be obtained by executing a Time Division Multiplexing (TDM) pattern where only one node at a time is transmitting in a certain time slot, while all the others are receiving. The experiment was executed during night hours, to ensure a steady environment. Such TDM pattern subsumes time synchronization among the nodes, which can be achieved by relying on the Network Time Protocol (NTP). The accuracy of the NTP is in the order of tens on milliseconds, and poses a constraint on the duration of each time slot. In

our testbed, the slot duration of the TDM frame is set to 0.2 seconds. With 8 nodes in the network, a TDM pattern of 8 time slots is then required for estimating the entire $8 \times 8$ complex channel matrix, with a total duration of 1.6 seconds. Note that each of the entries of the channel matrix has the dimension of the $2 \times 2$ MIMO configuration. The estimated channel matrices at each node, are then sent through a backhaul network (Ethernet or WiFi) to a centralized server, which log them for offline analysis.

During the post processing, desired and interfering channels are fed as an input to a Signal-to-Interference plus Noise (SINR) estimator. Different SINR estimators are used depending on the selected receiver. Besides the aforementioned IRC receiver, for the sake of comparison we also consider the Maximum Ratio Combining (MRC) receiver, which maximizes the power of the desired signal, but is unaware of the inter-cell interference. Further details on the used detectors can be found in [9]. Based on the calculated SINR we derive the maximum achievable throughput using the Shannon-Hartley formula, assuming the highest order modulation being 256QAM (maximum spectral efficiency of 8 bits/s/Hz).

A simple rank adaptation is adopted, where each AP selects the number of streams to be transmitted as the one which maximizes its throughput given the estimated interference conditions. Further, each cell also selects a transmit precoding matrix with the same criterion. We are adopting the same precoding codebook used in Long Term Evolution (LTE) air interface [10].

Different network loads are also emulated. In case of a $X\%$ activity factor, a certain AP is assumed to be active only in $X\%$ of the frames, randomly selected.

# 4  Performance Evaluation

In this section, we present the experimental results obtained with our SDR testbed in the indoor office deployment. Both traditional FRP and the novel MRP are evaluated, for the two different receiver types. In the following, we will refer to FR$x$ to denote frequency reuse $x$, i.e. the overall bandwidth divided in $x$ chunks, and MR$x$ to denote the maximum transmission rank $x$. Since the testbed nodes feature $2 \times 2$ MIMO, only the two options MR1 and MR2 are possible. MR1 corresponds to forcing rank 1 to all the cells, while in the MR2 case the rank adaptation can decide for rank 1 or rank 2. In order to ensure a fair comparison, also two options are considered for the FRP case (FR1 and FR2). In FR1 case, all the four cells are transmitting over the entire bandwidth, while in the FR2 case the bandwidth is divided in two chunks which are assigned to the cells in a way that the same chunk is allocated to the couple of cells located at the largest physical distance in our deployment. Results are presented in terms of Empirical Cumulative

Distribution Function (ECDF) of the cell throughput. As mentioned in the previous section, a throughput estimate for each cell is obtained by mapping their estimated SINR to the Shannon rate. Note that the results are scaled from the operational bandwidth of the USRP N200 boards to the 200 MHz bandwidth targeted by the envisioned 5G concept for cm-waves [1].
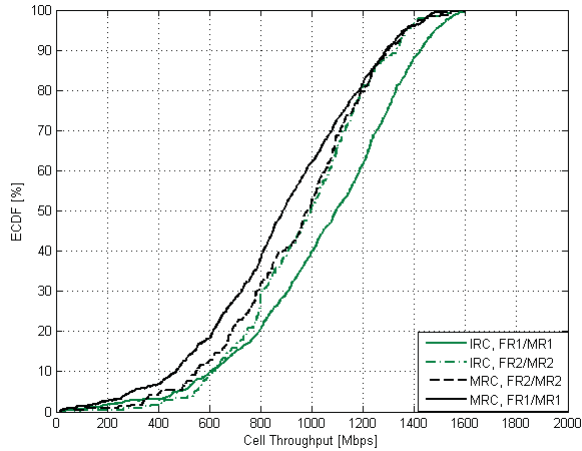


**Fig. D.4:** Cell throughput ECDFs for MRP and FRP at high load (100% cell activity factor).

**Table D.1:** The data rate performance in Mbps for both receiver types (MRC and IRC) at high load (100% cell activity factor)

| IRC | | | |
|---|---|---|---|
| | FRP | MRP | Gain (MRP over FRP) |
| Outage | 549.0 | 494.1 | -10.0 % |
| Median | 996.2 | 1095.0 | 9.0 % |
| Peak | 1371.0 | 1480.0 | 8.0 % |

| MRC | | | |
|---|---|---|---|
| | FRP | MRP | Gain (MRP over FRP) |
| Outage | 426.9 | 297.6 | -30.3 % |
| Median | 990.1 | 881.1 | -11.0 % |
| Peak | 1362.0 | 1362.0 | 0.0 % |

Figure D.4 shows the cell throughput performance of the network assuming 100% activity factor (corresponding to the case when each cell is in full buffer traffic mode), for different FRP/MRP combinations and the two receiver types, while Table D.1 reports the outage (5%-tile), median (50%-tile) and peak (95%-tile) data rates extracted from the figure. As already verified in our previous experimental activity [4], the usage of IRC clearly improves the performance for all the cells with respect to the MRC receiver, which is unable of suppressing any interferer. As a consequence, for the MRC receiver case the usage of FRP is more beneficial than MRP since it reduces the overall amount of interfering power, while MRP only reduces the rank of the interfering cells. In the case of IRC receivers, MRP leads instead to better performance than FRP in 90% of the cases. The possibility of suppressing one interfering stream enabled by the usage of the IRC receiver with MR1 turns out to be beneficial for the situation characterized by a dominant interferer, which can easily appear in the specific scenario of our experimentation. The walls and/or corridor separation between the cells makes indeed very likely that each cell is mainly interfered by one neighbor. On the other hand, FRP has still better outage performance; this represents the cases in which the specific deployment of the APs/UEs creates more equally strong interferers, limiting the benefit of being able to suppress only one, and then benefiting from a division of the spectral resources.
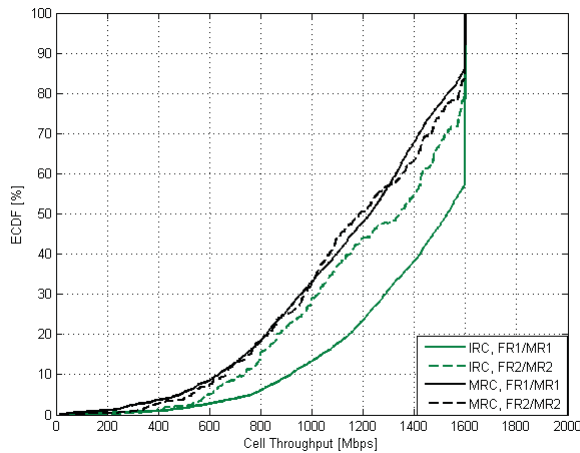


**Fig. D.5:** Cell throughput ECDFs for MRP and FRP at low load (50% cell activity factor).

The results with 50% activity factor are depicted in Figure D.5, and the corresponding extracted outage, median and peak data rates are reported in Table D.2. In this case, MRP clearly boosts its performance gain with respect to FRP, also improving the outage performance (+29%). Such throughput

**Table D.2:** The data rate performance in Mbps for both receiver types (MRC and IRC) at low load (50% cell activity factor)

| IRC | | | |
|---|---|---|---|
| | FRP | MRP | Gain (MRP over FRP) |
| Outage | 594.2 | 763.9 | 29.0 % |
| Median | 1343.0 | 1530.0 | 14.0 % |
| Peak | 1600.0 | 1600.0 | 0.0 % |

| MRC | | | |
|---|---|---|---|
| | FRP | MRP | Gain (MRP over FRP) |
| Outage | 529.1 | 485.2 | -8.0 % |
| Median | 1188.0 | 1228.0 | 3.4 % |
| Peak | 1600.0 | 1600.0 | 0.0 % |

improvement is due to the fact that a lower activity factor reduces the number of active interferers in each frame. This enhances the probability of presence of a dominant interferer, which represents the favourable condition for the IRC receiver task. Note that, in the FR1/MR1 combination, around 45% of the cells achieve the maximum throughput. Conversely, the performance of the MRC receiver is approximately the same for both MRP and FRP.

In general, the experimental results promote MRP as a simple and effective solution for interference mitigation in small cells networks.

## 5 Conclusions and future work

In this paper, we have presented an experimental evaluation of interference mitigation techniques in an indoor office scenario characterized by four small cells. Our SDR testbed is based on the USRP N200 hardware by Ettus Research and the ASGARD software platform, and each node features a $2 \times 2$ MIMO configuration. In particular, we have compared traditional frequency reuse planning (FRP) with the novel maximum rank planning (MRP) technique, which aims at suppressing the interference by exploiting the degrees of freedom offered by the multi-antenna techniques. Experimental results in the case of a fully loaded network reveal the benefit of using MRP as main interference mitigation technique since it outperforms FRP in 90% of the cases when IRC receivers are used, with only a penalty in terms of outage data

rates. In the case of moderate load (50% cell activity factor), the gain over FRP is further boosted, providing better performance for all the cells.

Our future work will focus on the evaluation of inter-cell interference mitigation solutions in larger testbed setup (e.g., eight cells) and as well as higher order MIMO configuration ($4 \times 4$), which offers higher degrees of freedom for balancing spatial multiplexing gain with interference resilience capabilities. In addition, advanced rank adaptation algorithms will also be considered.

# References

[1] P. Mogensen *et al.*, "5G small cell optimized radio design," *Globecom, International workshop on emerging techniques for LTE-Advanced and Beyond 4G*, 2013.

[2] F. M. L. Tavares, G. Berardinelli, N. H. Mahmood, T. B. Sørensen, and P. Mogensen, "Inter-cell interference management using maximum rank planning in 5G small cell networks," *11th International Symposium on Wireless Communications Systems (ISWCS), ISWCS2014*, 2014.

[3] T. O., G. Berardinelli, F. M. L. Tavares, A. F. Cattoni, I. Z. Kovács, T. B. Sørensen, P. Popovski, and P. Mogensen, "Experimental validation of a distributed algorithm for dynamic spectrum access in local area networks," *IEEE 77th Vehicular Technology Conference, VTC2013-Spring*, 2013.

[4] D. A. Wassie, G. Berardinelli, F. M. L. Tavares, O. Tonelli, T. B. Sørensen, and P. Mogensen, "Experimental evaluation of interference rejection combining for 5G small cells," *IEEE Wireless Communications and Networking Conference (WCNC 2015)*, 2015.

[5] (2014) NI USRP: Software defined radio platform,. [Online]. Available: http://www.ni.com/usrp/

[6] (2014) The asgard software radio,. [Online]. Available: http://asgard.lab.es.aau.dk

[7] J. Choi, *Optimal Combining and detection Statistical Signal Processing for Communications*. Camberidge University Press, 2010.

[8] Y. Ohwatari, N. Miki, T. Asai, T. Abe, and H. Taoka, "Performance of advanced receiver employing interference rejection combining to supress inter-cell interference," *IEEE Vehicular Technology Conference, VTC2011-Fall*, 2011.

[9] F. M. L. Tavares, G. Berardinelli, N. H. Mahmood, T. B. Sørensen, and P. Mogensen, "On the potential of interference rejection combining in B4G networks," *IEEE 78th Vehicular Technology Conference, VTC2013-Fall*, 2013.

[10] G. T. 36.211, "Evolved universal terrestrial radio access (E-UTRA); physical channels and modulation," 2012.

References

# Paper E

An Experimental Study of Advanced Receivers in a
Practical Dense Small Cells Network

Dereje Assefa Wassie, Gilberto Berardinelli, Fernando M. L.
Tavares, Troels B. Sørensen, Preben Mogensen

# Abstract

*5G is targeting a peak data rate in the order of 10Gb/s and at least 100Mb/s data rate is generally expected to be available everywhere. For fulfilling such 5G broadband targets, massive deployment of small cells is considered as one of the promising solutions. However, inter-cell interference leads to significant limitations on the network throughput in such deployments. In addition, network densification introduces difficulty in network deployment. This paper presents a study on the benefits of advanced receiver in a practical uncoordinated dense small cells deployment. Our aim is to show that advanced receivers can alleviate the need for detailed cell planning. To this end we adopt a hybrid simulation evaluation approach where propagation data are obtained from experimental analysis, and by which we analyse how MIMO constellation and network size impacts to the aim. The experimental data have been obtained using a software defined radio (SDR) testbed network with 12 testbed nodes, configured as either access point or user equipment. Each node features a $4 \times 4$ or a $2 \times 2$ MIMO configuration. The results demonstrate that advanced receivers with a larger MIMO antenna configuration significantly improves the throughput performance in a practical dense small cells network due to the interference suppression capability. In addition, the results prove that the operators can rely on uncoordinated deployment of small cells, since the resulting interference can be suppressed by the advanced receiver processing with sufficiently capable MIMO antenna configuration.*

# 1   Introduction

Currently, users located in indoor environment consume around 80% of all the mobile broadband traffic [1]. In addition, the data traffic demand is expected to increase at a tremendous pace year by year due to the proliferation of new services, broadband applications, rapid adoption of smartphones & devices and so on. To attain the demands, industry and academia are spending a significant effort on the design of a new 5th Generation (5G) radio access technology (RAT). 5G is expected to accommodate a wide range of diverse services, including new mission critical communication services targeting ultra-high reliability and very low latency transmission for e.g. industrial automation & vehicular to vehicular communication, massive machine type of communication and enhanced Mobile Broadband (eMBB) services.

5G is targeting a peak data rate in the order of 10Gb/s and at least 100Mb/s data rate is generally expected to be available everywhere [2] with respect to broadband applications. For fulfilling such 5G targets, network densification is crucial and a massive deployment of small cells is foreseen [3]. However, network densification complicates the network planning and raises challenging issues for site selection and acquisition in indoor small cells scenario. Furthermore, in dense small cells networks, the throughput perfor-

mance is mainly limited by inter-cell interference. With respect to that, an accurate site planning, i.e. selecting the locations and the number of cells, may reduce the impact of inter-cell interference and boosts the network throughput performance. However, this is very complicated in indoor environment due to a large number of walls and the different floor plans in each building. Therefore, operators are forced to make complex plans to find out where each cell should be installed in such a way that the interference is not a burden or operator can employ traditional inter-cell interference mitigation where the cells are configured to operate in different portions of the available spectrum. However, this approach will limit efficient usage of spectrum. In addition, the spectrum allocation will face a huge challenge due to a massive number of small cells. Alternatively, operators can employ uncoordinated deployment, which requires less planning and relies on advanced baseband processing at the receiver side to mitigate inter-cell interference.

The authors in [4] presented the envisioned 5G small cells concept in which the interference mitigation technique lies on the usage of the Interference Rejection Combining (IRC) receiver. The key working principle of the receiver relies on exploiting degrees of freedom of MIMO transceiver antenna for projecting the significant interfering signal over an orthogonal subspace of the desired signal to diminish the detrimental impact of inter-cell interference [5]. In addition, the envisioned 5G system frame structure design employs Time Division Duplex (TDD) mode, aiming to support efficient estimation of the interference covariance matrix, which is the key factor for the good performance of the IRC receiver [13]. Moreover, we have previously verified the potential of the IRC receiver towards boosting the network throughput in dense small cell scenarios based on both system level simulations [6] and experimental testbed networks [7].

In this paper, we address the potential benefit of the IRC receiver with different MIMO antenna configurations in a practical indoor dense small cells deployment and show its' inherent capability to cope with challenging interference conditions, and attain the best effort throughput improvement without the need for cell planning. We are adopting a hybrid simulation evaluation approach where the propagation models are replaced with actual measurement data obtained from a large testbed network. These field channel measurements provide the complete and factual information about all existing link combinations in a given deployment. The large testbed network consists of 12 software defined radio (SDR) testbed nodes which can be classified as 6 cells with one access point (AP) and one user equipment (UE), and the SDR nodes are equipped with a $4 \times 4$ MIMO antenna transceiver. Our previous work [7] on the experimental evaluation of advanced receivers considered a lower order MIMO antenna configuration and a limited number of cells. Here, we are assuming a larger, and more realistic, configuration of cells which can provide a further insight on the potential capability of the

IRC receiver where the interference conditions become challenging in practical dense small cell deployments dominated by inter cell interference. We also examine the impact of MIMO constellation size in combination with different number of cells, which configured to operate on the same carrier frequency, with the aim of showing that advanced receivers can alleviate the need for planning.

The paper is organized as follows. Section II presents our multi-link MIMO channel sounder testbed setup, while Section III presents the channel measurement campaign in an indoor office environment. Section IV discusses the experimental performance results of advanced receiver toward dealing with inter-cell interference in a practical uncoordinated dense small cells network. Finally, conclusions and future work are recalled in Section V.

# 2 Multi-Link MIMO Channel Sounder Testbed Setup

In this section, we present the multi-link MIMO channel sounder testbed. The testbed adopts Universal Software Radio Peripheral RIO (USRP-2953R) boards by National Instruments [9]. Each testbed node is composed of two USRP-2953R boards connected with PCI express cable to a host computer, as shown in Figure E.1. The USRP boards are used only as a radio-frequency front end, while the entire baseband processing runs on the host computer. The host computer runs a multi-link MIMO channel sounder application which is developed by using LabVIEW communications suite design environment [8]. Each USRP-2953R board has two radio frequency chains, and connecting the two URSP boards creates a testbed node with 4x4 MIMO transceiver configuration. The board's clock are synchronized, for ensuring synchronous transmission or reception, in such a way that the slave USRP-2953R board is exploiting the reference clock from the master USRP-2953R board.
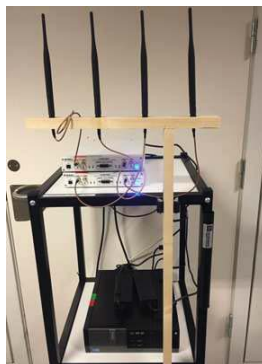


**Fig. E.1:** Testbed node with 4x4 MIMO transceiver configuration.

The channel sounder application is based on Orthogonal Frequency Division Multiplexing (OFDM) modulation, where the reference sequences (pilots) are mapped onto the sub-carriers in a frequency interleaved fashion and transmitted by the multiple antenna ports. At the receiver side, the channel frequency response is computed over the positions where the reference sequences are mapped based on Least Square estimator, and then linearly interpolated in order to obtain a response across the entire transmission bandwidth. Furthermore, the reference sequences are generated using constant amplitude zero autocorrelation sequence (CAZAC); since the sequence has a constant amplitude property [10], which contributes a prominent advantage for good channel estimation.

Moreover, the multi-link MIMO channel sounder provides the possibility to sound carrier frequencies spanning from 1.2 to 6 GHz with 40 MHz of bandwidth. Given a network with N testbed nodes, the channel sounder application allows estimating the $N \times N$ complex matrix of the channel responses between every couple of nodes within the network. The multi-link MIMO channel sounder application is based on the time division duplex (TDD) transmission mode; each node transmits his reference signals and receives the reference signals sent by the other nodes in a time interleaved fashion, as shown in Figure E.2. An estimate of the complex channel response for each link is obtained by demodulating the reference signals. The estimated complex channel response is sent to the testbed network controller through a backhaul network (Ethernet or WiFi) and logged for offline analysis.
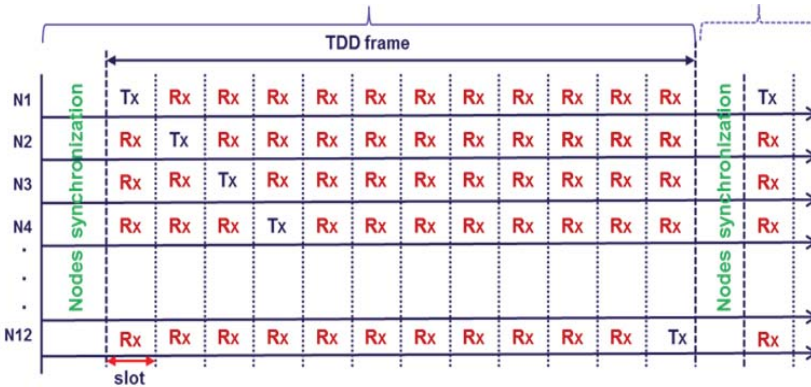


**Fig. E.2:** The multi-link channel sounder with TDD transmission mode for 12 SDR nodes.

During the offline processing, the estimated complex channel matrices of desired and interfering signal are provided as an input to the Signal-to-Interference plus Noise (SINR) estimator based on selected receivers type using a hybrid simulation approach. This estimated SINR is mapped to

throughput using the Shannon-Hartley formula, taking into account the highest order modulation being 256QAM (maximum spectral efficiency of 8 bits/s/Hz).

# 3 Measurement campaign in indoor environment

In wireless networks, the reliability of the network performance studies notably depends on the employed scenarios and propagation models. For instance, in any simulation study, it is expected that the propagation model should be able to reproduce precisely the conditions of any link as it is in real network deployment. However, this condition will not be achieved all the time due to the presence of several indoor building irregularities and also ever change of building materials. The work in [11] investigated the WINNER II path loss model in an indoor environment, and their observations show that such model does not accurately predict the path loss on the selected links. In this paper, the evaluation employs real channel measurement data rather than relying on the statistic based propagation models as described in previous section 1.

The channel measurement campaign has been executed in an indoor office scenario using our Multi-link MIMO channel sounder testbed. The measurement campaign is carried out at 5GHz band with a transmission bandwidth of 20MHz, and a transmit power of 10 dBm per antenna. During the campaign, the channel measurements are collected over 20 carrier frequencies spanning from 4.9GHz to 5.8GHz in order to experience different propagation conditions. Furthermore, multiple deployments with different propagation and geometrical characteristics have been taken into account to create different interference characteristics.

The channel measurement is attained in a typical indoor office environment with two pairs of adjacent rooms separated by a corridor as shown in Figure E.3, located at Aalborg University premises. As the figure depicts, the rooms have different size and divided by a concrete and plaster wall. These characteristics affect the signal propagation. In addition, there are also office furniture, black/white boards, and large office table lamps in the rooms which introduce a significant impact on the signal propagation pattern. Furthermore, the widespread presence of clutters and different building geometries plays a major role in shaping the interference characteristics.

The indoor office channel measurement campaign considered 18 possible different spatial locations as shown in Figure E.3. The campaign is carried out using 12 testbed nodes with 6 different deployments conditions for emulating different interference levels. For instance, one possible deployment of testbed node locations is highlighted with red dot circle in Figure E.3.
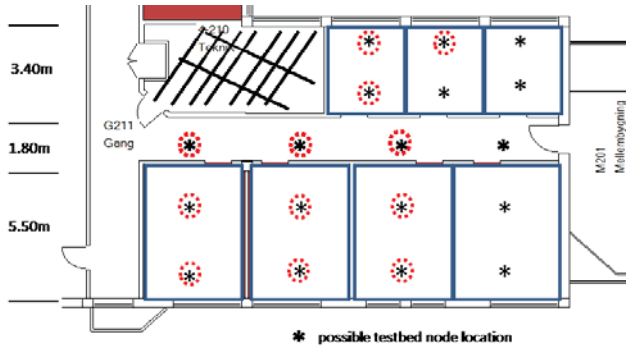
**Fig. E.3:** Indoor Office Scenario - 18 testbed node location.

# 4 Performance Evaluation

In this section, we present the network throughput performance results of our experimental analysis. The throughput results are computed for both an interference suppression receiver such as IRC, and an interference-unaware MIMO receiver, known as Maximum Ratio Combining (MRC), which exploits the MIMO antenna cardinality to maximize the power of the desired signal.

The performance results are generated using hybrid simulation approach considering 6 User Equipment (UEs), with Open Subscriber Group (OSG) access mode. The AP selection is based on the received power signal strength; each UE is connected to the AP which provides the highest received power. If there is an AP which does not serve any UE, it will be switched off and if an AP serves more than one UE, the UEs will equally share the available frequency resources.

The network performance is illustrated by the Empirical Cumulative Distribution Functions (ECDF) of users downlink throughput. In addition, three key performance indicator, namely Outage (5%-tile), median (50%) and peak (95%-tile), which are extracted from the ECDF results, are used in our performance analysis. Furthermore, during offline analysis, the throughput is scaled from transmission bandwidth of 20MHz to bandwidth of our envisioned 5G concept (200MHz) [12].

Figure E.4 shows the ECDF of UEs throughput for different MIMO transceiver antenna configurations, considering a single stream transmission. The performance results are generated for both IRC and interference-unaware receivers considering 6 cells with the OSG access mode. The IRC receiver boosts the throughput performance with respect to the interference-unaware receiver for both MIMO configurations in such dense small cells network. The outage data rate gain of IRC receiver over the interference-unaware receiver is

around 45% for a $2 \times 2$ MIMO configuration and 107% for a $4 \times 4$ MIMO configuration. The IRC receiver with single stream transmission mode uses the extra degree of freedom to suppress one interfering stream in $2 \times 2$ MIMO configuration cases and suppress up to three interfering streams in a $4 \times 4$ MIMO configuration case.
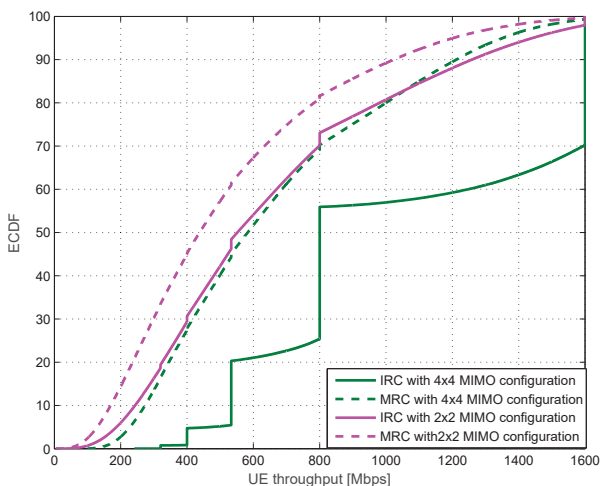


**Fig. E.4:** The ECDF of users throughput with different MIMO transceivers configuration, considering six deployed cells using both IRC and MRC receivers.

The higher order MIMO antenna configuration improves the throughput performance in such uncoordinated dense small cells network for both receivers as demonstrated by extracted KPIs in Table E.1; this is conventionally due to the gain on desired signal strength, and the IRC equipped system exploits the MIMO antenna cardinality for interference resilience purpose rather for spatial multiplexing. The results indicate that such deployments which lead to interference challenging situation are benefiting from a higher MIMO antenna configuration. Furthermore, the outage data rate gain of higher order MIMO configuration with respect to a lower MIMO configuration is significant when the users employ IRC receiver. Such significant gain is indeed achieved by the interference suppression capability of IRC receiver by suppressing three interferer cells 70% of the time in the case of $4 \times 4$ MIMO configuration with a single stream transmission mode. Since the number of active cells are less than or equal to four for 70% of the time as shown in Figure E.5, which means the users will face a maximum of three interfering streams with a single stream transmission mode.

Figure E.6 illustrates the ECDF of the user's throughput for a different number of deployed cells, considering both interference suppression and

**Table E.1:** The data rate performance in Mbps for both 2x2 and 4x4 MIMO antenna configurations for both receiver types (MRC and IRC), considering six deployed cells.

| Outage | | | |
|---|---|---|---|
| | 2x2 MIMO configuration | 4x4 MIMO configuration | Gain (4x4 over 2x2) |
| IRC | 187.6 | 470.3 | 150.7% |
| MRC | 129.5 | 227.9 | 75.9% |

| Median | | | |
|---|---|---|---|
| | 2x2 MIMO configuration | 4x4 MIMO configuration | Gain (4x4 over 2x2) |
| IRC | 550.4 | 800.0 | 45.7% |
| MRC | 440.2 | 581.6 | 32.1% |

| Peak | | | |
|---|---|---|---|
| | 2x2 MIMO configuration | 4x4 MIMO configuration | Gain (4x4 over 2x2) |
| IRC | 1443.0 | 1600.0 | 10.9% |
| MRC | 1205.0 | 1353.0 | 12.3% |
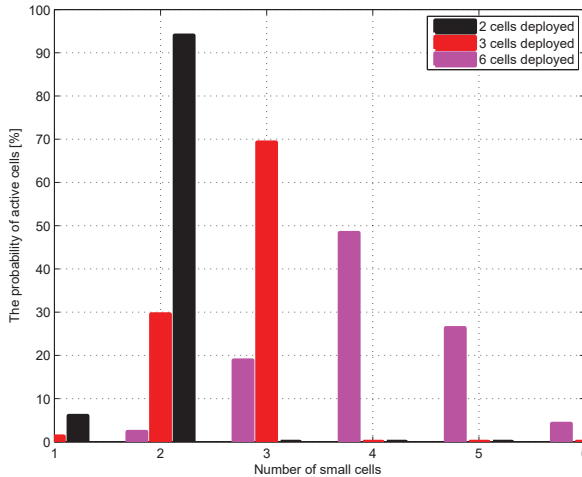


**Fig. E.5:** The probability of active cells with respect to a number of deployed cells.

interference-unaware MIMO receivers with a single stream transmission. The user's throughput performance is improved with increasing number of deployed cells when the system employs IRC receiver. In the contrary, this does not hold for the interference-unaware system. Further, when the number of deployed cells is increasing, the coverage of the network will increase and the number of users sharing the available resources per cell will decrease since the users will select other cells which provide them strong signal strength. This is illustrated with the probability of active cells, which are selected by the six users, as depicted in Figure E.5. On the other hand, the interference conditions are becoming more challenging and introduce a limitation on the throughput performance. However, interference suppression receiver equipped users are coping with increasing number of uncoordinated cells. This is also illustrated in Table E.2 in terms of outage, median, and peak data rate gain with respect to one cell deployment. The peak and median throughput gains are significant for a higher number of cells for both receivers. Increasing the number of deployed cells induces a loss in the outage data rate when the system employs inter-cell interference-unaware receiver. For instance, when the number of deployed cells is increased to three, the user's' outage data rate gain is severely compromised with the interference-unaware receiver. However, the IRC receiver provides up to +33% outage data gain with respect to having one deployed cell, by using the extra degree of freedom to suppress the two interfering cells. Therefore, one can claim that uncoordinated dense small cell deployments will significantly suffer from interference if the system utilizes interference-unaware receivers; increasing the number of cells will not alleviate the performance of vulnerable users substantially. On the contrary, increasing the number of uncoordinated cells can alleviate the performance if the system applies advanced receiver processing with a sufficient MIMO antenna configuration.

Table E.3 presents the outage data rate of a different number of cells when the users are equipped with a $2 \times 2$ MIMO configuration. The IRC throughput performance improvement with increasing number of cells does not hold. This is mainly because the IRC receiver has only one extra degree of freedom to suppress a strongest interferer stream in a $2 \times 2$ MIMO configuration equipped system with a single transmission mode. In addition, the IRC receiver throughput performance improvement will be challenged due to the lack of dominant interferer when the network consists of multiple cells with lower interfering levels. This has been noticed for a higher number of deployed cells. Generally, the operator can employ uncoordinated small cells deployment (which requires less planning) and rely on the advanced receiver with an acceptable MIMO antenna configuration to alleviate the interference burden.
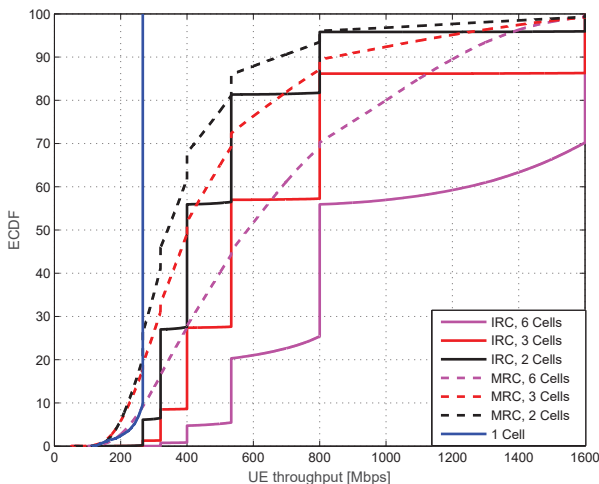
**Fig. E.6:** The ECDF of users throughput with different number of deployed cells using both IRC and MRC receivers - the APs and the UEs are equipped with 4x4 MIMO transceivers.

## 5 Conclusions and future work

In this paper, we demonstrated the usage of interference suppression receivers in a practical dense small cells network with a higher MIMO antenna configuration using a hybrid simulation evaluation approach where propagation data are obtained from experimental analysis. The experimental study has been carried out in a typical indoor office scenario, using a multi-link MIMO channel sounder testbed with 12 testbed nodes which can be configured as AP or UE, where each node can also feature a $4 \times 4$ or a $2 \times 2$ MIMO configurations. The testbed is developed using USRP-2953R hardware and LabVIEW communication suite software package by National Instruments. The evaluation results prove that the interference suppression receiver improves the throughput performance with respect to the interference-unaware MIMO receiver for both a $2 \times 2$ and a $4 \times 4$ MIMO configuration setup. The outage data rate gain of IRC receiver over the interference-unaware receiver is around 45% for a $2 \times 2$ MIMO configuration and 107% for a $4 \times 4$ MIMO configurations. Advanced receiver processing with a higher order MIMO antenna configuration boosts the throughput performance significantly in practical dense small cells deployment. With respect to that, the IRC receiver with 4x4 MIMO antenna configuration achieves +150% outage throughput performance gain with respect to 2x2 MIMO configuration. The evaluation results also show that increasing the number of cells will not alleviate the throughput performance when the system utilize interference-unaware receiver. On

**Table E.2:** The data rate performance gain of increasing number of deployed cells with respect to one cell for both receiver types (MRC and IRC), the nodes are equipped with a $4 \times 4$ MIMO configuration.

| | Outage | | |
|---|---|---|---|
| | Gain | Gain | Gain |
| | 2 Cells over 1 Cell | 3 Cells over 1 Cell | 6 Cells over 1 Cell) |
| IRC | 11.0% | 33.2% | 95.8% |
| MRC | -19.5% | -19.3% | -5.3% |

| | Median | | |
|---|---|---|---|
| | Gain | Gain | Gain |
| | 2 Cells over 1 Cell | 3 Cells over 1 Cell | 6 Cells over 1 Cell) |
| IRC | 50.0% | 100.0% | 200.0 % |
| MRC | 28.1% | 50.0% | 118.6 % |

| | Peak | | |
|---|---|---|---|
| | Gain | Gain | Gain |
| | 2 Cells over 1 Cell | 3 Cells over 1 Cell | 6 Cells over 1 Cell) |
| IRC | 200.0% | 500.0% | 500.0% |
| MRC | 200.0% | 345.4% | 406.9% |

**Table E.3:** The outage data rate in Mbps for different number of deployed cells considering both receiver types (MRC and IRC), the nodes are equipped with a $2 \times 2$ MIMO configuration.

| | 1 Cell | 2 Cells | 3 Cells | 6 Cells |
|---|---|---|---|---|
| IRC | 207.6 | **266.7** | 196.7 | 187.6 |
| MRC | 207.6 | 116.9 | 112.4 | 129.1 |

the contrary, increasing the number of uncoordinated cells can alleviate the performance if the system applies advanced receiver processing with a sufficient MIMO antenna configuration. Furthermore, the results indicate that the operator can deploy the dense small cells uncoordinated and the interference can be tackled by advanced receiver processing with sufficiently capable MIMO antenna configuration.

Our future work will focus on the experimental investigation on the potential benefit of uncoordinated dense small cell deployment with interference suppression receivers capability with respect to distributed antenna system in an indoor office environment.

# References

[1] Nokia Solutions and Networks.: Ten key rules of 5G deployment Enabling 1 Tbit/s/km2 in 2030. Nokia Networks white paper (2015)

[2] IMT Vision Framework and overall objectives of the future development of IMT for 2020 and beyond. International Telecommunication Union (ITU), radio communication Study Groups (2015)

[3] Bhushan, N. *et al.*: Network densification: the dominant theme for wireless evolution into 5G. IEEE Communications Magazine (2014)

[4] Mogensen, P. *et al.*: Centimeter-wave concept small cells. IEEE 79th Vehicular Technology Conference (2014)

[5] Choi, J.: Optimal Combining and detection Statistical Signal Processing for Communications. Camberige University Press (2010)

[6] Tavares, F. M. L. and Berardinelli, G. and Mahmood, N. H. and Sørensen, T. B. and Mogensen, P.: On the Potential of interference rejection combining in B4G networks. IEEE 78th Vehicular Technology Conference, VTC2013-Fall (2013)

[7] Wassie, D. A. and Berardinelli, G. and Tavares, F. M. L. and Sørensen, T. B. and Mogensen, P.: Experimental Verification of Interference Mitigation techniques for 5G small cells. IEEE 81st Vehicular Technology Conference, VTC2015-Spring (2015)

[8] National Instrument.: http://www.ni.com/labview-communications (2016)

[9] National Instrument.: http://www.ni.com (2016)

[10] Wen, Y. and Huang, W. and Zhang, Z.: CAZAC sequence and its application in LTE random acess. IEEE Information Theory Workshop (ITW) (2006)

[11] O. Tonelli.: Experimental analysis and proof-of-concept of distributed mechnisms for local area wireless network. PhD Thesis (2014)

[12] Mogensen, P. *et al*.: 5G small cell optimized radio design. IEEE Globecom, International workshop on emerging techniques for LTE-Advanced and Beyond 4G (2013)

[13] M. Lampinen, F. D. Carpio, T. Kuosmanen, T. Koivisto, and M. Enescu.: System-level modeling and evaluation of interference suppression receivers in LTE system. IEEE 78th Vehicular Technology Conference, VTC2013-Fall (2013)

References

# Part IV

# Radio Propagation and Multi-connectivity System Studies in Indoor Industrial Scenarios

# Radio Propagation and Multi-connectivity System Studies in Indoor Industrial Scenarios

This part addresses the radio propagation characterization study of indoor industrial scenarios, which is carried out in the context of very high reliable wireless communication. This section also presents the experimental validation of multi-connectivity solutions toward combating harsh propagation conditions of industrial scenarios - for improving the reliability of the wireless network. The experimental validation is performed using measured channel conditions which are obtained from measurement campaigns conducted in real indoor industrial scenarios.

## 1 Motivation

To automate the current industrial processes using a wireless network, very high reliable and robust wireless connections are required. In industrial scenarios, the reliability is mainly affected by the radio propagation conditions due to the rise of shadowing levels and a higher probability of Non-Line-of-Sight communication links [1]. These are caused by the presence of big machinery and different industry equipment. These features are expected to make the radio propagation conditions further harsh. However, limited studies have been carried out to characterize such severe propagation conditions. The work in [2], [3] investigated the large-scale propagation conditions of indoor industrial environments, using one-slope path loss models, i.e., alpha-beta (AB) model and close-in (CI) free-space reference [4]. The results indicated that the propagation conditions are challenging and have a waveguide effect due to the presence of big metal machinery and concrete

walls. Their analyses were based on limited spatial measurement samples, which were obtained only in specific locations or routes in a given industry hall environment. Therefore, the results may not comprehensively describe the propagation conditions of the scenarios. In that respect, one aim of this project is to investigate large-scale fading conditions in industrial scenarios using spatially distributed channel measurement system. The investigation is discussed in this section of the thesis.

Furthermore, to enhance the wireless network reliability in industrial scenarios, it is vital to improve the immunity of the radio coverage against the challenging propagation conditions. In such a scenario, the reliability could be enhanced by utilizing spatial diversity for the transmissions of the same data packets from multiple access points [1]. In fact, packet duplication is also seen as a fundamental technique for enhancing the reliability in the 5G wireless network, as agreed in 3GPP 5G new radio standard [5]. Such methods have been investigated using numerical analysis, and have shown significant potential for improving the reliability. The work in [6] analyzed the advantage of transferring the same data packet through uncorrelated channels from multiple access points. Similar work has also been carried out to show the benefit of such schemes using computer simulations in urban scenarios [7]. However, there is a lack of investigation toward validating the potential of such systems in real indoor industrial scenarios. In such scenarios, a very highly reliable wireless connection may increase the productivity of the industrial process. In that respect, besides the radio propagation study, this part of the thesis addresses the potential benefits of the multi-connectivity system in real indoor industrial scenarios.

## 2    Objectives

The aims of this part of the thesis are the following:

- Characterizing the large-scale propagation conditions of indoor industrial scenarios, and evaluating the one-slope path loss models (AB and CI models) toward predicting the severe propagation conditions in the given indoor industrial environments.

- Investigating the potential benefits of the multi-connectivity solutions toward enhancing the wireless network reliability using real channel conditions, in indoor industrial scenarios.

## 3    Included Articles

The articles that make the main body of this part of the thesis are:

**Paper F: Radio Propagation Analysis of Industrial Scenarios within the Context of Ultra-Reliable Communication**

This article discusses the large-scale radio propagation investigations in indoor industrial scenarios. The analysis is based on an extensive propagation measurement campaign that is performed using the testbed platform presented in Paper A. The study is conducted in different industrial topologies such as open production space and dense factory clutter. The impact of these industrial topologies is described using large-scale fading models. Besides, the models' capability towards capturing the occurrence of severe fading is also examined.

**Paper G: Multi-Connectivity for Ultra-Reliable Communication in industrial scenarios**

This article addresses the benefit of multi-connectivity techniques toward enhancing the reliability of wireless network in indoor industrial scenarios. Such a study is conducted using real channel measurement data collected from measurements campaigns carried out in two factories. The promising advantage of various multi-connectivity techniques is assessed and discussed in the article.

# 4 Main Findings

**The radio propagation large-scale fading behavior in industrial scenarios**

In indoor industrial scenarios, the radio channels characteristics are impacted by deep shadowing and severe fading due to the concrete building structures and the presence of huge metallic machinery, and these conditions become more challenging when the factory clutter (e.g., metallic machinery, cranes, robots) increases. The results in Paper F confirms that the radio channel conditions indeed become challenging due to the presence of more metallic machinery; which can be explained by higher path loss exponents and shadow fading levels observed in dense factory clutter, compared to the open production space factory environments. Further, such presence of machinery and confined indoor industrial buildings affect the line-of-sight (LOS) radio propagation channels to have a waveguiding effect. This is observed in the analysis in terms of lower path loss exponents compared to the free-space path loss.

Besides, Paper F demonstrated that widely used AB and CI large-scale propagation models can provide further insight into the observed radio propagation trends with respect to scenarios, frequencies, and antenna heights. However, it is observed that such models failed to predict the shadow fad-

ing levels correctly for the cases when the shadow fading distribution (i.e., log-normal distribution expressed by the average standard deviation which is computed using the models) is below the probability level of $10^{-2}$ percentile (99% of availability ). Therefore, it is essential to give close attention to the usage of the models to express the propagation conditions with a signal availability above the 99%, particularly in indoor industrial scenarios.

**The multi-connectivity system benefits in indoor industrial scenarios**

The learning from paper F indicated that radio propagations are harsh and challenging in Indoor industrial scenarios. Indeed, these will significantly impact the reliability of the wireless network since radio signal coverage is affected by the harsh conditions. Multi-connectivity techniques can improve signal quality by counteracting poor channel conditions. The initial experimental results in Paper G verified the potential benefit of the multi-connectivity solutions in indoor industrial scenarios. The benefit of multi-connectivity solutions comes from the use of additional communication links. The additional links increase the robustness of the signal transmission against harsh propagation effect due to the presence of industrial machinery. The results showed that the use of physical layer multi-connectivity techniques considerably improved the lower percentile of the SINR distribution. For example, at $10^{-2}$ percentile the usage of the multi-connectivity solutions improved the SINR by 8 dB compared with the system that employed single connectivity. In fact, such improvement of SINR is achieved due to the use of additional communication paths for transmitting a redundant packet to a user terminal which demands high reliability. Furthermore, it has been observed that physical layer multi-connectivity solutions (i.e., Single Frequency Network and Joint Transmission) provided better signal quality performance compared with higher layer solution (i.e., packet duplication at PDCP). The reasoning behind is that, in higher layer solution, multiple access points serving a user terminal generate mutual interference since they transmit the same packets at different time instances. However, the use of multi-connectivity solutions for improving reliability impacted the throughput performance of the mobile broadband users that are sharing the same network resource. This is because some resources of the network are taken from the broadband users to serve users requesting high reliability. The results in Paper G showed that the overall network capacity of mobile broadband users is significantly dropped while using multi-connectivity solutions to improve the reliability of a specific user terminal. This learning indicates that the use of multi-connectivity solutions for enhancing reliability should be carefully treated not to impact the mobile broadband users that are sharing the same network resource.

# References

[1] B. Singh, Z. Li, O. Tirkkonen, M. A. Uusitalo and P. Mogensen, "Ultra-reliable communication in a factory environment for 5G wireless networks: Link level and deployment study," 2016 IEEE 27th Annual International Symposium on Personal, Indoor, and Mobile Radio Communications (PIMRC), Valencia, 2016, pp. 1-5.

[2] E. Tanghe et al., "The industrial indoor channel: large-scale and temporal fading at 900, 2400, and 5200 MHz," in IEEE Transactions on Wireless Communications, vol. 7, no. 7, pp. 2740-2751, July 2008.

[3] S. Phaiboon,"Space diversity path loss in modern factory at frequency of 2.4GHz,"in WSEAS transactions on communications, vol. 13, 2014.

[4] M. Peter, W. Keusgen and R. J. Weiler, "On path loss measurement and modeling for millimeter-wave 5G," 2015 9th European Conference on Antennas and Propagation (EuCAP), Lisbon, 2015, pp. 1-5.

[5] 3GPP Tech. Spec. 38.323, "NR; Packet Data Convergence Protocol (PDCP) Specification," v0.21, Aug. 2017.

[6] J. Rao and S. Vrzic, "Packet Duplication for URLLC in 5G: Architectural Enhancements and Performance Analysis," IEEE Network, vol. 32, no. 2, pp. 32-40, March 2018.

[7] Melisa López Lechuga, "Multi-Connectivity in 5G New Radio: Configuration Algorithms and Performance Evaluation ," Mater thesis, Aalborg University, 2018.

References

# Paper F

Radio Propagation Analysis of Industrial Scenarios within the Context of Ultra-Reliable Communication

Dereje Assefa Wassie, Ignacio Rodriguez, Gilberto Berardinelli, Fernando M. L. Tavares, Troels B. Sørensen, Preben Mogensen

# Abstract

*One of the 5G use cases, known as ultra-reliable communication (URC), is expected to support very low packet error rate on the order of $10^{-5}$ with a 1 ms latency. In an industrial scenario, this would make possible replacing wired connections with wireless for controlling critical processes. Industrial environments with large metallic machinery and concrete structures can lead to deep shadowing and severe fading in the radio propagation channel, and thus pose a challenge for achieving the outage levels in connection with URC. In this paper, we present and analyze the large-scale propagation characteristics of two different industrial environments - open production space and dense factory clutter - based on measurements conducted at 2.3 and 5.7 GHz*

*By including a large number of spatially distributed samples, as per our experimental approach, we show the importance of properly characterizing the large-scale fading outage for URC. For instance, we show that based on a simple one-slope distance dependent path loss model, the conventional log-normal model for large-scale shadow fading is by far too simple for this environment. Our results show that at the $10^{-4}$ percentile, the tail of the shadow fading distribution can deviate by up to 10-20 dB from the log-normal model with respect to the average NLOS values (around 6 dB and 8 dB at 2.3 and 5.7 GHz, respectively). The simplicity of the one-slope path loss model, and its ability as we show, to express the trends with respect to scenarios, frequencies, and antenna heights, makes it an attractable option. However, there is a need for further experimental insight, possibly in combination with deterministic analysis, to get a better understanding of the large-scale fading for the study of URC in industrial environments.*

# 1 Introduction

One of the key features of the 5G wireless communication system is the support of new mission-critical applications which demand high reliability, known as ultra-reliable communication. Most of ultra-reliability communication services require 99.999% reliability and usually very low latency [1]. Furthermore, ultra-reliable communication opens a wide range of use cases, such as industry automation, vehicular communication for traffic safety/control, and energy management.

With respect to industry automation, ultra-reliable communication enables a significant benefit on monitoring and controlling the physical process of the industry, such as assembly lines and logistics, by offering a more flexible communication infrastructure compared with the existing wired communication. However, there are many challenges to be addressed for verifying the potential of ultra-reliable communication in an industrial environment, such as the radio propagation conditions. The radio propagation conditions

in large industrial buildings are expected to be severe due to concrete structure and presence of large metallic machinery. This condition may affect the spatial availability of the wireless communication signal. In that respect, extensive radio propagation measurements are crucial to understand the radio channel characteristics in the context of ultra-reliable communication in such environments. Particularly for this context, one needs to understand the occurrence and characteristics of severe fading, which is commonly expressed in the tails of the shadow fading distributions. A considerable effort on the measurement campaign is therefore needed to ensure a large number of measurement samples over multiple locations, containing representative information about the diverse radio propagation possibilities in the environment.

Limited works have been done on characterizing the radio propagation aspects of the industrial environments. The work in [2] investigated the large-scale radio propagation characteristics at a frequency of 1.3 GHz in different factories like food processing, engine factory, and aluminum manufacturing. The measurements were performed at three measurement locations in each factory where the transmitter and receiver separation range was between 10 m and 80 m and the transmitter/receiver antennas were 2 m above the ground. A similar narrow-band study was also executed at a carrier frequency of 2.4 GHz in a chemical pulp factory, a cable production hall, and a nuclear power plant [3]. The measurements were executed along two measurement routes with a maximum distance of 95 m. The work in [4] also explored the propagation characteristics in a nuclear power plant environment with the measurements being executed at nine positions with a maximum transmitter and receiver separation distance of 13 m. In [5], propagation measurements were carried out at frequencies of 900 MHz, 2.4 GHz, and 5.2 GHz in wood and metal processing factories. The measurements were performed with a transmitter antenna height of 6 m and receiver antenna height of 2 m with a maximum distance of 140 m in between, and a different number of path-loss samples were also collected for the three frequencies. The work in [6] investigated different empirical path loss models for industrial environment radio coverage by measuring the received signal strength indicator (RSSI) of the beacon frame transmitted by IEEE802.11a/b/g access points. The measurements were conducted along two measurement routes using two access points installed at 2 m and 4.85 m with the receiver being at 1 m above the ground. Measurements spanning over a large frequency band 200-2500 MHz were also carried out in an industrial environment [7] where the transmitter/receiver antennas were mounted 1 m above the floor. The measurements included 1601 measurement points with a maximum distance of 18 m between the transmitter and receiver locations. In addition, large-scale radio propagation in the civil engineering laboratory, which consists of soft and hard structure besides machinery, was also investigated in [8] at a

frequency of 2.4 GHz with a 36 path loss samples, where the transmitter was mounted at three different heights like 1.5 m, 2 m, and 3 m and the receiver installed only at 1.71 m above the floor.

In most of aforementioned works, the spatial measurement coverage over a given industrial environment was restricted, and had relatively low number of representative measurement points (in the order of tenths to few thousands). In addition, most of the measurements were carried out over specific measurement routes on a limited set of locations; with the objective to characterize the tails of the distribution, viz ultra-reliable communication, this is likely insufficient.

This paper presents an empirical analysis of wideband large-scale radio propagation in two industrial scenarios at 2.3 GHz and 5.7 GHz. Compared to previous studies, extensive measurement campaigns are performed for obtaining a total of 8,832 wideband path loss measurement samples per frequency and scenario. The measurements are conducted at 24 uniformly spatial-distributed locations in each scenario for multiple antenna configurations considering all possible link combinations between two different heights: 0.25 and 1.75 m. Our measurement approach allows better spatial coverage of the environments, facilitating, at least, a partial characterization of the tails of the shadowing distributions.

The rest of the paper is organized as follows. In Section II, the measurement setup and industrial scenarios are introduced. Section III discusses the wideband large-scale propagation measurement results and derived models, and presents the results in the perspective of ultra-reliable communication. Finally, the conclusion of the study is drawn in Section IV.

# 2   Measurement setup and scenarios

## 2.1   Industrial Scenarios

Two industrial production lab facilities were selected as scenarios for the measurements. These facilities are located at the Department of Mechanical and Manufacturing Engineering, Aalborg University. The first lab is an "open production space" (OPS) which consists of laboratory machinery, robots and a production line, surrounded by relatively large empty areas around the different production equipments. The second lab is a "dense factory clutter" (DFC) facility where large metallic machinery is present like metal welding machines, hydraulic press, and material processing machines. Both labs have a similar size of approximately $35 \times 14 \times 6$ m. As it can be seen in Figures F.1 and F.2, which display an overview of both scenarios, the DFC represents a denser industrial clutter type than the OPS.

The measurements are performed at 24 locations which are approximately

**Fig. F.1:** View of Lab1, open production space (OPS).



**Fig. F.2:** View of Lab2, dense factory clutter (DFC).

uniformly spatial-distributed over each lab facility with a minimum and maximum distance of 2 m and 34 m respectively. The measurement locations are carefully selected based on visual inspection to investigate the radio propagation in LOS (Line-of-Sight) and NLOS (Non-Line-of-Sight) conditions. In the OPS lab facility, 15% and 85% of the measurement points are classified to be in LOS and NLOS conditions respectively, while the DCF lab facility has slightly less measurement points in LOS condition (11%). During the static measurement campaign, the measurement acquisition nodes are deployed at 12 different locations and the path loss between each node antennas is estimated from measured channel transfer function. Multiple redeployments of this setup are executed for each frequency to estimate the path loss between all possible combinations of the measurement locations; with this, a total of $24 \times 23$ spatial combinations considering all the different antenna configurations (higher link 1.75 m -1.75 m, lower link 0.25 m - 0.25 m, and the cross-link between the high and low antenna heights 1.75 m - 0.25 m) are estimated, resulting in 8,832 measurement links. These antenna heights were both selected below average surrounding clutter height, in order to increase the shadowing probabilities and levels in NLOS conditions as compared to clear LOS (which would have been the case of having antennas above average clutter height). By doing this we have two different references of, for example, two representative heights at which sensors or controllers in future automation systems will be deployed.
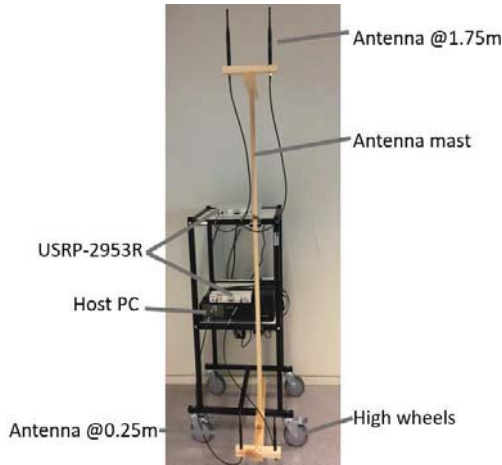
## 2.2 Measurement setup



**Fig. F.3:** Measurement acquisition node.

The measurement setup is based on a software-defined radio (SDR) platform. Our platform is based on USRP-2953R [9] which supports synchronized transmission and reception of wireless radio signal over two radio frequency (RF) chains within the frequency range 1.2-6 GHz. A measurement acquisition node is built from two USRP boards which allow a synchronized transmission or reception of RF signal over four RF chains. Figure F.3 depicts the measurement acquisition node with a support of two selected antenna heights (1.75 m and 0.25 m) and two dipole antennas mounted at each specific height. The overall testbed measurement setup consists of 12 acquisition nodes, where coordinated transmission and measurement acquisition are based on time-division multiplexing (TDM); while only one node is transmitting a reference signal with a 24 MHz bandwidth over four transmitter antennas in a time-interleaved fashion, the other nodes are simultaneously receiving and recording the signal over the four antennas. The wideband received power [1] on each antenna port is calculated for estimating the path loss between all possible 16 combinations of transmitter and receiver antennas among the nodes.

Each antenna port transmits a calibrated power of about 6 dBm and 5 dBm for 2.3 GHz and 5.7 GHz, respectively. Each of the receivers has a sensitivity level of -100 dBm. The antennas at both sides were similar with a peak gain of approximately 2 dBi at both frequencies. By exploiting noise averaging

---

[1]Complex channel transfer function measurements were performed so it will also possible to estimate other channel parameters such as power delay profile, however, the focus of this paper is only on large-scale propagation.

techniques (which provides a 29.5 dB processing gain) and considering a 10 dB SNR level, the maximum measurable path loss is about 126 dB at 2.3 GHz and 125 dB at 5.7 GHz. The measurement setup has been calibrated in an outdoor open space environment within LOS conditions, where the measured path loss was verified to match with free-space path loss with a maximum deviation of $\pm 1.5$ dB.

# 3 Results and discussion

Large-scale propagation refers to the received signal power attenuation (path loss) with distance where the relation can be expressed by using statistical models which capture the logarithmic distance-dependence [10]. The general formulation is given as follows:

$$PL(d) = PL(d_0) + 10\gamma log_{10}\left(\frac{d}{d_0}\right) + X_\sigma \tag{F.1}$$

Where $PL(d)$ is the path loss at distance $d$ (in m) between the transmitter and receiver in dB, $PL(d_0)$ is the intercept/reference point which is known as the mean path loss in dB at reference distance $d_0$ in m, $\gamma$ is the path loss exponent and $X_\sigma$ is a zero-mean Gaussian random variable with standard deviation $\sigma$ in dB. The parameters $PL(d_0)$, $\gamma$ and $\sigma$ are commonly estimated by least-square fitting of measurement data using different models, such as the alpha-beta (AB) model and the close-in (CI) free-space reference distance model [10]. The main difference between the models relies on the statistical linear regression intercept; in the AB model, the intercept (known as $\beta$) is determined by the least-square fit of measurement data while in CI model the intercept is equal to the free-space path loss at a reference distance $d_0=$ 1 m. In this work, the path loss exponent $\gamma$ of AB and CI models is expressed as $\alpha$ and $n$ respectively. In addition, $X_\sigma$ is usually modeled as log-normal distribution, with a variability equal to the standard deviation of the residuals. The residuals are calculated from the deviations of the measurement data from the model least-square fitting; these provide an indication on the shadow fading level. We use both the AB and CI models for highlighting the large-scale propagation differences among the considered industrial scenarios, frequencies, and antenna heights.

## 3.1 Large-scale propagation measurement results and derived models

In this subsection, large-scale propagation measurement results and parameterization of the AB and CI path loss models are presented. These models are well known and widely used statistical large-scale propagation models [10].

They are also considered as a baseline for comparison of the propagation in different conditions, frequencies, and scenarios.
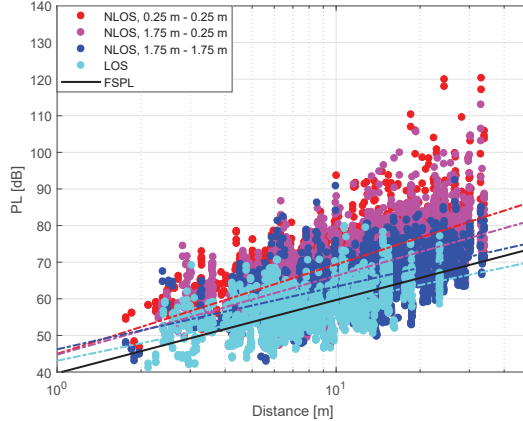


**Fig. F.4:** Measured path loss and AB model for OPS industrial lab facility at 2.3 GHz frequency, LOS condition and NLOS condition with different antenna heights.

Figure F.4 shows the measured path loss results and the least-square fitted AB model for the OPS facility at 2.3 GHz. In the figure, path loss results are categorized in LOS conditions and NLOS conditions for the different antenna configurations (higher, cross and lower links). The derived AB model for each of the cases is represented with a dashed line of a different color. As a reference, the figure also depicts the free-space path loss (FSPL) at 2.3 GHz. As it can be seen, the LOS propagation follows the free-space path loss. In addition, the figure shows that the path loss versus distance slope becomes steeper for configurations with low antenna height. This is caused by obstacles in the propagation paths since the lower transmitter/receiver antennas are mounted 0.25 m above the floor and located clearly below the average factory equipment height as compared to the highest antenna location. Similar trends, with different numerology are observed at 5.7 GHz as compared to 2.3 GHz at both lab facilities, but we have decided not to show them explicitly as they will result in a very similar plot to Figure F.4. A summary of the parametrization of all derived path loss models, considering all cases, can be found in Table F.1.

As it can be seen in the table, both the AB and CI models exhibit similar trends. The LOS path loss exponent of the CI model is close to the free-space path loss exponent ($n = 1.9 - 2.0$) for both frequencies and industrial environments. However, in the AB model prediction, which is the direct fit of the measurement data, the path loss exponent is lower than free space ($\alpha = 1.0 - 2.0$). This indicates that waveguiding effects are introduced by

Table F.1: Summary of the large-scale propagation parameters for both Industrial Lab facilities across different frequency and antenna height configurations.

| Frequency | Conditions | Transmitter - Receiver Antenna Height Configurations | AB Model $\beta$ [dB] | $\alpha$ | $\sigma$ [dB] | CI Model $n$ | $\sigma$ [dB] |
|---|---|---|---|---|---|---|---|
| **Lab1, open production space (OPS)** | | | | | | | |
| 2.3 GHz | LOS | 1.75 m-1.75 m (higher) | 43.1 | 1.6 | 5.1 | 2.0 | 5.2 |
| | | 1.75 m-0.25 m (cross) | 46.2 | 1.7 | 6.0 | 2.3 | 6.1 |
| | NLOS | 1.75 m-0.25 m (cross) | 44.7 | 2.2 | 6.0 | 2.6 | 6.1 |
| | | 0.25 m-0.25 m (lower) | 45.0 | 2.4 | 6.2 | 2.9 | 6.3 |
| 5.7 GHz | LOS | 1.75 m-1.75 m (higher) | 46.2 | 2.0 | 5.6 | 1.9 | 5.6 |
| | | 1.75 m-0.25 m (cross) | 48.6 | 2.2 | 7.0 | 2.3 | 7.0 |
| | NLOS | 1.75 m-0.25 m (cross) | 48.8 | 2.5 | 7.6 | 2.7 | 7.6 |
| | | 0.25 m-0.25 m (lower) | 42.5 | 3.4 | 9.1 | 3.0 | 9.2 |
| **Lab2, dense factory clutter (DFC)** | | | | | | | |
| 2.3 GHz | LOS | 1.75 m-1.75 m (higher) | 47.8 | 1.0 | 5.1 | 2.0 | 5.4 |
| | | 1.75 m-0.25 m (higher) | 42.7 | 2.0 | 5.6 | 2.3 | 5.6 |
| | NLOS | 1.75 m-0.25 m (cross) | 42.0 | 2.5 | 6.5 | 2.7 | 6.5 |
| | | 0.25 m-0.25 m (lower) | 42.6 | 2.8 | 7.6 | 3.1 | 7.7 |
| 5.7 GHz | LOS | 1.75 m-1.75 m (higher) | 52.9 | 1.3 | 5.5 | 1.9 | 5.6 |
| | | 1.75 m-0.25 m (higher) | 46.5 | 2.5 | 7.2 | 2.4 | 7.2 |
| | NLOS | 1.75 m-0.25 m (cross) | 47.2 | 2.8 | 8.3 | 2.8 | 8.3 |
| | | 0.25 m-0.25 m (lower) | 42.9 | 3.5 | 9.1 | 3.1 | 9.1 |

the confined environment and the presence of many large metallic machines. Some evidence to this can be seen in the fact that the DFC environment, having more metallic machines, exhibits lower path loss exponents compared with the OPS scenario. Similar findings were also reported in [3], [5] and [8]. In NLOS condition most of the propagation paths are obstructed by the presence of factory machinery, which leads to extra losses, resulting in higher path loss exponents for both of the AB and CI modeling approaches.

The path loss exponents in NLOS conditions are clearly dependent on the antenna height; the path loss exponents are increaseing for configurations with lower transmitter/receiver antenna height. For instance, with focus on 2.3 GHz and the OPS scenario, it can be seen that the path loss exponent of the AB model ($\alpha$) increases from 1.7 to 2.4 when we look at the higher and the lower link, respectively. A similar conclusion can be reached by looking at the CI model fit in the same scenario, where in this case the path loss exponent ($n$) increases from 2.3 to 2.9. As it was explained in connection to Figure F.4, the configurations with lower antenna heights have a higher probability of propagation paths blockage and lead to larger path loss exponents as compared to the configurations with higher antenna heights, which are closer to LOS conditions. This fact also explains the larger shadow fading standard deviation ($\sigma$) for configurations with lower antenna height. For instance, and with focus on the same scenario, OPS at 2.3 GHz, the standard deviation considering the AB model increases from 6.0 dB in the higher link to 6.2 dB in the lower link. Very similar standard deviation values are observed with both the AB and CI modeling approaches. This indicates a very similar fit in both cases.

The DFC scenario presents larger shadow fading levels as a consequence of the higher NLOS probability due to the presence of more metallic machinery as compared to the OPS scenario. This results into a higher NLOS path loss exponent and standard deviation. For 2.3 GHz, the path loss exponents ($\alpha$) in the DFC scenario are in the range 2-2.8 (as compared to the 1.7-2.4 in the OPS), and the standard deviation is up to 1.4 dB larger than in the OPS scenario.

By looking at the frequency dependency, the path loss exponents and shadow fading standard deviation increase when the frequency increases from 2.3 GHz to 5.7 GHz for both LOS and NLOS conditions. On the other hand, the work in [5] reported that the path loss exponent and shadow fading standard deviation decrease with increasing frequency. These can be explained by the antenna height difference; in [5] the transmitter and receiver antenna height were mounted in 6 m and 2 m above the floor respectively, this transmitter antenna height is far above the height of the large metallic machinery, whereas in our setup the transmitter and receiver are mounted 1.75 m or 0.25 m above the ground whose heights are comparable with the height of the large machines or below. Because of this height difference, our

NLOS scenario seems to be driven by diffraction and blockage, while the scenario in [5] seems to driven by reflection due to the elevated transmitter height clearly above the average machinery clutter height.

In perspective of exploring the challenge related to achieving higher levels of reliability, it is worth to be mentioned that the worst propagation conditions are observed in the DFC with a maximum mean path loss exponent of up to 2.8 and 3.5 for 2.3 and 5.7 GHz, respectively. In terms of shadow fading standard deviation, the maximum observed values are 7.6 dB at 2.3 GHz and 9.1 dB at 5.7 GHz.

## 3.2 Measurement results in perspective of ultra-reliable communication

In order to remove cable connections in industrial scenarios and replace them with 5G wireless units, very stringent requirements in terms of maximum packet error rate ($10^{-5}$) and latency (1 ms) should be met [1]. Regarding that matter, the work in [11] indicated that to provide such ultra-reliable communication, the focus should be on the behavior of the channel at probabilities of $10^{-5}$ or less in the signal reception. These probabilities reflect the occurrence of rare events which may have significant impact on the radio signal availability, and thus in the reliability in a given scenario. Based on that argumentation, any channel model used in the design and evaluation of 5G ultra-reliable systems should be derived or validated based on well planned and extensive measurement data sets, containing enough representative information of the propagation in the scenario to capture the occurrence of those rare events.

Following the previous premises, we try to illustrate and highlight the impact of such rare events in the ultra-reliability regime, by analyzing the shadow fading distributions extrapolated from our measurements. Figure F.5 depicts the complementary cumulative distribution function (CCDF) of the empirical shadow fading distributions, considering all the LOS and NLOS samples and all the different antenna configurations, computed over the AB model for both the OPS and DFC scenarios at 2.3 and 5.7 GHz. As a reference for the analysis, the figure also displays a theoretical reference based on the model in (F.1), in which the common assumption of log-normal shadow fading has been applied with average NLOS standard deviation (6.1 dB at 2.3 GHz and 8.3 dB at 5.7 GHz). As it can be seen, the different empirical OPS and DFC distributions follow closely the log-normal reference distribution, with deviations smaller than 1 dB up to levels of approximately $10^{-1}$ (90% of availability). Below that probability, large-scale fading levels deviate considerably from the assumed model, despite being parametrized with the same standard deviation. This deviation is as large as 20 dB at the $10^{-3}$ percentile (observed at 2.3 GHz in the DFC scenario) and larger for

lower percentiles (24 dB close to the $10^{-4}$ percentile – 99.99% of availability).
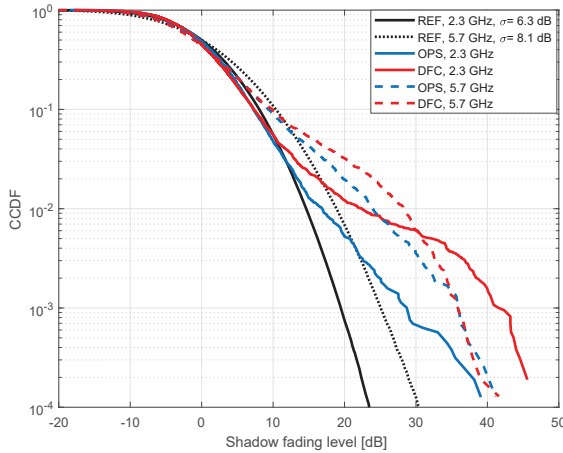


**Fig. F.5:** Complementary cumulative distribution function of the measured shadow fading level in both the OPS and DFC facilities for both frequencies.

Further, the empirical shadow fading distributions show that the scenario (clutter type) has a larger impact at 2.3 GHz than at 5.7 GHz. In the DFC the shadowing can be as severe as 46 dB close to the $10^{-4}$ level while the OPS is approximately 8 dB better. For the same probability level, at 5.7 GHz, both the OPS and DFC exhibit a similar shadowing level of approximately 40 dB. The same conclusion can be reached by looking at the overall distribution trends, where it is clearly visible that both the OPS and DFC distributions are very similar at 5.7 GHz. On the other hand, at 2.3 GHz, the DFC distribution presents larger shadowing levels than the OPS distribution. A possible explanation for the observed trends can be that, in the industrial scenarios, at 2.3 GHz, diffraction is dominant over other propagation mechanisms, which translates into larger losses for larger NLOS probabilities, and thus a larger loss in the DFC as compared to the OPS. Differently, at 5.7 GHz, other propagation mechanisms may have relatively larger impact, e.g. reflection (and scattering) losses, to reduce the difference between the two clutter types.

One can speculate that the deviations from the log-normal reference will continue to increase for even lower outage probabilities like the targeted $10^{-5}$ which should set the margin for the planning of ultra-reliable systems. Experimentally verifying this is proven to be difficult. Despite our measurement effort to collect a large number of spatially distributed samples, further work is needed to make accurate predictions on the lower tail of the distribution.

### 3.3 Point-cloud simulations as a complement to the measurements

In order to extend further the statistics from measurements and to characterize the environment with higher resolution, we are exploring the feasibility of basing the analysis on deterministic field predictions built on point-cloud methods [12]. These ray-tracing techniques use as an input detailed maps of the environment rather than simplified geometrical descriptions of it. These maps are based on the laser scan of the physical environment, and take the shape of a cloud of points representing the different interaction points of the laser ray with the obstacles present in the environment. Based on this cloud of points, it is possible to simulate the propagation between two locations inside the scenario by considering these points of interaction as potential sources of diffraction, reflection or scattering. The simulation will be calibrated by using a subset of the measurements, while another will be kept for verification. From the calibrated predictions, we expect to be able to match the channel statistics for the higher percentiles, getting more detailed insight onto the lower tails. The advantage of using such prediction methods is the possibility of running "virtual" measurement campaigns over a much larger number of locations, situations, or link combinations than in a real-world measurement campaign.

## 4 Conclusions

This paper presented the results and analysis of wideband large-scale propagation based on extensive measurements performed in two different industrial scenarios (open production space and dense factory clutter) at 2.3 GHz and 5.7 GHz. The measurements were conducted over a total of 24 uniformly spatial-distributed locations in each of the labs, considering multiple antenna configurations at 0.25 and 1.75 m heights. The results show that in both scenarios, the path loss exponents ($\alpha$) are below 2 in LOS, due to the waveguiding effects caused by multiple reflections on the many metallic machines. In NLOS conditions, the path loss exponents increase for lower antenna heights, reaching values of up to 2.4 and 3.4 at 2.3 and 5.7 GHz, respectively, in the open production space. This values are larger in the dense factory clutter, reaching values of 2.8 at 2.3 GHz and 3.5 at 5.7 GHz. The same increasing trend with lower antenna heights is observed for the shadow fading standard deviations ($\sigma$). In this case, the maximum values at 2.3 GHz and 5.7 GHz are, respectively, 6.2 and 9.1 dB and in the open production space and 7.6 and 9.1 dB in the dense factory clutter. From the analysis of the lower percentiles of the shadow fading distributions, it is possible to see that the shadow fading levels can be as severe as 38-46 dB at 2.3 GHz, and approxi-

mately 40 dB at 5.7 GHz, close to the $10^{-4}$ level (99.99% of spatial availability). It is also possible to see that the commonly applied log-normal distributions fail to predict for probabilities lower than $10^{-1}$, finding deviations of up to 20 dB for that low percentiles. It is expected that further insight on lower percentiles will be achieved by exploiting the ability of running much more extensive virtual measurement campaigns by means of advanced calibrated simulation methods.

# Acknowledgment

The authors would like to thank the Robotic and Automation research group at at the Department of Mechanical and Manufacturing Engineering, Aalborg University, for providing the access to the industrial lab facilities. The authors would also like to express their gratitude to Tomasz Izydorczyk from the Department of Electronic Systems, Aalborg University, for his collaboration during the execution of the measurement campaign.

# References

[1] 3GPP TR 38.913 v14.1.0, "Study on Scenarios and Requirements for Next Generation Access Technologies," Mar. 2017.

[2] T. S. Rappaport and C. D. McGillem, "UHF fading in factories," in IEEE Journal on Selected Areas in Communications, vol. 7, no. 1, pp. 40-48, Jan. 1989.

[3] S. Kjesbu and T. Brunsvik, "Radiowave propagation in industrial environments," 2000 26th Annual Conference of the IEEE Industrial Electronics Society. IECON 2000. 2000 IEEE International Conference on Industrial Electronics, Control and Instrumentation. 21st Century Technologies, Nagoya, 2000, pp. 2425-2430 vol.4.

[4] H. Farhat, L. Minghini, J. Keignart and R. D'Errico, "Radio channel characterization at 2.4 GHz in nuclear plant environment," 2015 9th European Conference on Antennas and Propagation (EuCAP), Lisbon, 2015, pp. 1-3.

[5] E. Tanghe et al., "The industrial indoor channel: large-scale and temporal fading at 900, 2400, and 5200 MHz," in IEEE Transactions on Wireless Communications, vol. 7, no. 7, pp. 2740-2751, July 2008.

[6] C. B. Andrade and R. P. Fabris Hoefel. " On Indoor Coverage Models for Industrial Facilities". 7th international telecommunication symposium (ITS2010).

[7] J. Ferrer-Coll, P. Angskog, J. Chilo and P. Stenumgaard, "Characterisation of highly absorbent and highly reflective radio wave propagation environments in industrial applications," in IET Communications, vol. 6, no. 15, pp. 2404-2412, October 16 2012.

[8] S. Phaiboon,"Space diversity path loss in modern factory at frequency of 2.4GHz,"in WSEAS transactions on communications, vol. 13, 2014.

[9] National Instruments USRP-2953R [Online], 2017. Available: http://www.ni.com/da-dk/support/model.usrp-2953.html

[10] M. Peter, W. Keusgen and R. J. Weiler, "On path loss measurement and modeling for millimeter-wave 5G," 2015 9th European Conference on Antennas and Propagation (EuCAP), Lisbon, 2015, pp. 1-5.

[11] P. C. F. Eggers and P. Popovski,"Wireless channel modeling perspectives for ultra-reliable commnications," [Online], 2017. Available: http://arxiv.org/abs/1705.01725

[12] J. Jarvelainen, K. Haneda and A. Karttunen, "Indoor Propagation Channel Simulations at 60 GHz Using Point Cloud Data," in IEEE Transactions on Antennas and Propagation, vol. 64, no. 10, pp. 4457-4467, Oct. 2016.

# Paper G

Multi-Connectivity for Ultra-Reliable
Communication in industrial scenarios

Emil J. Khatib, Dereje Assefa Wassie, Gilberto Berardinelli,
Ignacio Rodriguez, and Preben Mogensen

# Abstract

*In the last years, wireless communications in industrial scenarios are becoming an increasingly important market. Some of these communications have tight reliability requirements, but harsh propagation conditions in industrial scenarios represent a major challenge. In this paper, multi-connectivity is explored as a solution for assuring high reliability in industrial scenarios. Several multi-connectivity techniques are compared, using real channel measurements from two factories. The impact over the mobile broadband terminals in the same network is also measured to assess for the cost of implementing multi-connectivity.*

# 1   Introduction

In the last decades, industrial processes have undergone a new revolution with the Industry 4.0 paradigm [1] and technologies such as the Internet of Things [2]. Telecommunication technologies and, more specifically, wireless data networks play a central role in these technological trends. The new cellular network generations, such as 5G, offer a competitive alternative to wired networks in the industry, allowing for an agile deployment and reduced installation complexity and costs.

The development of 5G takes into account the requirements of industrial communication. Specifically, two main communication profiles are supported [3]:

- Massive Machine Type Communications (MMTC): it represents non mission-critical messages coming from a large number of sources. Typically used by sensors that monitor a process continuously.

- Ultra Reliable Low Latency Communications (URLLC): mission-critical messages that require a very high reliability and a low latency. Used for alarms, special events measured by sensors for a closed loop control.

These two Machine Type Communication (MTC) profiles are complemented with Enhanced Mobile Broadband (eMBB), which is commonly associated with personal communications, but that also has its use in industrial scenarios, for instance in surveillance video feeds.

In order to accommodate the requirements of these communication profiles, a large network capacity is required. In previous generations, cell densification was exploited to increase the network capacity [4]. In the upcoming 5G network, this trend will continue. It is expected that in geographical areas where the number of devices is higher, or the requirements are more stringent, small cell deployments will be used to increase network capacity. This is precisely the case for the industrial scenarios where a large number

of MTC devices are expected to be deployed. To that end, a massive number of small cells is foreseen for supporting not only a higher capacity, but also the tight reliability requirements of industrial communications. However, cell densification suffers from increased level of interference. To deal with this, several interference mitigation techniques such as inter-cell interference coordination and advanced receivers have been used [5]. In particular, advanced receivers such as Interference Rejection Combining (IRC) have shown significant benefits in dense small cells deployments [6]. Besides the interference challenge, harsh propagation conditions in industrial scenarios [7] is another limiting factor, for improving the capacity and fulfilling the tight reliability requirements of mission-critical services.

This paper focuses on the usage of multi-connectivity for improving the reliability of wireless communication in industrial scenarios [8]. In multi-connectivity, one User Equipment (UE) terminal may be connected to more than one Access Point (AP) simultaneously. It has been proposed, for instance, for increasing the capacity of a UE for eMBB services [9] or for ensuring connectivity at the cell edge [10]. In this paper, multi-connectivity is used for the sake of improving the reliability of the communication by increasing the redundancy of data transmission.

Multi-connectivity can be analyzed via system level Monte Carlo simulations by reproducing a network of dense small cells. Nevertheless, standard propagation models may not fully capture the real propagation characteristics of a given scenario. For instance, the work in [11] indicated that commonly used path loss models such as WINNER II do not correctly predict the real measured path loss in indoor scenarios. This discrepancy will be further exacerbated in indoor industrial scenarios due to its specific characteristics, such as the presence of massive metallic machinery; therefore, a pure simulation study may not provide a realistic assessment of the advantages of using multi-connectivity techniques for mission-critical communications. Hence, in this paper, the performance of multi-connectivity is analyzed using a hybrid simulation approach where the channel models are superseded by real channel measurements. For this analysis, radio propagation measurements are run in two different factory scenarios using a Software Defined Radio (SDR) testbed [12].

The paper is structured as follows. Section 2 describes how multi-connectivity can be used to enhance the reliability, and the considered techniques. In Section 3, the measurement process, as well as the hybrid simulation technique will be described, detailing the configuration parameters for the scenario. The results are shown and discussed in Section 4; and finally, in Section 5, the conclusions are presented.

# 2 Multi-connectivity for industrial URLLC communications

Typically, in wireless networks, a UE is served by a single AP. In multi-connectivity, a single UE may be connected simultaneously to more than one AP at a given time. In case the multiple serving links are spatially uncorrelated, multi-connectivity can provide the required diversity for counteracting poor channel conditions. This is particularly important in harsh propagation scenarios, which is the case of industrial environments. In large factories with a large amount of heavy metallic structures, as well as concrete walls, shadowing is indeed the major limiting performance factor [7], and can jeopardize the possibility of establishing a reliable communication in case proper countermeasures are not taken into account.

Packet duplication is a multi-connectivity solution meant at improving reliability by increasing redundancy of the transmission [8]. When a packet reaches a certain AP which acts as primary node (PN), such packet is duplicated and transmitted to a secondary node (SN); both APs take care of transmitting the same packet to UEs demanding reliable communication. There are several ways to implement packet duplication in multi-connectivity, depending on the layer where the duplication is performed:

- Physical layer duplication: the APs coordinate at physical layer to transmit the packet. On the receiver side, the UE combines the received packet at physical layer, with the rest of the layers being agnostic to multi-connectivity. In this paper, we consider two possibilities for physical layer duplication:

  - Single Frequency Network (SFN) [13] : the APs transmit simultaneously the same waveform over the same frequency resources. The UE will then receive the superposition of the same signal from several points. SFN exploits opportunistically constructive interference for boosting the power of the signal.

  - Joint Transmission (JT) [14]: the APs transmit simultaneously the same physical layer packet over the same or different frequency resources; however, the waveforms are multiplied by an AP-specific precoding matrix which is calculated upon the estimated channel matrix. Such scheme requires then channel knowledge at the transmitter, and allows for coherent receive combining with the promise of further strengthening the signal power. Note that we are not considering here the case of coherent JT known in literature (e.g., [15]), where the precoding matrices are designed according to shared channel state information among the APs, but each AP applies its precoding matrix individually according to its own

155

channel. Further details on the scheme used in our evaluation will be provided in the implementation section.

• Higher layer (HL) duplication [8]: the packet is duplicated at PDCP (Packet Data Convergence Protocol) layer or above (e.g. network via multi-path TCP [16], or application). The packet will then undergo independent Radio Link Control (RLC), Medium Access Control (MAC) and physical layer processing at each AP. As a consequence, the packet can eventually be transmitted at different time instants, over different frequency resources and with different physical layer parameters such as modulation and coding scheme (MCS). On the receiver side, the UE will receive the multiple versions of the same packet, and eventually discard replicas in case the packet has already been correctly received. Duplication at PDCP layer is studied by the 3GPP for its inclusion in 5G [17].

Figure G.1 shows the distribution of the different packet duplication schemes over the network layers.
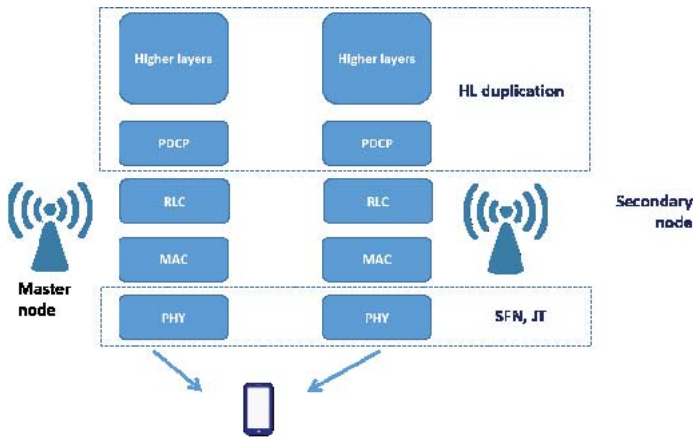


**Fig. G.1:** Summary of the different packet duplication techniques

Physical layer duplication requires tight synchronization. In particular, when using OFDM, the synchronization error must be below the cyclic prefix duration of the symbols. Such tight synchronization needs a high capacity connection between the APs, which increases the costs of deployment. Higher layer duplication has more relaxed requirements in terms of backhaul connection since the duplicated packets are not to be transmitted simultaneously. On the other side, this may translate to a latency increase.

# 3   Evaluation

For evaluating multi-connectivity in industrial scenarios, a hybrid simulation approach is used. In this approach, the higher layers will be emulated, while the physical layer will use real channel measurements instead of standard channel models.

The scenario that is emulated in this paper consists of 4 APs and 4 UEs, as shown in Figure G.2. We assume that one of the 4 UEs is demanding reliable communication (RC), while the other 3 UEs are eMBB users. Our focus in on the downlink. An Open Subscriber Group (OSG) mode is assumed, where each UE connects to the AP for which it measures the highest receive signal power. We assume that the APs (either PN or SN) serving the RC UE do not serve other users. Conversely, the other APs can instead serve multiple eMBB UEs by equally dividing its transmission bandwidth. Frequency reuse one is assumed, i.e. each UE suffers from the interference generated by the APs not serving itself.
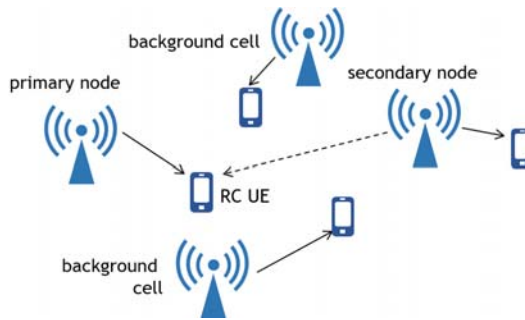


**Fig. G.2:** Basic emulated scenario.

Two main Key Performance Indicators (KPIs) are extracted for performance assessment:

- Signal to Interference plus Noise Ratio (SINR) for the RC UE, calculated assuming different multi-antenna receiver types. Specifically, we consider a Maximum Ratio Combining (MRC) receiver, which exploits spatial diversity to boost the power of the received signal, and an Interference Rejection Combining (IRC) receiver, which is able to suppress the strongest interference sources. Both receivers exploits the degrees of freedom offered by multi-antenna reception to strengthen the power of the useful signal. A packet is correctly received in case the measured SINR is above a minimum value necessary for a correct detection.

- eMBB throughput on the occupied resources: it measures the amount of data successfully transferred to the entire set of eMBB UEs over the

used bandwidth. Note that the throughput is not a relevant performance indicator for RC traffic, which is characterized by small packets to be transmitted with a high reliability. In this study, it is then only measured for the eMBB users. In particular, we aim at analyzing the eMBB throughput losses due to the usage of resources of multiple APs for serving the RC UE when multi-connectivity is activated.

## 3.1   Channel Measurement setup

The channel measurements are taken in two industrial scenarios, which we denote as Factory A and Factory B. The clutter in each scenario depends on the type of industrial machinery, as well as on the density of the installation. Factory A (Figure G.4) has a reduced amount of clutter, so line-of-sight (LOS) conditions for radio communication are more probable. Factory B (Figure G.5) is a cluttered environment, where the probability of shadowing is higher.

Measurements have been taken by using an SDR testbed consisting of 12 nodes. Out of the 12 nodes, 4 of them are configured as transmitters, and the other 8 nodes as receivers. Each node consists of 2 USRP RIO devices and a host PC that runs the measurement software. Figure G.3 shows two of the SDR nodes. Each USRP device is considered as an independent terminal and has two RF chains enabling $2\times2$ MIMO; this means, each testbed node has two co-located terminals. The node setup is mounted over a movable trolley to ease redeployments. The transmitter locations are deployed as shown in Figures G.4 and G.5. The receivers are distributed over 24 predefined positions via several redeployments. Furthermore, panel antennas with $60°$ aperture are used for the transmitter nodes, and omnidirectional dipole antennas are used for the receiving nodes. The transmit antennas are set at a 2.6 m height, while different heights per terminal are set for the receive nodes (1.75 m and 0.25 m, as shown in Figure). This is meant to emulate the diverse positions of industrial devices such as sensors an actuators in the factory environment.

Each transmitter generates a known signal, specifically a Zadoff-Chu sequence [18]. The Zadoff-Chu sequence is generated in the frequency domain and mapped over 600 subcarriers. The time domain signal is then generated via Inverse Fast Fourier Transform (IFFT) and repeated a number of times in order to fit a predefined slot duration. The system operates at a 3.5 GHz carrier frequency, and the transmission bandwidth is 18 MHz. The transmission of the Zadoff-Chu sequences is done by using a Time Division Multiple Access (TDMA) scheme with the approach shown in [12]. A frame structure with 4 slots is defined, where the transmission by the 4 transmitters are time multiplexed. This allows the receiver to discriminate the transmitter identity and the measured link. The receivers use the reference sequence to estimate the Channel Transfer Function (CTF) in the downlink. We refer to [12] for

**Fig. G.3:** Nodes of the SDR testbed. The left image shows a transmitter node and the right image a receiver node.
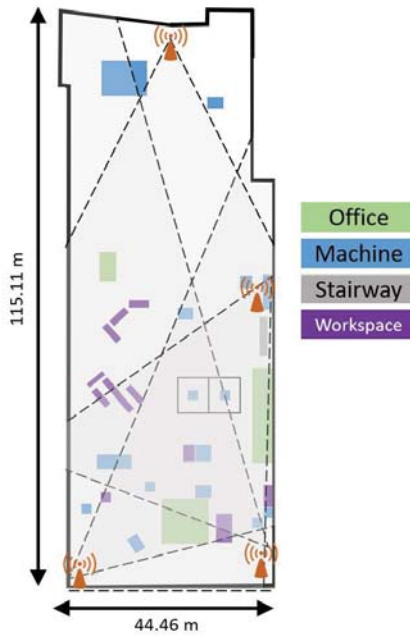


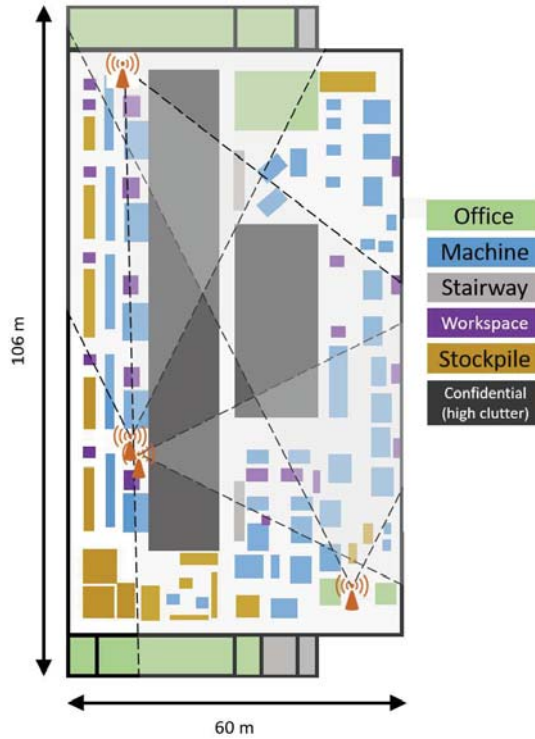**Fig. G.4:** Floorplan of Factory A with the AP positions.

**Fig. G.5:** Floorplan of Factory B with the AP positions.

further details on the adopted measurement approach.

Table G.1 summarizes the main radio parameters of the system. The outcome of the measurement campaign is a set of channel matrices representing the channel responses between the 4 transmitters and the 48 receiver locations (2 antenna heights per the 24 measurement positions).

## 3.2 Emulation

The performance of multi-connectivity is analyzed via hybrid simulations, where the channel measurements are replacing standard channel model. The scenario presented in Section III is used as a reference for the simulations. At each iteration of the simulation, four of the locations where the measurements have been taken are selected, representative of the 4 UEs. The role of the RC UE is assigned to a receiver of each of the selected locations in turn, and the rest of the receivers are assigned the role of eMBB UEs, resulting in four different scenarios per iteration. In each turn, an A/B testing is performed; first with only single connectivity and then with the different

**Table G.1:** Radio parameters.

| | |
|---|---|
| Frequencies | 3.5 GHz |
| Modulation | OFDM |
| Reference sequence | Zadoff-Chu |
| Reference sequence length | 601 |
| FFT length | 1024 |
| Sampling rate | 40 MS/s |
| Symbol duration | 25 $\mu$s |
| Signal bandwidth | 18 MHz |
| Tx power | 10 dBm |
| Antennas AP | 1 Panel XP (2.6 m) and 1 Panel HV (2.65 m), 60° aperture |
| Antennas UE | 2 dipole onmidirectional |

multi-connectivity options for the RC UE. In each case, the RC UE selects the serving APs; and the remaining APs are then serving the eMBB users. Once the assignations have been done, the CTFs measured by the UEs are used to obtain the downlink KPIs (SINR and throughput). The SINR is calculated according to the receiver type, by following the same approach as in [19], and then mapped to Shannon throughput. This loop is repeated until all the possible location combinations are emulated.

The SINR of the RC UE depends on the specific multi-connectivity scheme, and is calculated as follows:

- SFN: the received signal is the superposition of the signal of the assigned APs (PN and SN), so the SINR will be calculated upon a modified CTF which is the complex sum of the two individual CTFs.

- JT: The channel-aware precoding allows for coherent combining of the signals generated by the APs at the receiver. The SINR will be the sum of the individual SINRs: $SINR_{JT} = SINR_p + SINR_s$, where $SINR_p$ and $SINR_s$ denote the SINR of the PN and SN, respectively. It is worth to mention that this reflects the ideal case of full channel knowledge at the transmitter, which may not be feasible in the practice; however, it represents an upper bound on the JT performance.

- HL duplication: since two separate packets are received, the one with the highest SINR will be chosen as the received packet. Therefore, $SINR_{HL} = max(SINR_p, SINR_s)$.

Note that, for both SFN and JT, both signals coming from primary and secondary AP are useful signals. In case of HL duplication, packets are transmitted by the two APs in different time instants; this means, they would also suffer from their mutual interference, besides the interference from the other APs.

## 4   Results

Figure G.6 shows the Empirical Cumulative Distribution Function (ECDF) of the SINR of the RC UE in the two different scenarios and receiver types (MRC and IRC).
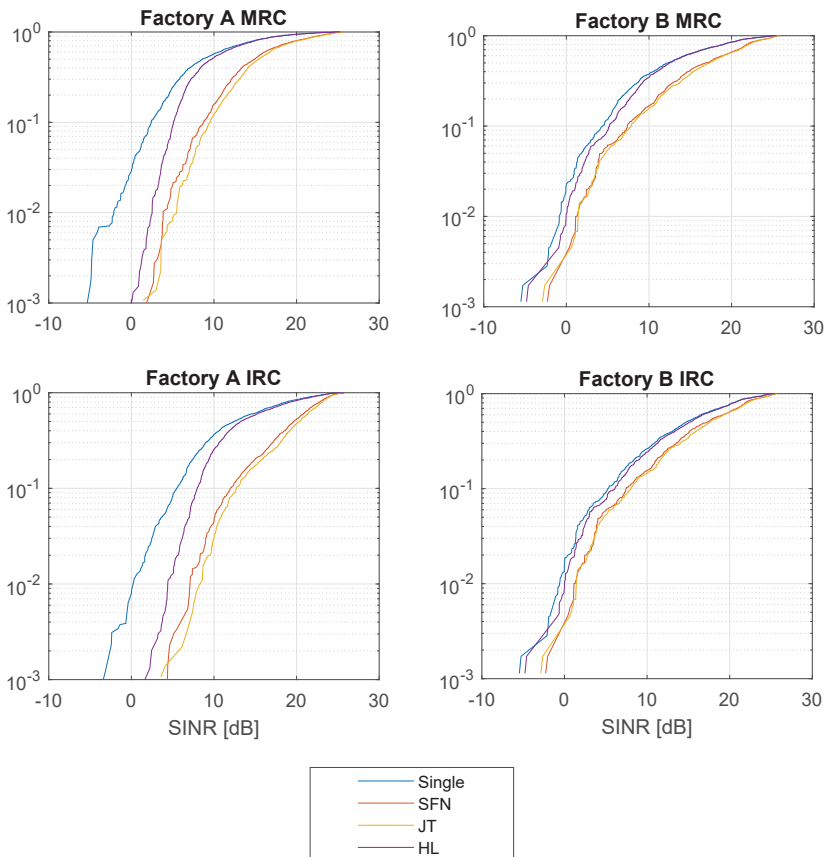


**Fig. G.6:** ECDF of the measured SINR in the two scenarios.

The multi-connectivity solutions clearly lead to a higher SINR gain with respect to single connectivity in Factory A. In particular, the gain is in the order of ~8 dB at a $10^{-2}$ percentile for the physical layer multi-connectivity solutions compared to the ~ 1-2 dB gain in Factory B. By assuming for example a 0 dB SINR threshold for correct packet detection, in Factory A transmission appears to be successful for all the measured samples in case physical layer multi-connectivity is used, while in Factory B a remaining failure rate persists. The LOS conditions in Factory A cause indeed a high level of interference, leading to a significant performance improvement in case the strongest interfering link in single connectivity mode becomes a useful signal when multi-connectivity is used. In Factory B, on the other hand, the massive presence of obstructors protects the receiver from a high level of interference, diminishing the benefits of an additional useful link.

As expected, both SFN and JT clearly outperform HL duplication. As explained in Section III, this is due to the fact that in HL duplication, both primary and secondary AP still suffer from their mutual interference since they transmit the duplicated packets at different time instants. However, the physical layer duplication improvements come at a significantly higher cost. It is worth to observe that no significant gain of JT with respect to SFN is visible. In this scenario, performance appear to be dominated by the instantaneous stronger link such that the benefits of signal combining enabled by JT are negligible.

The usage of an IRC receiver has a minor benefit with respect to MRC in Factory A (around ~ 2 dB gain at the $10^{-2}$ percentile), while its impact is negligible in Factory B. Given the two receive antenna terminals, IRC is able to suppress at most a single relevant interferer; the high amount of obstructors reduces the possibility of experiencing a relevant interferer in Factory B while this is more likely to happen in Factory A, therefore leading to a higher gain in the latter scenario.

When activating multi-connectivity, some resources of the network are redirected to serve the RC UEs, so the resources available for eMBB are lower in that instant. Figure G.7 shows the throughput of the eMBB users over the occupied resources of the network when the RC UE is served in single and multi-connectivity mode, averaged over all the instances of the simulation. The calculated throughput is the sum of the ideal Shannon capacity of each eMBB UE, based on the measured SINR and considering the total bandwidth of 18 MHz divided by the number of eMBB users served by the same AP. In both scenarios, the maximum throughput is about ~36 % lower when comparing the multi-connectivity with respect to single connectivity. This is because, in multi-connectivity, a second AP is dedicated to RC and the eMBB UEs can only choose between the remaining two APs. This increases the chances that the selected AP offers a lower receive power (and therefore a lower SINR) and that it is shared with other eMBB UEs; resulting in lower

throughput. Figure G.7 also shows a high standard deviation (represented by the thin red line). This is due to the high variability in the scenarios, caused by moving objects and the high variety of conditions found in the different locations where the measurement nodes were deployed. In Factory B the standard deviation is higher, responding to a higher clutter and movement of people and machines.
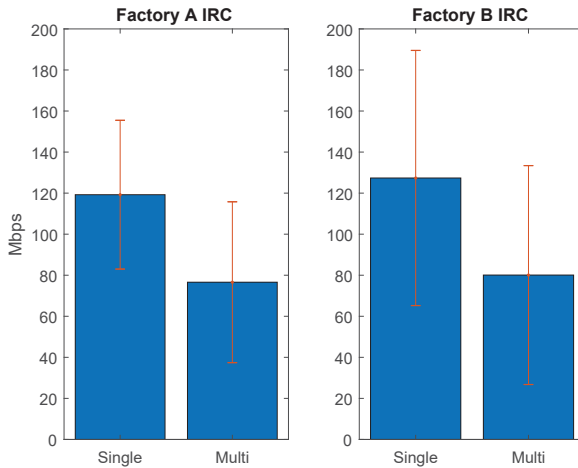


**Fig. G.7:** eMBB throughput of the network in the assigned resources with single and multi connectivity.

# 5   Conclusions

In this paper, multi-connectivity has been studied as a solution for reliable communications. The analysis is based on a large set of channel measurements obtained in two industrial scenarios characterized by different amount of clutter. Both physical layer and high layer duplication have been studied, considering multi-antenna Maximum Ratio Combining (MRC) and Interference Rejection Combining (IRC) receivers.

Multi-connectivity is shown to provide larger gains in the industrial scenario characterized by a low amount of clutter, given the dominance of LOS links which allow to convert relevant interfering links to useful signals. Minor benefits are instead visible in the scenario characterized by large shadowing levels. Physical layer duplication leads to the higher performance benefit, at the cost of additional implementation complexity with respect to packet duplication performed at a higher layer (e.g., PDCP).

Overall, multi-connectivity comes at a cost in the form of network throughput. Since resources are redirected to the UEs demanding reliable communication, a reduction in terms of eMBB throughput is observed.

# 6 Acknowledgements

# References

[1] H. Lasi, P. Fettke, H.-G. Kemper, T. Feld, and M. Hoffmann, "Industry 4.0," *Business & Information Systems Engineering*, vol. 6, no. 4, pp. 239–242, 2014.

[2] A. Al-Fuqaha, M. Guizani, M. Mohammadi, M. Aledhari, and M. Ayyash, "Internet of things: A survey on enabling technologies, protocols, and applications," *IEEE Communications Surveys & Tutorials*, vol. 17, no. 4, pp. 2347–2376, 2015.

[3] M. Series, "IMT vision–framework and overall objectives of the future development of IMT for 2020 and beyond," *Recommendation ITU*, pp. 2083–0, 2015.

[4] V. Chandrasekhar, J. G. Andrews, and A. Gatherer, "Femtocell networks: a survey," *IEEE Communications Magazine*, vol. 46, no. 9, pp. 59–67, September 2008.

[5] P. Mogensen, K. Pajukoski, E. Tiirola, J. Vihriala, E. Lahetkangas, G. Berardinelli, F. M. Tavares, N. H. Mahmood, M. Lauridsen, D. Catania *et al.*, "Centimeter-wave concept for 5G ultra-dense small cells," in *Vehicular Technology Conference (VTC Spring), 2014 IEEE 79th*. IEEE, 2014, pp. 1–6.

[6] D. A. Wassie, G. Berardinelli, F. M. L. Tavares, T. B. Sorensen, and P. Mogensen, "Experimental verification of interference mitigation techniques for 5g small cells," *IEEE Vehicular Technology Conference*, pp. 1–5, 2015.

[7] D. A. Wassie, I. Rodriguez, G. Berardinelli, F. M. L. Tavares, T. B. Sorensen, and P. Mogensen, "Radio propagation analysis of industrial scenarios within the context of ultra-reliable communication," in *2018 IEEE 87th Vehicular Technology Conference (VTC Spring)*, June 2018, pp. 1–6.

[8] J. Rao and S. Vrzic, "Packet duplication for URLLC in 5G: Architectural enhancements and performance analysis," *IEEE Network*, vol. 32, no. 2, pp. 32–40, 2018.

[9] Y. Li, S.-H. Kim, B. L. Ng, Y.-H. Nam, J. Zhang, and A. Papasakellariou, "Methods and apparatus for inter-eNB carrier aggregation," Feb. 9 2016, uS Patent 9,258,750.

[10] M. Polese, M. Giordani, M. Mezzavilla, S. Rangan, and M. Zorzi, "Improved handover through dual connectivity in 5G mmWave mobile networks," *IEEE Journal on Selected Areas in Communications*, vol. 35, no. 9, pp. 2069–2084, 2017.

[11] O. Tonelli, *Experimental analysis and proof-of-concept of distributed mechnisms for local area wireless network*. Aalborg University, 2014.

[12] D. Assefa Wassie, I. Rodriguez, G. Berardinelli, F. M. L. Tavares, T. B. Sørensen, T. L. Hansen, and P. Mogensen, "An agile multi-node multi-antenna wireless channel sounding system," *accepted for publication in IEEE Access*, 2019.

[13] F. B. Tesema, A. Awada, I. Viering, M. Simsek, and G. P. Fettweis, "Mobility modeling and performance evaluation of multi-connectivity in 5G intra-frequency networks," in *2015 IEEE Globecom Workshops (GC Wkshps)*, Dec 2015, pp. 1–6.

[14] P. Baier, M. Meurer, T. Weber, and H. Troger, "Joint transmission (JT), an alternative rationale for the downlink of time division CDMA using multi-element transmit antennas," in *Spread Spectrum Techniques and Applications, 2000 IEEE Sixth International Symposium on*, vol. 1. IEEE, 2000, pp. 1–5.

[15] D. Lee, H. Seo, B. Clerckx, E. Hardouin, D. Mazzarese, S. Nagata, and K. Sayana, "Coordinated multipoint transmission and reception in lte-advanced: deployment scenarios and operational challenges," *IEEE Communications Magazine*, vol. 50, no. 2, pp. 148–155, February 2012.

[16] Y.-C. Chen, Y.-s. Lim, R. J. Gibbens, E. M. Nahum, R. Khalili, and D. Towsley, "A measurement-based study of multipath TCP performance over wireless networks," in *Proceedings of the 2013 Conference on Internet Measurement Conference*, ser. IMC '13. New York, NY, USA: ACM, 2013, pp. 455–468. [Online]. Available: http://doi.acm.org/10.1145/2504730.2504751

[17] 3GPP, *NR and NG-RAN Overall Description*, ts 38.300 ed., 3rd Generation Partnership Project, December 2017.

[18] M. M. U. Gul, S. Lee, and X. Ma, "Robust synchronization for OFDM employing Zadoff-Chu sequence," in *Information Sciences and Systems (CISS), 2012 46th Annual Conference on*. IEEE, 2012, pp. 1–6.

[19] D. A. Wassie, G. Berardinelli, F. M. L. Tavares, O. Tonelli, T. B. Sørensen, and P. Mogensen, "Experimental evaluation of interference rejection combining for 5g small cells," in *2015 IEEE Wireless Communications and Networking Conference (WCNC)*, March 2015, pp. 652–657.

# Part V

# Conclusions

# Conclusions

## 1  Summary and Conclusions

Dense small cells deployment, in indoor environments, is foreseen to be one of the main components of the next-generation 5G mobile networks - to improve the capacity and reliability of the wireless network. The first deployments of such 5G small cells are anticipated to operate at below 6 GHz frequency bands. Unfortunately, the available spectrum in these bands is limited, and due to this, the cells are expected to operate over the same spectrum bands. Deploying a massive number of cells to operate over the same limited spectrum will increase inter-cell interference levels. Therefore, the interference mitigation study is crucial in a dense deployment scenario. Practically, a dense deployment brings plenty of active links, and these, on the other hand, can be harnessed to enhance the received signal quality by connecting a user to multiple access points (known as multi-connectivity).

Typically, to reduce the interference levels, different interference mitigation techniques such as inter-cell interference coordination, or advanced receivers that rely on the receiver signal processing capability and the availability of multiple receiver antennas, are utilized. Notably, advanced receivers are envisioned to be a good candidate in the dense deployments of small cells. This is mainly due to the reason that they do not require cells coordination which is challenging to apply in the presence of a massive number of cells. Besides, the technology is improving, and the current user terminals are equipped with multiple antennas.

In literature, the performance of those techniques is evaluated using system level simulations. This approach employs simplified statistical channel models; also, the employed scenarios are commonly based on a geometrically regular layout. However, in indoor environments, the building structures and materials are very diverse, and also the building layout is mostly irregular. These will impact the propagation conditions, and commonly used channel models may not efficiently describe the real propagation characteristics. Due to these, the system evaluation based on the simplified channel models may not fully grasp the complexity of the real scenario. Therefore, the objective

of this thesis is to validate the potential of those techniques in real scenarios using an experimental methodology. To that end, the validation of those techniques is based on a hybrid-simulation approach, where the channel models are substituted with the real channel measurements data. The measurements data are obtained from field experiments considering a real network deployment setup.

In this PhD project, a multi-node channel sounder testbed has first been developed to facilitate the experimental validation activities. The testbed was designed using a software-defined radio (SDR) platform and built from multiple nodes, and each testbed node consists of 2-4 antennas. The multiple SDR nodes enabled the testbed to support a distributed network deployment architecture and easy reconfigurability. The testbed accommodates measurements of composite channel links among deployed network nodes, and these allow to capture the instantaneous interference levels among cells. Such channel knowledge increases the accuracy and realism of the employed hybrid experimental validation approach.

The first experimental validations focused on the benefit of advanced receivers and spatial interference mitigation techniques towards dealing with inter-cell interference, in real indoor small cells deployment scenarios. Extensive channel measurements were conducted by deploying the testbed nodes, in a small cells network context, in typical indoor office and open hall environments. Several deployments with different propagation conditions and geometrical characteristics have been considered to create different realistic interference conditions. The measurements data were provided as an input to the hybrid-simulator to analyze the performance of the techniques mentioned above. The experimental results from the analysis essentially verified the effectiveness of the advanced receivers towards increasing the network throughput in interference-limited scenarios. The advanced receivers such as interference rejection combining (IRC) significantly improved the network throughput compared to interference unaware maximum ratio combining (MRC) receiver, in both indoor office and open hall scenarios. In particular, in an open hall indoor environment, considerable higher throughput gain was observed. In such an environment, there are not any walls that may reduce the neighboring interferers levels, and due to this, the presence of dominant interferers was observed. This condition benefited the IRC receiver since the receiver is capable of suppressing the strongest interferers by utilizing the available spatial degree of freedom (DoF). Besides, It has been observed that the IRC performance gain improved further using higher order MIMO antenna configurations. In fact, this is due to the extra spatial DoFs that can be exploited by the use of higher-order MIMO configurations.

Techniques that provide a means for the effective use of the available MIMO antenna configurations, such as Maximum Rank Planning (MRP) and Rank Adaptation are also experimentally evaluated in indoor small cells sce-

narios using real radio propagation conditions. The experimental results confirmed the usefulness of the MRP technique that limits the maximum number of transmission streams in a network. The experimental study revealed that limiting each cells transmission rank to one, even in a network that employed $2 \times 2$ antenna configuration, significantly improved the network throughput performance compared to a static Frequency Reuse Planning (FRP), in particular when IRC receivers are employed. This is achieved because MRP offered an extra DoF to the IRC receivers for suppressing at least one strong interferer. In fact, indoor office small cells scenario favors this because each cell is likely to experience one strong interferer from the adjacent neighboring cell due to the presence of walls and corridors between cells. In such low interference condition, the use of static FRP scheme reduced the network throughput since the frequency chuck allocated to each cell was minimized. Besides, the experimental results demonstrated the effective benefit of rank adaptation algorithms (that manage the trade-off between spatial multiplexing gain and interference resilience) towards facilitating interference suppression capability of advanced receivers. When the cells used interference-aware rank adaptation algorithms, the outage data rate gain of the IRC receivers prominently improved. This is because when a cell experienced strong interferers, the algorithm discouraged the selection of higher rank transmission for enabling the receiver capability towards suppressing the interferers. Also, It was observed that the gain was further improved when a strong discouragement level was applied. Moreover, the experimental analysis proved the suitability of advanced receivers with efficient use of spatial domain resource as a solution providing interference mitigation in indoor dense small cells deployments.

The second experimental validation focused on multi-connectivity solutions toward improving the wireless network reliability in indoor industrial scenarios. Before this has been carried out, the large-scale radio propagation characteristic study was performed in indoor industrial scenarios. Such study did not have enough coverage in existing literature compared with the indoor office scenarios. Besides, most of the existing industrial propagation studies are limited with the spatial measurements coverage in a given industrial environment. In this project, extensive propagation measurements with better spatial coverage were performed in indoor industrial environments. The results obtained from the measurements confirmed that the propagation conditions are profoundly affected by the presence of many metallic machines: those impact the propagation channels to have a waveguiding effect and high shadowing levels. Besides, the results indicated that the existing widely-used large-scale propagation models might not be adequate for predicting the lower tail of the large-scale fading statistics. In fact, the lower tail of the statistics illustrates the occurrence of the rare circumstances that may have a vital impact on the radio signal availability. Therefore, the wireless

network reliability study should not only be based on channel models since managing the rare events are a crucial ingredient for reliability. Moreover, this study indicated that a detailed analysis of the lower tail of the channel statistics requires further investigations by running much more extensive measurement campaigns or using advanced ray tracing tools.

The propagation study demonstrated that larger shadowing levels are observed in the presence of metallic machinery, and this affects the wireless network reliability. To address this challenge, multi-connectivity could be a viable solution in such a scenario. In this regard, an initial experimental validation of multi-connectivity solutions was addressed in this thesis. The performance validation was carried out using real channel measurements obtained from an extensive measurement campaign performed in real factory environments. The preliminary results obtained from the experimental analysis indeed verified the effectiveness of multi-connectivity solutions toward improving signal quality. It was observed that the use of multi-connectivity provided higher SINR gain compared to single connectivity. Such gain of multi-connectivity is achieved since an additional communication link is used to improve the signal quality. This, however, decreased the network throughput of mobile broadband users since some network resources are taken from them to improve reliability. Also, it was observed that the benefit of an additional link was diminished in the industrial scenario where the presence of clutters (i.e., metallic machinery) was higher. In this scenario, a massive presence of clutters impacted the propagation of the additional communication link. These learnings lead to a conclusion that the selection of an additional link should carefully consider both the signal quality and the cost on mobile broadband users.

## 2 Recommendations

To answer the research questions described in Part I - Section 3, the following recommendations are worth considering:

- The experimental analysis demonstrated that advanced receivers are a viable solution for counteracting interference in uncoordinated dense small cells deployment. Therefore, to decrease indoor dense small cells deployment planning cost, the operator can consider uncoordinated deployments and rely on advanced receiver processing with sufficient MIMO antennas configuration to tackle interference. Such benefit of the advanced receiver can be achieved considering that the cells are tightly synchronized, and the channel response of interfering links are adequately estimated.

- Employ interference aware rank adaptation algorithms to improve fur-

ther the performance of interference suppression receivers. However, such algorithms may add inter-cell signaling burden for estimating the interference levels introduced to the adjacent cells. Therefore, such signaling burden should be considered. In addition, the benefit of the algorithms is exploited if the assumptions discussed in the above list are also fulfilled.

- Consider a sufficient margin from commonly used channel models for analyzing the performance of the algorithms that are employed to enhance the reliability of the wireless network. To calculate the margin, an extensive measurement campaign is essential to be held with the adequate spatial coverage of the targeted scenario.

- Use multiple serving links which are spatially uncorrelated to enhance the reliability of the wireless network in industrial environments. However, such an approach will reduce the capacity of mobile broadband users who share the same network resource. Therefore, such an impact on broadband users should be considered during the use of multi-connectivity for improving reliability.

# 3  Future Work

Experimental validation allows verifying the feasibility of new technologies in realistic operating conditions. Designing a testbed platform which can support the experimental validation of technologies in the context of network performance requires many network nodes. However, in this regard, the main challenge lies in the cost and the complexity in the design and development of such a testbed network. A design approach which is based on software-defined radio concept provides benefit towards alleviating those challenges. In fact, continuous growth of software-defined radio device capability is expected to drive experimental validation activities in the future.

In this thesis, a multi-node software-defined radio testbed has been developed for enabling experimental validation. However, various aspects of the platform could still be improved. First, further developments are required to better exploit the available field-programmable gate array (FPGA) processor on the employed software-defined radio devices. Efficient use of the FPGA processor will enable a real-time validation of the new 5G concepts. Furthermore, the testbed time synchronization approach can be further improved using high precision reference clock signals. Such synchronization approach will support a shorter transmission interval, and this will enable the testbed channel sounding capability toward capturing the time-varying channel characteristics.

The experimental activities discussed in this thesis focused on 5G wireless technology applications, enhanced broadband communications and highly reliable communication for industrial automation. Currently, the industrial automation application is the main focus of the research activity at Aalborg University. The initial radio propagation and multi-connectivity studies presented in this thesis are one of the examples among the ongoing research activities. In this thesis, the early experimental activity of multi-connectivity schemes are presented, and an extension of the study is required in order to further evaluate the promising potential of the multi-connectivity technique in industrial scenarios. Besides, other research aspects are also expected to be carried out. For example, one interesting research direction related to propagation study in an industrial scenario would be to investigate further the lower tail of channel statistics (capturing the rare events which significantly impact the reliability of wireless network) using advanced ray-tracing tools. Since such analysis requires a massive number of spatially distributed channel measurement samples in a given scenario, this is somehow difficult to achieve using just field measurements. An extensive channel measurement can be used to calibrate ray tracing tools for increasing the accuracy of the tool. In this way, the tool precision towards estimating a propagation condition of a given network link can be increased. Therefore, the tool can be exploited for further validation of the 5G technologies potential towards improving the reliability of the wireless network in ultra $(10^{-9})$ level context.